DAMPING OF STREAM TEMPERATURE TIME SERIES BY HYPORHEIC EXCHANGE

by

KRISTIN ANN KRASESKI

(Under the Direction of C. Rhett Jackson)

ABSTRACT

Stream temperature is an important water quality attribute that influences instream processes, reaction rates, and species distributions. Solar radiation has the largest effect on water temperatures, but heat exchange also occurs at the streambed interface. Hyporheic exchange is a type of streambed interaction that occurs when channel water advects through the streambed. Studies of thermal regimes suggest that mean temperature of hyporheic and surface waters are similar on daily timescales, but that patterns and timing extreme values are sufficiently different that this exchange is a common contributor to thermal heterogeneity within streams. This study seeks to investigate how temperature changes may occur based on the rates of heat transfer in hyporheic pathways between water and hyporheic sediments. An extensive literature review identified reported ranges of common hyporheic characteristics that affect movement and heat transfer within hyporheic flowpaths. A laboratory experiment was used to measure heat transfer rates between water and sediment. Four bed sediments (sand, fine gravel, coarse gravel, and a mix) were initially different temperatures and then added to room temperature water. Water-sediment temperatures were measured every

half second during the resulting interaction. The majority of heat transfer, or conduction, consistently occurred within the first few seconds of sediment addition. This, combined with the slow velocities in most hyporheic flow paths, would imply near-instantaneous conduction for these systems. This information was used to develop two spreadsheet models: one that subjects stream temperature time series to a set of calculated “damping coefficients” based on travel time in the hyporheic zone, and another that explicitly calculates heat transfer terms based on common literature values. Results showed that heat transfer in the hyporheic zone damps temperature patterns, and water present in a flow path for four daily cycles would have temperature patterns almost indistinguishable from the average temperature. Assuming near-instantaneous conduction, this model should be applicable to most stream systems where hyporheic characteristics and travel times can be estimated.

INDEX WORDS: Hyporheic Exchange, Stream Temperature, Riverbed Thermal Conduction

DAMPING OF STREAM TEMPERATURE TIME SERIES BY HYPORHEIC EXCHANGE

by

KRISTIN ANN KRASESKI

B.A., Binghamton University, 2005

M.S., Long Island University, 2010

A Dissertation Submitted to the Graduate Faculty of The University of Georgia in Partial Fulfillment of the Requirements for the Degree

DOCTOR OF PHILOSOPHY

ATHENS, GEORGIA

2015

DAMPING OF STREAM TEMPERATURE TIME SERIES BY HYPORHEIC EXCHANGE

by

KRISTIN ANN KRASESKI

Major Professor:	C. Rhett Jackson
Committee:	Todd C. Rasmussen
	Jeffrey Hepinstall-Cymerman
	Mary C. Freeman

Electronic Version Approved:

Julie Coffield
Interim Dean of the Graduate School
The University of Georgia
May 2015

DEDICATION

To my family for always being supportive and to Matthew for sticking with me through it all and always making me laugh.

ACKNOWLEDGEMENTS

I would like to acknowledge my committee, but especially Rhett Jackson and Todd Rasmussen. As my advisor, Rhett has really guided me through this project and I am deeply indebted to him for his help. He was instrumental in redirecting my project (and especially the experiments) when I encountered problems, and brought a real focus to this dissertation through his helpful revisions. Todd has been invaluable in helping me with the modelling aspects of this project – he always has a way of making seemingly complex ideas understandable, and there are parts of this project that would have seemed unachievable without his help.

TABLE OF CONTENTS

Page

ACKNOWLEDGEMENTS v

LIST OF TABLES viii

LIST OF FIGURES ix

CHAPTER

1 INTRODUCTION 1

1.1 Stream energy budgets 4

1.2 Lack of hyporheic effect on net energy budget 6

1.3 Stream temperature time series 9

1.4 Ideas on temperature effects – cooled, damped, or lagged? 11

2 LITERATURE REVIEW 23

2.1 Hyporheic flow and exchange 23

2.2 Ecological implications of hyporheic exchange 28

2.3 Factors controlling the amount of hyporheic exchange 34

2.4 Inclusion of hyporheic exchange on water temperature and water quality modeling 37

3 THERMAL AND HYDRAULIC CHARACTERISTICS OF STREAM SUBSTRATES RELEVANT TO HYPORHEIC TEMPERATURE EXCHANGE 45

3.1 Sediment porosities and densities 47

3.2 Hyporheic hydraulic conductivities 49
3.3 Hyporheic path lengths and velocities 53
3.4 Sediment specific heats and thermal conductivities 55
3.5 Bucket experiments 57
3.6 Calorimeter experiments 60
3.7 Calibration of specific heats of sediments 63
3.8 Calibration of thermal conductivity 65
3.9 Conclusions 66
4 DAMPING OF TEMPERATURE VARIATION WITH HYPORHEIC TRAVEL DISTANCE 86
4.1 One-dimensional heat transfer equation 87
4.2 Instantaneous conduction model for hyporheic damping 88
4.3 Heat flux EXCEL model 95
4.4 Conclusions 107
5 CONCLUSION 124
REFERENCES 127

LIST OF TABLES

Page

Table 3.1: Hyporheic porosities from the literature....69

Table 3.2: Hyporheic bulk densities from the literature....70

Table 3.3: Porosity and bulk density of sediments (based on Shen and Julien, 1993)....70

Table 3.4: Bulk densities of sand and gravel taken from the literature....71

Table 3.5: Hyporheic hydraulic conductivities from the literature....72

Table 3.6: Hyporheic flowpath lengths from the literature....73

Table 3.7: Hyporheic flow velocities from the literature....74

Table 3.8: Different systems of classifying particle sizes (Soil Survey Division Staff, 1993)....76

Table 3.9: Calculated bulk density and porosity of sediments used in bucket and calorimeter experiments....77

Table 3.10: Calculated sediment specific heat for each calorimeter trial....78

Table 4.1: Descriptive information for Holloway Branch and Shope Fork....109

Table 4.2: Damping coefficients based on number of half cycles that water is present within the hyporheic zone – used in Instantaneous Conduction Excel Model....109

Table 4.3: Initial parameters for Heat Flux Excel Model....110

LIST OF FIGURES

Page

Figure 1.1: A conceptual model of a stream energy budget, taken from Li, 2006, with the addition of a hyporheic exchange term 16

Figure 1.2: Conceptual diagram of how hyporheic exchange occurs in stream with pool-riffle-pool morphology.....17

Figure 1.3: Shope Fork riparian gap stream temperature data, summer, 2012 18

Figure 1.4: Shope Fork riparian gap stream temperature data, winter, 2014.....19

Figure 1.5: A time series temperature comparison of shaded and unshaded streams.....20

Figure 1.6: Diagram explaining the possible temperature patterns of the hyporheic zone compared to channel water (from Arrigoni *et al*., 2008) 21

Figure 1.7: Conceptual diagram showing the processes that influence hyporheic water temperature in a gravel bar (from Burkholder et al., 2008) 22

Figure 2.1: Conceptual longitudinal model of a pool-riffle-pool sequence (from White, 1993) 43

Figure 2.2: Conant's (2005) conceptual model showing different directions and magnitude of hyporheic flowpaths and sediment characteristics 44

Figure 3.1: Values of hydraulic conductivity of river-lining materials (taken from Calver, 2001) 79

Figure 3.2: 3D plot of Unit travel time as a function of typical ranges of slope and characteristic travel time (all scales are logarithmic) 80

Figure 3.3: Principle of the steady-state longitudinal heat-flow method for measuring thermal conductivity (taken from Berman, 1976).....80
Figure 3.4: Bucket experiment: Mixed sediment trial temperature time series.....81
Figure 3.5: Bucket experiment: Sand trial temperature time series.....82
Figure 3.6: The hypothetical peak missing from temperature time series in the bucket experiment.....83
Figure 3.7: The experimental set-up for the calorimeter study.....83
Figure 3.8: Temperature time series for the sand trials of the calorimeter experiment.....84
Figure 3.9: Temperature time series for the fine gravel trials of the calorimeter experiment.....84
Figure 3.10: Temperature time series for the coarse gravel trials of the calorimeter experiment.....85
Figure 3.11: Temperature time series for the mixed sediment trials of the calorimeter experiment.....85
Figure 4.1: A schematic of water traveling through pores conceptualized as sheet flow111
Figure 4.2: A schematic of how heat flow will occur within the sheet flow conceptualization of water movement through the hyporheic zone 111
Figure 4.3: Schematic showing the components of a daily temperature time series 112
Figure 4.4: Locations of Streams: Holloway Branch and Shope Fork, North Carolina ..113
Figure 4.5: Holloway Branch, North Carolina.....114
Figure 4.6: Shope Fork, North Carolina 115
Figure 4.7: 24-hour temperature time series from Holloway Branch in the Nantahala National Forest, North Carolina.....116

Figure 4.8: 24-hour temperature time series from Shope Fork, North Carolina.....117

Figure 4.9: Model results for the Instantaneous Conduction Model at Holloway Branch, North Carolina 118

Figure 4.10: Model results for the Instantaneous Conduction Model at Shope Fork, North Carolina.....119

Figure 4.11: Conceptual visualization of Heat Flux model, with red arrows representing heat exchanges within the system.....120

Figure 4.12: A screenshot from Microsoft Excel showing how information within the Heat Flux model was organized.....121

Figure 4.13: Screenshots from the Heat Flux model showing the components that were used to calculate advection and dispersion for downstream cells within the model….....122

Figure 4.14: Results from the Heat Flux model, looking a heat concentrations through time for different locations within the grid of hyporheic cells, and including input temperatures.....123

CHAPTER 1

INTRODUCTION

Stream temperature is a fundamental aspect of water quality: it affects rates of chemical reactions, dissolved oxygen levels, species distributions, and the overall health of aquatic ecosystems (Caissie, 2006). Interest in stream temperature has been heightened due to recent evidence of a consistent long-term warming trend in rivers and streams in many parts of the U.S. (Kaushal et al., 2010). This warming trend seems to be present even when taking into account seasonally dependent cooling periods (Isaak et al., 2012), but, this picture is more complex because not all streams are warming equally (Luce et al., 2013).

Streams vary in their sensitivity to air temperature changes associated with climate change, with the coolest streams (often the ones at the highest elevations) being less sensitive than naturally warmer streams - they are sourced from groundwater and are therefore less affected by weather conditions and sunlight (Luce et al., 2013). Yet, groundwater temperatures may also be expected to rise in response to rising air temperature during the season of highest recharge, and these changes would likely manifest themselves in changes to stream temperature. For example, Taylor and Stefan (2009) found that shallow groundwater temperatures respond to ground surface temperature cycles, which in turn are affected by seasonal cycles and climate change; in northeastern temperate regions these influences upon ground surface temperatures can penetrate 10-15 meters into the ground. It is likely that climate change-related stream

temperature variation will differ by region and in more complex ways than by temperature alone – this includes changes in vegetation type or precipitation patterns (Dori, 2005).

Stream temperatures are determined by a complex set of interacting factors that include atmospheric conditions, latitude, topography, riparian shade, stream discharge and streambed morphology (Caissie, 2006). Stream water temperatures vary in a cyclical manner in concert with daily solar radiation fluctuations: they vary seasonally, due to longer term fluctuations in solar radiation; they can vary due to external anthropogenic inputs, like dam releases or wastewater effluent releases (Kinouchi, 2007); and they can be affected spatially by differences in riparian shading and variations in contributing system inputs such as hyporheic exchange and groundwater discharge (Loheide and Gorelick, 2006). A combination of these types of factors will lead to the temperature of a stream at any moment.

The sources of stream temperature variation can range from highly localized, to watershed-scale factors, and even to regional climatic factors. Localized variations in stream shading can greatly influence the amount of solar radiation reaching the stream surface – the factor with the largest effect on stream temperature. Li et al. (2012) developed a stream shading model that speaks to the complexity of shading and how it shifts throughout the day. This model, although it does not directly predict stream water temperatures, uses factors such as azimuth, channel width, bank height, vegetation height, and vegetation overhead to describe how solar radiation reaches - or rather, does not reach - a stream (Li et al., 2012).

Larger scale factors can also be examined to determine their relative impact on stream temperature variation. A study by Booth et al. (2014) in the Puget Sound area of Washington State did not include local factors like stream shading, but rather looked at landscape-scale factors at a large number of sites, including watershed size, the percentages of urbanization or outwash soils within the watershed, and the amount of watershed area covered by lakes, all of which, in the past, have been found to affect stream temperature (Booth et al., 2014). A statistical analysis indicated that for the study year with the most voluminous data (1999), outwash soils - used as a proxy for groundwater inputs into the system - alone seemed to be having the greatest effect on summertime stream temperatures (Booth et al., 2014). Although interesting, in that level of urbanization wasn't recognized as a larger contributing factor, it is likely that these results are regionally specific and reliant on geology, rain patterns and climate. Conversely, regions with intense, but short-lived, mid-afternoon summer thunderstorms are more likely to be affected by warmed direct runoff from paved surfaces (e.g. Herb et al., 2008), and one may find that level of urbanization is a more important factor than geology. These larger-scale factors may be very context-specific, rather than localized factors like shading, which will tend to be of more universal importance, but all scales will contribute to temperatures in some way.

This chapter will introduce some of the basic concepts in stream temperature research: how heat can be conceptualized within a stream system, common sources of heat and/or energy within the system, how temperature is commonly measured, and most importantly for this work, where hyporheic exchange fits into the study of stream temperature.

1.1 Stream energy budgets

A stream energy budget takes into account all of the energy inputs and outputs of a stream segment, and estimates how they contribute to its water temperature. Energy budget equations and conceptual models such as Figure 1.1 (From Li, 2006) are common ways to visualize the different influences of energy within a system. This can include advected water into and out of the reach, interactions at the stream surface including short- and long-wave radiation, and interactions with the streambed. G.W. Brown (1969) gave an early and well-cited example of a stream energy budget to predict stream temperature in three small streams in western Oregon. In this study, Brown measured water temperature at the upstream boundary of a reach, tried to calculate the exchanges occurring within the reach using the following equation:

$$\Delta S = Q_{NR} \pm Q_E \pm Q_C \pm Q_H \pm Q_A \qquad \text{(Equation 1.1)}$$

where

ΔS = net change in energy stored;
Q_{NR} = net thermal radiation flux;
Q_E = evaporative flux;
Q_C = conductive flux;
Q_H = convective flux;
Q_A = advective flux.

He then compared his calculations to temperature measurements at the downstream boundary of his study reaches. Hourly predictions based on estimated losses and gains of energy were within 1°F of the measured temperature for 21 of the 24 predictions, demonstrating the energy budget technique of predicting stream temperature appears to be effective, for these streams, at least. However, Brown effectively disregarded the effect of water traveling through stream sediments in his predictive models, and his

model cannot account for spatial variation in energy inputs (e.g. shade). His is effectively an infinite reach model.

A more recent example of a stream temperature energy budget model is from LeBlanc et al. (1997), who developed a Critical Urban Stream Temperature (CrUSTe) model to examine summer extreme temperatures associated with low flow conditions. LeBlanc et al., (1997) began with the same energy balance equation used by Brown, but then translated that net change in energy stored into a corresponding temperature change using the specific heat capacity of water and the equation,

$$\Delta T = (\Delta H \cdot A/Q) \cdot 0.000664 \qquad \text{(Equation 1.2)}$$

where ΔT is the change in water temperature, ΔH is the net change in energy stored (denoted as ΔS in Brown, 1969), A is the stream surface area and Q is the discharge. An initial sensitivity investigation of input parameters demonstrated that transmissivity, stream width, and groundwater discharge were having the largest influence on stream temperature and were affected by urbanization (LeBlanc et al., 1997); these parameters were then modeled in more detail as component models for the CrUSTe. The LeBlanc et al. (1997) study demonstrates how a simple energy budget equation can be expanded and used to make predictions about consequences of land use changes and urbanization on stream temperatures.

Many early models based on stream energy budgets conceptualize energy inputs and outputs as occurring either at the stream surface (including solar radiation, net radiative fluxes, and evaporative fluxes), or at the stream bed (conduction, groundwater contributions, and hyporheic exchange) (Caissie, 2006), but because hyporheic exchange has historically been difficult to measure or even estimate in the field, it has rarely been

included in these water temperature models. The conceptual model presented in Figure 1.1 is modified from the original source (Li, 2006) to include a term for hyporheic exchange, illustrating that hyporheic exchange has no net effect on the energy budget at the reach scale where advective hyporheic inputs and outputs are balanced. Figure 1.2 presents a basic introductory longitudinal schematic of how hyporheic exchange occurs within a mid-size stream dominated by pool-riffle-pool sequences. Due mostly to pressure gradients, water moves from the stream, into the sediment, and back out again. Temperature patterns within the hyporheic zone will differ from surface temperatures and are affected by path lengths, gradients, conductivities, travel times, porosity, thermal capacity, thermal conductivity, and heat transfer rates. These concepts will be discussed more thoroughly in the following chapters. The difficulty is in capturing the spatial and temporal effects of hyporheic exchange on the stream energy budget and resulting temperatures.

1.2 Lack of hyporheic effect on net energy budget

Although it has been estimated that about 15% of the total energy fluxes in a stream channel occur at the channel bed (Evans et al., 1998), no consensus techniques have been developed to estimate the effect of hyporheic exchange on energy fluxes or temperature. Average hyporheic zone temperatures on daily, or longer term time scales, tend to be similar or nearly identical to average stream channel temperatures (Arrigoni et al., 2008). This occurs because of the cyclical nature of temperature time series - bed temperatures and stream water temperatures will likely have similar means or averages over the period of a day (unless there is a strong influence from groundwater discharge,

which may have vastly different temperatures from channel water, especially during air temperature extremes), even though they reach their minimum and maximum temperatures at different times of the day. The water present in the hyporheic zone, especially at shorter time scales has come directly from the stream, and therefore shares many characteristics with stream water. In addition, the stream bed goes through daily temperature cycles similarly to the stream itself, although the time each day that it reaches its maximum and minimum are somewhat offset from the stream diel temperature cycle. This implies that water in the hyporheic zone will not likely reach temperatures outside of the range of the stream water itself; however, it is conceivable that this may occur when hyporheic flowpath lengths are long and reflect the patterns of different upstream reaches or are heavily influenced by groundwater inputs. Some researchers have found that net cooling seen in some hyporheic flow paths is likely due to conduction with adjacent cooler groundwater (Menichino and Hester, 2014). Generally speaking though, hyporheic exchange and bed conduction are internal drivers of temperature, and do not actually remove any heat from the system, but rather spatially and temporally redistribute it (Burkholder et al., 2008).

Even if hyporheic temperatures are similar, on average, to stream channel temperatures and do not technically add or remove any heat from the system, this doesn't imply that they are not important ecologically. Because zones of upwelling hyporheic water may be a different temperature than stream water at any one moment, even if only slightly, they are considered to be ecologically significant because they enhance temperature diversity in surface and subsurface habitats (Arrigoni et al., 2008). This may be especially important during the summer months for species, such as fish, that can

thermoregulate by moving to cooler patches within a stream system. Because temperatures are offset between the surface water and hyporheic zones, it is a common occurrence that when the stream water has reached its maximum temperature for the day, water in the nearby hyporheic zone will be comparatively cooler at that moment, and hyporheic upwelling sites can therefore act as cooler water patches during these extreme periods. This type of thermal heterogeneity, as well as those associated with deep pools and riparian shading, can greatly affect the distribution of stream fishes (Ebersole et al., 2003), although the interaction will likely be more complex than that. For example, growth rates of fish may be more affected by changes in food supply rather than direct temperature changes with removal of riparian vegetation (Leach et al., 2012).

Poole et al. (2008) introduced the concept of 'hydrologic spiraling,' which posits that there are a population of different flow paths that link the channel to the hyporheic zone, and these flow paths may blend or be returned to the channel in close proximity to each other, creating a complex picture of hyporheic water. These complex hyporheic flow nets can be influenced by channel morphology and gradients, hydraulic conductivities of sediments, and even changes in stream discharge during wet seasons or storm events (Wondzell, 2011). In other cases, it is not clear that hyporheic exchange will create significant spatial variation in stream temperatures at all. For example, Long and Jackson (2014) found no ecologically significant variation in stream temperatures across mesoscale habitat types in southern Appalachian streams, even though this is a region with pool-riffle morphology that was expected to display hyporheic exchange processes.

1.3 Stream temperature time series

Stream temperature time series are the most common way to examine stream temperatures over an extended period of time, and are considered to be more useful than one-time, instantaneous water temperature measurements (see Booth et al., 2014, for an example where individual point measurements were more suitable for the scope of the study). Time series allow you to see not only the cyclical nature of water temperatures, but also allow a closer investigation of the properties of a temperature cycle that are likely to be important to the health of ecosystems and particular species of interest. These significant characteristics can include daily temperature range or variation as well as maximum (or minimum) temperatures seen during the day. Maximum temperatures are often important when investigating whether certain streams have temperatures that surpass critical threshold levels for particular species, or statewide water quality criteria.

Perhaps less important, but useful in certain situations, are temperature means. Means can give an indication of overall temperature changes on large time scales. For example, Kaushal et al. (2010) looked at monthly mean temperatures and found that there were long-term warming trends in historical water temperature time series throughout the U.S. However, means may not be as vital in the understanding of stream water temperatures on short time scales because of their lack of specificity when it comes to ecologically important aspects of daily or seasonal temperatures. For example, temperatures with a very large range or variability can theoretically have the same mean as a temperature series with a very small range. Temperature time series can also give a good indication of short term changes within a system, like how water temperatures may

change when exposed to an external pulse of warmer or cooler water, assuming the time points of measurement are suitably close together to observe the change.

When water temperature time series are examined over a long time period, they can give an idea of maximum temperature ranges, average diurnal variation, or the number of days or hours or events when water temperature spends above certain thresholds (important for cold-water fish during summer). They can also give an indication of how stream systems respond to environmental changes. An interesting example of how temperature time series can be used to understand stream thermal processes is illustrated by Figures 1.3 and 1.4. These graphs show temperature measurements taken in and around a gap in the riparian zone at Shope Fork in Otto, North Carolina during the summer (Figure 1.3) and the winter (Figure 1.4) of 2012. Stream-side shading by riparian vegetation has long been acknowledged as an important factor for mitigating elevated stream temperatures (Brown, 1969), the importance of which can be seen at different streams in the region (Figure 1.5 shows two corresponding temperature time series, one at a fully shaded stream site and another at an unshaded stream site). Temperature measurements were taken at the Shope Fork to understand how far sudden changes in stream temperature, created by an abrupt reduction in riparian shading, are propagated downstream.

The Shope Fork summer temperature data (Figure 1.3) show that while there are elevated maximum daily temperatures encountered within the riparian gap, they are short-lived, and stream temperatures return to upstream levels within 50 meters of the end of the gap. An interesting note here is that although peak temperatures vary widely between the forested areas and the gap, minimum early morning temperatures do not; it is

unclear why this is occurring. During the winter of 2012 at this same location (Figure 1.4), it is apparent that the riparian gap is not exerting the same influence on water temperatures as it did in the summer. This is likely due to an increase in discharge that may have decreased the importance of solar radiation on the energy budget of the stream during this period. Although temperature patterns varied seasonally, the temperature time series does demonstrate that the riparian gap in this stream does seem to cause elevated, though spatially short-lived temperature maximums during the warm summer months. This is an example of the type of spatial and temporal analysis of stream temperature patterns that can be done using temperature times series.

1.4 Ideas on temperature effects – cooled, damped, or lagged?

Factors affecting steam temperature may interact in complex ways and although hyporheic exchange is known to have at least some effect on channel water temperature, in the past there have been relatively few studies examining the direct thermal interaction between the channel and the hyporheic zone. Comparing temperatures within the channel and the streambed at the same moment may lead to the erroneous view that they differ systematically from each other. Arrigoni et al. (2008) caution that taking instantaneous temperature measurements for the stream and the bed may lead to flawed results, but instead suggest examining the cycles occurring within the bed sediment, or hyporheic zone, as well.

In a study that investigated two reaches with extensive hyporheic zones within the Umatilla River, Oregon, Arrigoni et al. (2008) wanted to examine how the temperatures of hyporheic water differed from that of stream water, and hypothesized that hyporheic

water temperature cycles would be either cooled (or warmed, as evidenced by a difference in mean), buffered (had a difference in range), or lagged (denoted by a difference in phase) when compared to corresponding stream water temperatures (Figure 1.6). The larger purpose of this study was to determine whether water coming from locations of hyporheic discharge were responsible for the patterns of temperature diversity that were seen within channel water. The authors found that most areas of hyporheic discharge within the study reaches were dominated by relatively short hyporheic flowpaths (<100 m), and therefore closely resembled surface water temperatures, but were somewhat buffered and lagged; temperatures are not cooled compared to average surface temperatures unless they are affected by extremely long hyporheic flow paths and have lost that cyclical temperature pattern associated with surface waters and shallow sediments (Arrigoni et al., 2008).

An earlier study by Loheide and Gorelick (2006) used forward-looking infrared cameras to try to quantify groundwater discharge and hyporheic exchange in a stream based on their thermal signatures, and like Arrigoni et al. (2008) found that only areas associated with groundwater discharge (or perhaps a seasonal time lag) demonstrated a depression in temperature compared to channel temperature, whereas hyporheic fluxes seemed to have a time lag and buffering effect on temperature (Loheide and Gorelick, 2008). Because hyporheic waters are shielded from direct sunlight and air temperature effects, maximum temperatures do not tend to go as high, nor minimum temperatures as low as surface water temperatures (Burkholder et al., 2008).

The overall effect of hyporheic exchange on river temperature can vary widely depending on the system in question. For the Clackamas River, Oregon, Burkholder *et*

al. (2008), using a simple mixing model, found that although damping of hyporheic temperatures seems to be occurring and hyporheic and surface water temperatures are offset from each other, its impact on the daily river temperature cycle is minimal because of the large size of the river itself and the small fraction of water that hyporheic exchange actually contributes to this particular system. Damped and offset hyporheic temperatures will likely have a greater impact on smaller streams that have greater levels of hyporheic exchange occurring, and even at a larger scale where hyporheic discharge is not nominally affecting river temperatures, this exchange will still likely create some thermal heterogeneity that may be important for stream ecosystem health (Burkholder et al., 2008).

The main idea of the recent studies that show a buffering and lagging effect of temperatures during hyporheic exchange is that the hyporheic zone acts as a heat exchanger for stream water. Figure 1.7, taken from Burkholder et al. (2008), was the stimulus for thinking about how to model these exchange process. It shows the different processes that influence water temperatures as hyporheic water moves through a gravel bar. Of particular interest for this dissertation is the inset picture showing how heat exchange, through conduction, is occurring at the scale of the sediment particles. This part of the schematic was not explored much beyond stating that conduction occurs between sediment and water along hyporheic flow paths and that it is one of the important processes that transports heat within the hyporheic zone. There was no attempt in Burkholder et al. (2008) to calculate or estimate heat transfer rates or the importance of this process, however further investigation of this aspect of heat transport will lead to greater understanding of thermal exchanges in the hyporheic zone.

This dissertation is focused on improving our understanding of the spatial and temporal variation in stream water temperatures. Previous collaboration on two projects resulted in papers related to different factors that affect stream temperatures. One study designed a model (SHADE2) that uses stream characteristics such as stream azimuth, stream width, and canopy features (height, overhang, and height of maximum canopy overhang) to calculate a shading ratio at any time and location, and introduced a new field photographic technique for quantifying shade (Li et al., 2012). A sensitivity analysis was performed to test model parameters for the magnitude of their influence on the model, and found that tree height, canopy overhang, channel width, and latitude (for east-west facing streams) all had strong effects on the daily time series of shade, but that the height of maximum overhang was of little importance.

The second study was an analysis of local- and watershed-scale factors on summertime stream temperatures in the central Puget lowland of Washington State (Booth et al., 2014). Using extensive near-instantaneous temperature measurements collected during a 2-hour period in August in each of the years 1998-2001, and GIS-generated watershed-scale factors (total watershed area, and watershed percentages of urban development, upstream lakes, and permeable glacial outwash soils as an indicator of groundwater exchange), a determination of the relative importance of individual variables or sets of variables on determining stream water temperature was made. Through the use of Akaike's information criterion and temperature measurements from the most voluminous single year of data (1999), it was determined that percent outwash soils alone was the candidate model with the greatest support (Akaike weight of 0.44), perhaps refuting the idea that urban development is the most important determining factor

for summertime stream temperatures in certain regions. These previous studies have contributed to the understanding of some of the external causes of stream temperature variation, and this dissertation project allowed for a closer look at the influence of hyporheic exchange on water temperatures within both the channel and the hyporheic zone.

Within this dissertation, we further investigate the idea that hyporheic water temperatures are damped or buffered when compared to channel water and my goal was to explore the mechanisms by which this occurs. To do this, a set of laboratory experiments was completed, which examine how water temperature changes when it comes into contact with sediment of a different temperature and the temporal scale over which this occurs. Interestingly, it was found that conduction seems to occur almost instantaneously when water comes into contact with sediment of a different temperature, and may actually be an important term in heat transfer equations, where it often has been ignored as being insignificant for thermal variations in hyporheic exchange processes compared to larger magnitude terms such as advection and dispersion (Swanson and Cardenas, 2010), or only thought to be of importance at relatively low flow velocities, when advection becomes comparatively less significant (Hatch et al., 2006). In addition, two simple EXCEL models were developed to demonstrate this damping phenomena that seems to be occurring within the hyporheic zone, which may serve as a basis for the development of future models that will incorporate hyporheic exchange into water temperature and water quality models.

Figures

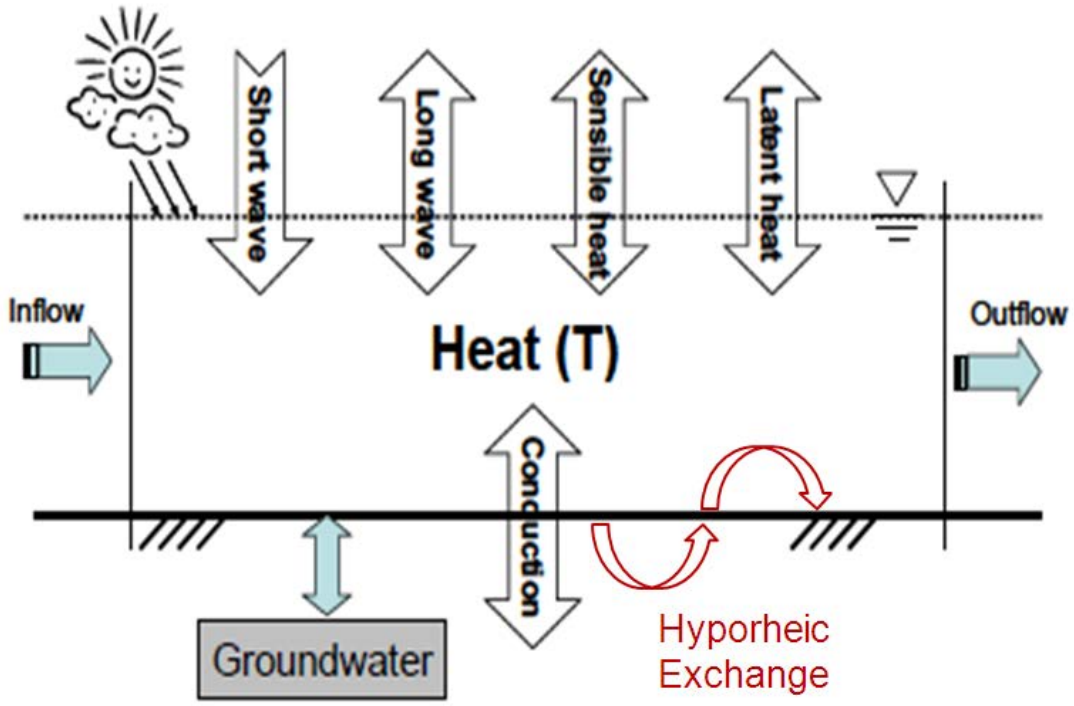

Figure 1.1: A conceptual model of a stream energy budget, taken from Li, 2006, with the addition of a hyporheic exchange term.

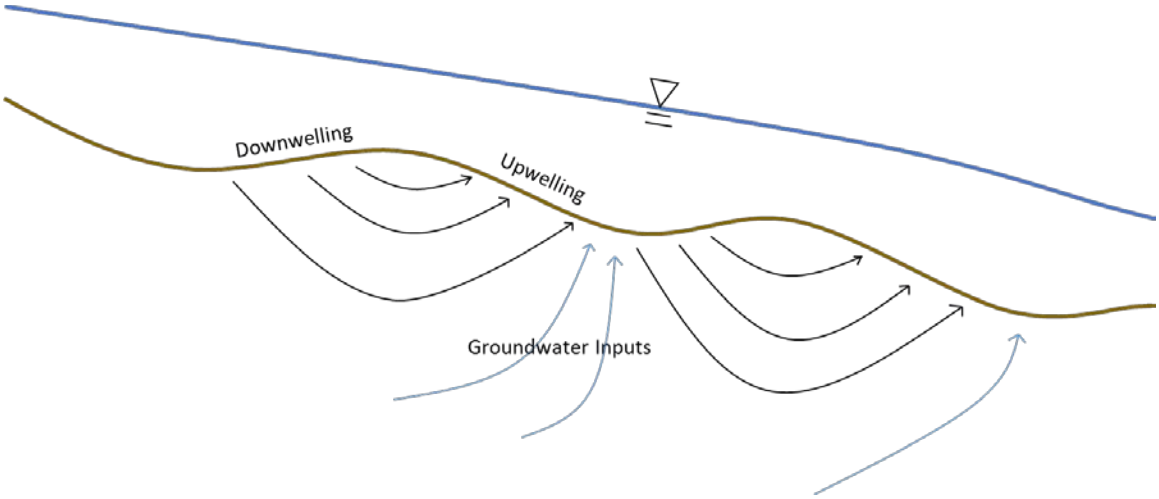

Figure 1.2: Conceptual diagram of how hyporheic exchange occurs in stream with pool-riffle-pool morphology. Temperature patterns within the hyporheic zone are affected by path lengths, gradients, conductivities, travel times, porosity, thermal capacity, thermal conductivity, and heat transfer rates.

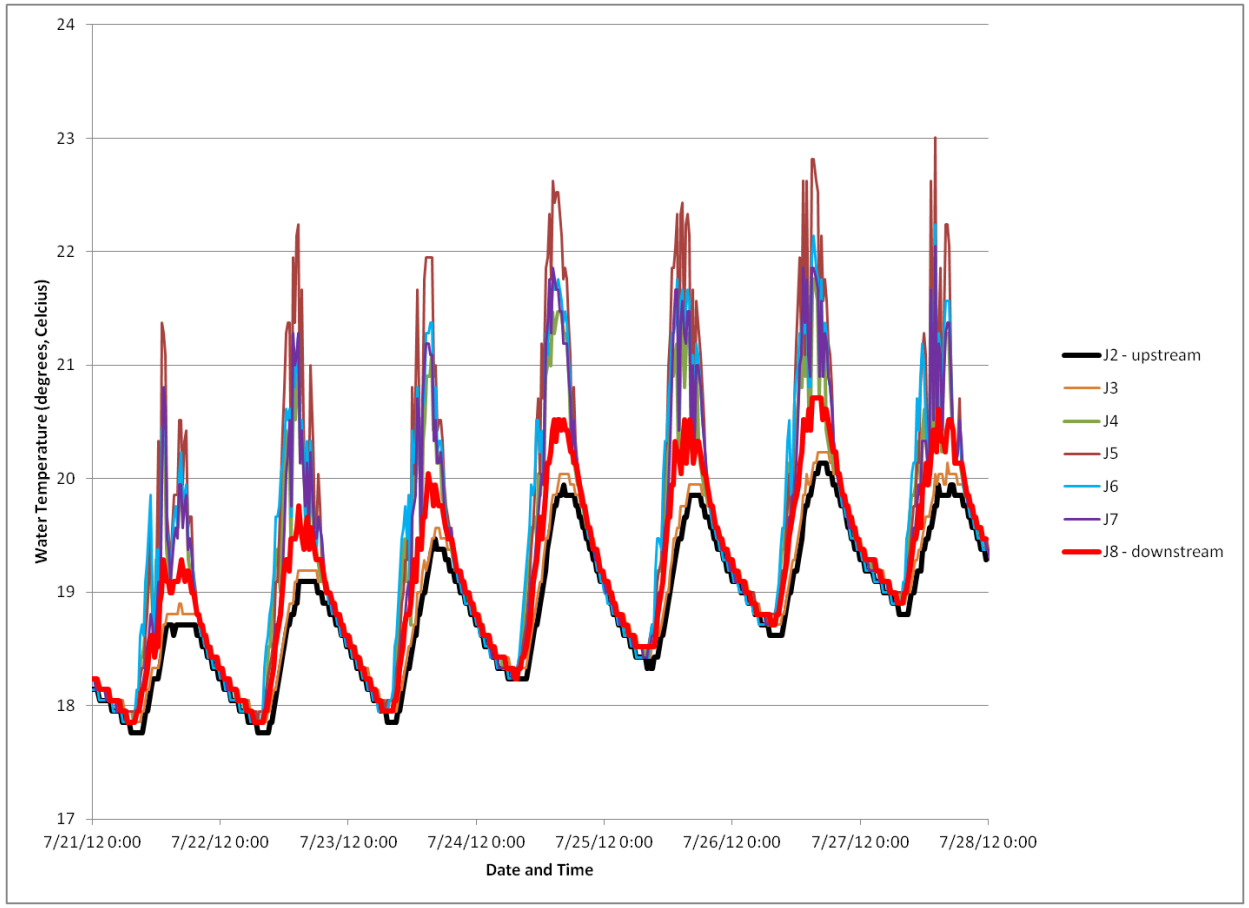

Figure 1.3: Shope Fork riparian gap stream temperature data, summer, 2012. Curves J2 through J8 represent the numbered temperature loggers placed in the stream, running sequentially from upstream to downstream.

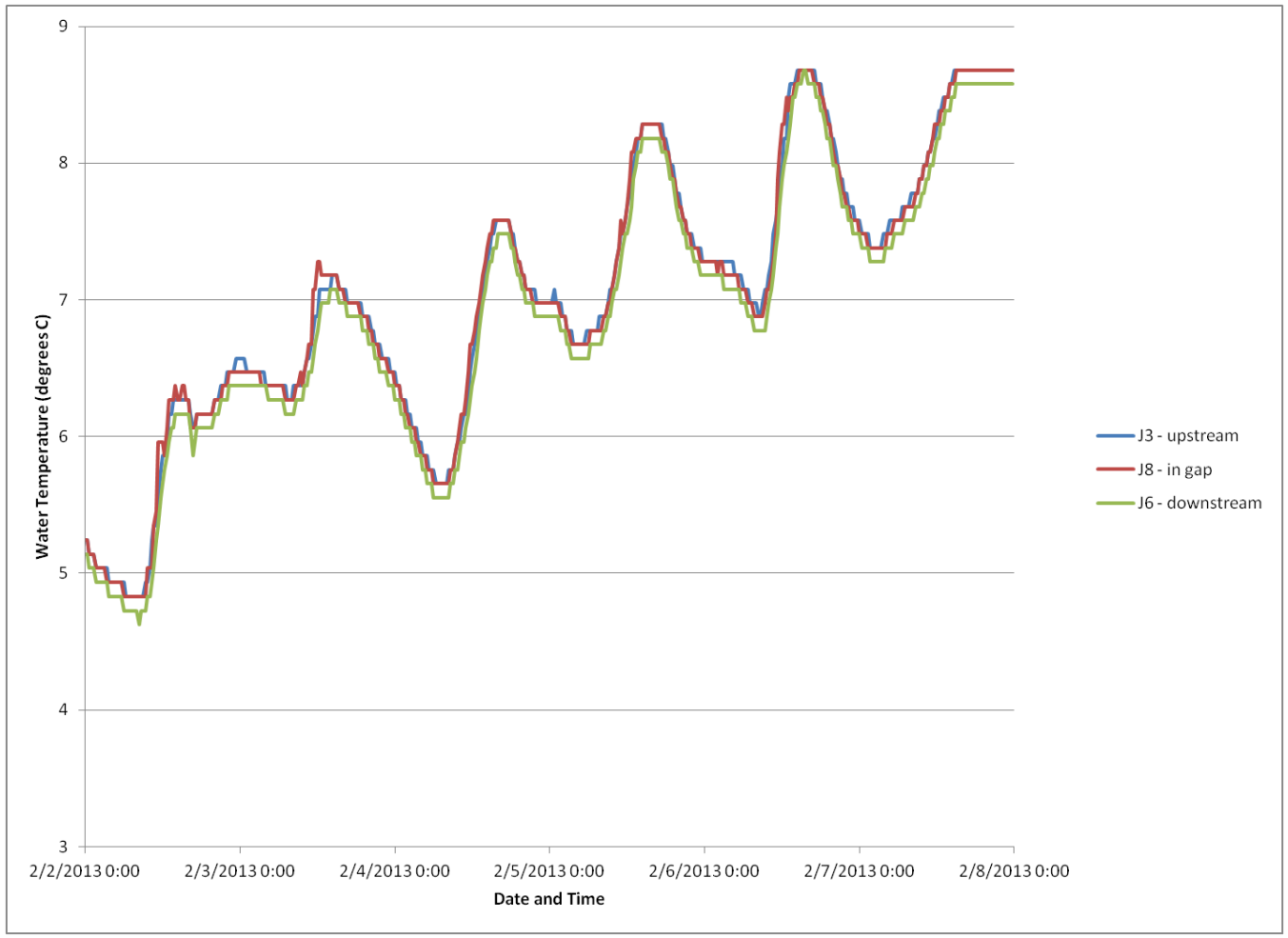

Figure 1.4: Shope Fork riparian gap stream temperature data, winter, 2014. J3, J8, and J6 represent temperature logger identification numbers.

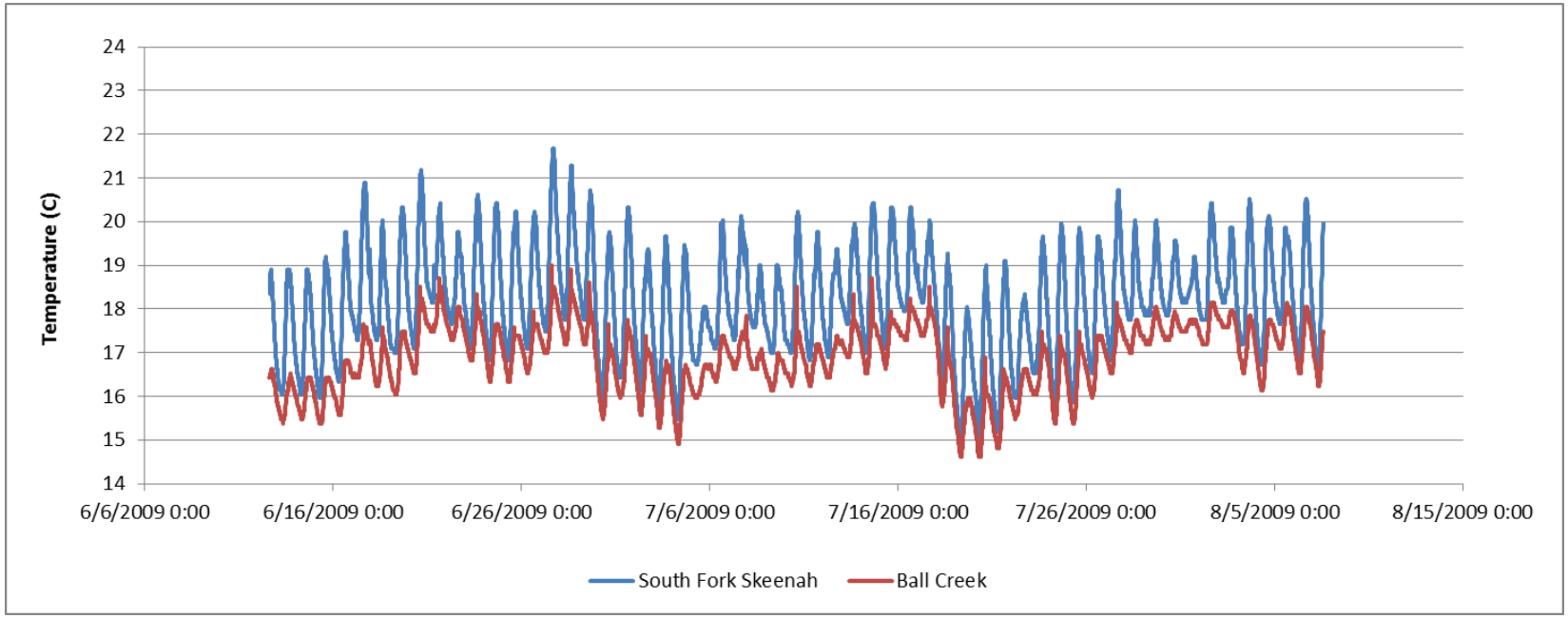

Figure 1.5: A time series temperature comparison of shaded and unshaded streams. Data from summer 2009 for shaded Ball Creek (red line) and unshaded South Fork Skeenah (blue line), located in North Carolina.

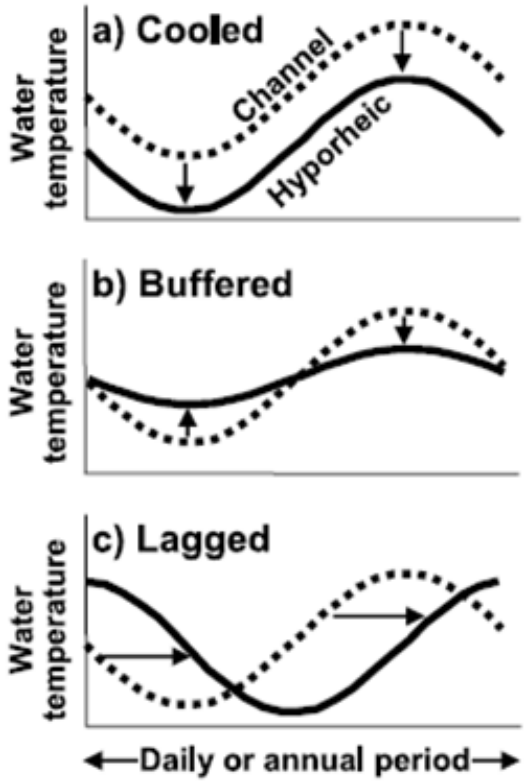

Figure 1.6: Diagram explaining the possible temperature patterns of the hyporheic zone compared to channel water (from Arrigoni et al., 2008).

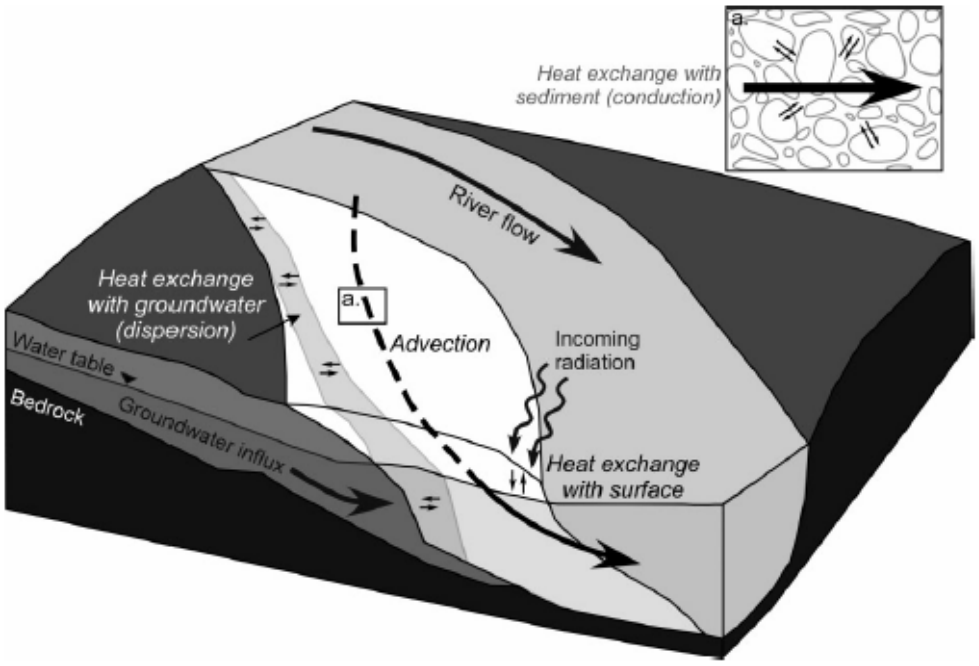

Figure 1.7: Conceptual diagram showing the processes that influence hyporheic water temperatures in a gravel bar (from Burkholder et al., 2008). The inset diagram demonstrates how heat exchange (conduction) occurs between the water and sediment of the hyporheic zone.

CHAPTER 2

LITERATURE REVIEW

2.1 Hyporheic flow and exchange

The term ‘hyporheic’ was coined in the late 1950s by Traian Orghidan, a Romanian hydrobiologist (Orghidan, 2010 – an English translation of the 1959 German version from *Achiv für Hydrobiologie*), but the concept had been studied, or at least acknowledged, in the decade or so before the publication of that seminal paper. The hyporheic zone can be defined as the region between the stream channel bed and the underlying groundwater aquifer where there are often spatially and temporally complex interactions occurring. This zone, however, may be defined in slightly different ways depending on the discipline (Smith, 2005). Some have tried to delineate the hyporheic zone based on chemical differences between channel water and groundwater (Triska et al., 1989), while others have based their designations on the type of aquatic invertebrates found there (Brunke and Gonser, 1999), but always with an understanding that these changes or shifts tend to be gradual, and that systems can be dynamic.

The hyporheic zone can also be thought of as an extension of the stream channel, where channel water flows down into the bed due to pressure gradient, flows for some distance in the interstitial spaces of the bed sediment and is then re-released back into the channel downstream. This exchange is important because water that has been in contact with these hyporheic sediments for extended periods of time will likely be changed in

some way, biologically, chemically or physically from original stream water inputs, and could have a significant effect on downstream channel water quality. It is a concept that is important in both the fields of hydrology and ecology because it connects groundwater and surface water systems, but in the past, its impact has been debated, as it tends to be so variable within and between stream networks (Wondzell, 2011).

The term 'hyporheic exchange,' although introduced rather early in the history of the field is not always applied when discussing similar processes to those mentioned above, and this differing terminology can be a source of confusion when examining the literature. Processes that are similar to, or have overlapping characteristics with hyporheic exchange can include intragravel flow (Vaux, 1968), referring to any flow within a porous streambed; transient storage (Bencala and Walters, 1983); surface-subsurface interactions (Acuña and Tockner, 2009; Jones and Holmes, 1996); and groundwater/surface water interactions (Conant, 2005; Silliman and Booth, 1993). Groundwater discharge into a stream may be mixed with advected channel water within the bed sediments, adding even more complexity to designations of water sources (White, 1993). These various terms are sometimes used in concert with hyporheic exchange, but may also be used alone. Although not all researchers use this term, likely due to the varied definitions of hyporheic exchange, overall, the concept does seem to be well studied and understood in the literature. The different ways of thinking about hyporheic exchange are often based on the motives of the study. For example, Conant (2005) was interested in how groundwater contaminant plumes might enter the stream, and therefore more concerned with direct flowpaths from the groundwater system or discharge that mixes groundwater with advected channel water rather than short hyporheic flow paths

that originate as channel water, whereas Cardenas (2009) focused on lateral hyporheic flux occurring in sinuous meandering rivers and had less of a focus on the effects of groundwater inputs.

In ecology, the hyporheic zone is most often thought of as an ecotone – an area of transition between two biomes, or distinct ecological communities (Gibert et al., 1990; Robertson and Wood, 2010). This ecotone differs from its surrounding environments in light and oxygen levels, flow velocities, thermal regimes, amounts of available food sources (Orghidan, 2010), and nutrient processing and detention (Robertson and Wood, 2010), with some aspects being more similar to surface waters and others more similar to groundwater. Often in nature, this type of transitional ecotone is found to have higher biodiversity than its two adjacent communities because it will likely be habitable for at least some organisms from both communities, but the hyporheic zone is unusual in that it seems to be a zone of intermediate biodiversity (Gibert et al., 1990) with decreased biodiversity when compared to the surface environment, and increased biodiversity compared to the groundwater system. This decrease in biodiversity from the above environment is most likely due to the decrease in oxygen and quantity of organic matter when compared to surface waters, which decreases more still within the groundwater (Gibert et al., 1990). In addition, organisms living within the groundwater system are highly specialized, and accustomed to specific conditions such as low oxygen concentrations and low current velocities, and even a slight increase in environmental variability may act as a barrier for organisms that are adapted to very stable conditions (Brunke and Gonser, 1997).

Hyporheic exchange can occur at various scales, from small-scale bedforms such as riffle-pool sequences or sudden drops in channel elevation, to larger scale exchanges due to channel sinuosity (channel meandering) and valley slope (Cardenas, 2009). Advective hyporheic exchange may not even occur at all if a stream has a straight channel with uniform slope and uniform bed materials, is directly underlain by bedrock, runs through an engineered channel (such as one underlain by concrete), or has bed sediments with a hydraulic conductivity so low that no appreciable amounts of water can actually pass through. Transition zones can also occur at the interface between terrestrial and aquatic ecosystems adjacent to stream systems, like floodplains (Gibert et al., 1990). It is common for short hyporheic flow paths to be nested within longer flow path networks (Poole et al., 2008), and this can add to the complexity of water discharging from the hyporheic zone into the stream (water in contact with hyporheic zone sediments for longer periods of time should differ more from the original downwelling channel water in both temperature and chemistry), as well as difficulty in tracing its source.

Interactions across hierarchical scales of both hyporheic exchange and the consequent biogeochemical processes that occur within sediments are still poorly understood, and as of now, there is little ability to extrapolate across scales (Boulton et al., 2010). The multiscale modeling and laboratory flume approach presented by Stonedahl et al. (2010) demonstrated that in the case of a naturally formed, weakly meandering stream that multiscale, three-dimensional hyporheic exchange is complex with interacting short (ripples) and long (multiple meander) flow paths. The authors argue that without specifying the correct boundary conditions that take into account fluxes occurring at a larger scale than a study reach, it will be difficult to adequately

model the hyporheic exchange processes occurring in most systems. However, the majority of hyporheic exchange is assumed to occur at a small or intermediate scale where pool-riffle-pool sequences dominate, as groundwater inputs tend to dominate headwater streams and advection dominates in the broader floodplains of larger rivers (White, 1993). Because hyporheic flowpaths lengths seem to scale accordingly with stream size (White, 1993), this intermediate reach scale may be the easiest scale to model and observe in real-time, and it is therefore a commonly studied scale in hyporheic flow research, although certainly there are likely to be interactions with varied hyporheic flow paths and discharges at this scale. The previously mentioned modeling study by Stonedahl et al. (2010) claims to be the first to confirm earlier, intuitively-made assertions by White (1993) and others that small-scale features (ripples) are, in fact, the dominant factor in driving interfacial flux in meandering streams.

The influence of hyporheic waters on the stream are often considered to be small due to the velocity differential between hyporheic waters and surface flow (Vaux, 1968), but depending on streambed and climatic characteristics, a large proportion of surface water can actually flow through the hyporheic zone in some streams (Fernald et al., 2001). For example, in the Sonoran Desert where sediments are highly porous, the volume of interstitial water can be up to 3-4 times that of the surface water, although this is highly dependent on discharge (Valett et al., 1990). In the Sonoran Desert area, during dry summer months, surface flow may be zero, with all water residing and flowing within the hyporheic zone (Valett et al., 1990). Even in wetter climates, the hyporheic zone can exert a large influence over streams and rivers. In the Willamette River in Oregon, when looking at flux patterns cumulatively over long river reaches (26 km), a large percentage

of total river flow may actually be passing through hyporheic pathways (Fernald et al., 2001).

Because it occurs on many interacting scales, amounts of hyporheic flow can be difficult to measure, but have been estimated through tracer studies (Fellows et al., 2001; Fernald et al., 2001; Wondzell, 2006) which can be scaled up for large reaches, or through purely mathematical estimations based on the hydraulic conductivity and longitudinal gradient of a river (Wondzell, 2011). However, Stonedahl et al. (2010) assert that simplified representations of stream topography do not characterize patterns and rates of hyporheic exchange adequately, and suggest a spectral scaling model that uses easily measureable characteristics such as channel planform morphology, bed morphology, sediment permeability, and average streamflow conditions. Because of the inherent complexity of interactions between co-occurring hyporheic flow paths, there does seem to still be some disagreement in the literature about the best way to estimate hyporheic exchange, especially at larger scales.

2.2 Ecological implications of hyporheic exchange

Hyporheic exchange is responsible for affecting many aspects of the stream system, including its biology, chemistry, and physical characteristics, including temperature (White, 1993). As a transition zone between two environments that is affected by external factors such as climate and rainfall events, the hyporheic zone is not easily delineated, and may shift spatially and temporally somewhat (Brunke and Gosner, 1997). Wondzell and Swanson (1996) found that although the overall pattern of subsurface flow changed little over the course of a year and seemed to be determined

mainly by bed forms within a 4th order stream in the western Cascade Mountains of Oregon, the proportions of that flow that were coming from either advected channel water or groundwater discharge changed among seasons and even during individual storms. In this case, rather than a shifting boundary of the hyporheic zone, the magnitude of flows seemed to remain moderately stable, but the relative fluxes of the different hyporheic water sources changed (Wondzell and Swanson, 1996). Here, whether or not the hyporheic zone expands or contracts may be based on terminology and the definition of the hyporheic zone or hyporheic exchange being used. Gariglio et al. (2013) found that the source of water in the hyporheic zone, whether originating from surface water or groundwater, can even vary spatially within a stream at the same moment, with interactions between stream flow and the streambed occurring near the center of the channel while interactions with groundwater are more common near the banks.

The hyporheic zone is subject to varying gradients of temperature, current velocity, nutrients, organic matter, and dissolved oxygen (Brunke and Gonser, 1997). Although distributions of temperature and some conservative chemical species like chloride and silica often resemble flowpaths of the water (in fact, temperature is often used as a flow tracer), more biologically reactive substances can become concentrated or reduced along the flowpath (White, 1993), and this has obvious implications for the associated ecosystems and any nutrient transport downstream. In addition, heterogeneity within the stream bed can affect patterns of water and nutrient transport. Gomez-Velez et al. (2014) found that low-permeability sedimentary layers (depending on their relative positions) can affect the geometry of the hyporheic zone and will likely act as a hotspots

for biogeochemical transformations by mixing younger hyporheic waters with older sequestered water and even older upwelling groundwater.

Many aquatic organisms inhabit the hyporheic zone for some or all of their life cycles. A diverse array of species, called the "hyporheos," live in the interstitial spaces within this zone and include many types of crustaceans, segmented worms, rotifers, water mites, and the juvenile stages of some aquatic insects (Boulton et al., 1998). These organisms can further be divided into species which complete their entire life cycles in the hyporheic zone (hyporheobiont species), hyporheophile species that sometimes migrate into the hyporheic zone and may include benthic organisms or stygobiont species (groundwater fauna), and species that obligatorily complete their larval stages in the hyporheic zone (amphibionts) (Brunke and Gonser, 1997). The hyporheic zone can also be utilized as refugia for benthic insects against strong currents, extreme temperature, and bedload movements (Brunke and Gonser, 1997). Density of hyporheic invertebrates seems to be most dependent on the amount of usable pore space and the ratio of particulate organic carbon to the total fine particulates, which indicates high assimilation efficiencies for detritivorous sediment feeders (Brunke and Gonser, 1999), but other factors that may be important include dissolved oxygen, fine inorganic particulate matter (which provide surfaces for biofilm development), and even season (Brunke and Gonser, 1999). Biofilms are a thin, superficial layer of bacteria, cyanobacteria, algae and fungi on fine sediment particles that are held in place by a polysaccharide matrix that they themselves secrete (Brunke and Gonser, 1997) and are a major food source for interstitial organisms.

The suitability of hyporheic interstices for certain organisms varies greatly among streams due to the variability in hyporheic exchange. The characteristics that control the amount of hyporheic exchange, and that are detailed in the next section, greatly influence the volume of and the speed at which water moves through the hyporheic zone, and this will have a big impact the processes that occur there. Photoautotrophic production does not occur within the hyporheic zone due to lack of light, and this has important implications for dissolved oxygen. Variations in oxygen content are due to factors like interstitial flow rates and hyporheic residence time, direction of flow and respiration rates within the sediment (Valett et al., 1990). The greatest oxygen depletion in the hyporheic zone occurs with the greatest contact time of water within that zone, and this can lead to systems that are periodically anoxic (Findlay, 1995).

In general, it has been found that streambeds act as sinks for DOC, oxygen, and ammonium, while nitrate shows a more complex relationship, which may be highly dependent on hyporheic velocities (Bardini et al., 2012). Increasing velocities imply a larger influx of solutes through the system as a whole, while at the same time decreasing the contact time for reactions to occur (Bardini et al., 2012). Flow into and through the hyporheic zone can also act as a filter, even for trace metals in mining-contaminated streams, as was demonstrated by Fuller and Harvey (2000) who found that uptake by Mn oxides within the hyporheic zone decreased metal loads between 12-68% in Pinal Creek, Arizona, depending on the metal. However, if organic or toxic contaminants are not adsorbed by these hyporheic sediments, the hyporheic zone can actually act as a passageway for the contamination of groundwater in influent reaches (Brunke and Gonser, 1997).

Beyond organisms living in or adjacent to the hyporheic zone and within the bed sediment, exchange processes can also affect aquatic organisms living in the stream channel. Although much of the nutrient flux in a river system occurs within the channel flow, there are many biological, hydrological, and chemical processes that slow this flow – this is known as hydrologic retention (Morrice et al., 1997). Exfiltrating, or upwelling water may have some benefits for aquatic species including enrichment in nutrients due to mineralization occurring within the hyporheic zone, it may be a different temperature from the stream water and act as a refugia that is cooler in the summer and warmer in the winter. Exfiltration may even prevent siltation, which may be important for species that require sediments with a high dissolved oxygen content, such as lithophilous fish who use sediments for spawning, however, upwelling zones are often associated with lower dissolved oxygen levels than other parts of the stream (Brunke and Gonser, 1997).

Locations of downwelling and upwelling strongly influence spawning site selection for fishes such as salmon, trout, and charr (Poole et al., 2008), with Chum salmon choosing spawning sites where warmer hyporheic water upwelled into streams (Geist et al., 2002). Bull trout were shown to select hyporheic discharge zones for spawning sites when low stream gradient was a covariate, but downwelling sites at the pool-riffle scale where there is high intragravel flow rates and a more constant supply of oxygen (Baxter and Hauer, 2000). These examples suggest a complex relationship between hyporheic exchange and the spawning behavior of different species of fish. Hyporheic exchange is often thought of as ecologically significant because it both creates temperature diversity and moderates both diel and annual temperature cycles in surface and subsurface habitats (Arrigoni et al., 2008), however recent research suggests that

factors formerly thought to be important for the dissolved oxygen regime of salmonids spawning sites, including the accumulation of fine sediment and thermal regime, are actually dwarfed by the effects of lower dissolved oxygen levels contributed by upwelling groundwater (Sear et al., 2014).

There is a newfound understanding in the literature that hydrologic measurements of surface water, groundwater and their interactions are vitally important in ecological studies of the hyporheic zone (Stanley and Boulton, 1993). A study comparing the hyporheos of two widely varying stream systems (the Rhône River, a highly regulated European river; and Sycamore Creek, a small, spatially intermittent desert stream), demonstrated that there were strong similarities, especially in longitudinal changes in hyporheic assemblage structure, which is associated with the transition from an upwelling to a downwelling zone (Stanley and Boulton, 1993). Understanding the direction of movement during hyporheic exchange processes can give important information about the type of biotic processes that are likely occurring there. For example, due to differing dissolved oxygen levels, downwelling zones may be more conducive to aerobic processes, such as respiration and oxidation reactions like nitrification, and upwelling zones will likely be more conducive to anaerobic processes, such as denitrification and ammonification (Hendricks, 1993). There is clearly something that is held constant between hyporheic zone processes across varied systems, and these can be better studied by understanding and incorporating the hydrology of these systems.

2.3 Factors controlling the amount of hyporheic exchange

In addition to external factors including seasonal variation in rainfall, and its effects on recharge and discharge (Wroblicky et al., 1998), the direction and duration of water flow through the hyporheic zone is highly dependent on streambed characteristics, most importantly the depth of the porous streambed (determined by geological constraints), hydraulic conductivity, and the pressure gradient. Hydraulic conductivity is a measure of how easily water moves though a soil or other media, and it is influenced by the size and shape of sediment particles as well as the interconnectedness of the pore spaces, or permeability. The pressure gradient, or hydraulic gradient is determined by head differences between two points, divided by the distance between the points.

Movement of water through the porous hyporheic zone of bed forms occurs through two processes: pumping and turnover, as described by Elliot and Brooks (1997). Turnover occurs when moving bedforms trap and release interstitial water, and pumping occurs when acceleration of stream flow over bed forms gives rise to spatial variations in pressure, which induce flow into and out of the bed. An easy way to conceptualize this idea of water movement during hyporheic exchange is by considering the hyporheic flow though the commonly studied pool-riffle sequence (Figure 2.1), which is caused by discontinuities in the slope of the streambed. As the stream depth decreases and the channel bottom becomes concave at the head, or upstream end of a riffle, pressure is increased and water is advected into the bed sediment (downwelling). Return flow, or upwelling then occurs when the bed becomes convex in the downstream direction, channel depth again increases and pressure decreases, and hyporheic water is released back into the stream.

However, hyporheic flow may be much more complex than this due to inherent heterogeneity of streambed sediments and within a reach there may be exchange paths of different lengths, directions, and velocities (Boulton et al., 1998). Exchange can also be influenced by groundwater recharge, large-scale variations in bed topography, such as bends, bank storage, preferential flow paths due to heterogeneity of the bed materials, and even small-scale and rapid exchange near the surface due to turbulent pressure fluctuations (Elliot and Brooks, 1997). It may have been thought that hyporheic exchange fluxes would be different between gaining and losing streams, but evidence from a laboratory flume experiment showed that actual exchange fluxes do not change based on differences in these types of flow conditions (Fox et al., 2014). Hyporheic exchange is inherently three-dimensional in character and is controlled by subsurface heterogeneity, geomorphology, and channel hydraulics (Cardenas, 2009).

Conant (2005) introduced a more complex conceptual model of hyporheic exchange, in that it takes into account the different sources of upwelling water and the bed sediment characteristics that make each type of flow possible, and was perhaps the first conceptual model to take into account the magnitude of the fluxes (Figure 2.2). This study found that streambed topography did not actually result in very much recharge and hyporheic zone mixing, nor did it seem to have much determination on discharge location. The model focuses on vertical movement of water into and out of the bed sediment rather than any horizontal or longitudinal water movement, however, purely vertical flow should not need to be assumed when estimating vertical fluxes (Cranswick et al., 2014). In Conant's (2005) model, the streambed is conceptualized as a mosaic of zones, some being no-discharge or recharge areas, and others being dominated by one of

three types of discharge: high, medium or low, or short-circuit discharge. Short-circuit discharge refers to localized points of extremely high discharge, such as might occur with artesian springs. High discharge areas also release groundwater directly to streams, but these flowpaths are determined by high conductivity deposits, and can be caused by large topographic changes in the streambed such as deep pools at the end of riffles. Areas of low to moderate discharge tend to have temperatures that fall in between groundwater and surface water temperatures, and they are by far the most common type of discharge measured in this stream system (Pine River, Angus, Ontario, Canada). Although streambed topography was not found to influence the location of these zones, geologic variations at depth and streambed sediment characteristics were clearly having a strong effect (Conant, 2005).

The relative size of the hyporheic zone is inversely proportional to stream discharge, likely due to the fact that longitudinal gradients change systematically with stream size, with smaller headwater streams having steeper gradients than do larger streams (Wondzell, 2011). The ratio of the total channel water that flows through the hyporheic zone, in small streams with low discharge, may actually be very large with turnover lengths (the distance over which the entire in-channel flow enters the hyporheic zone and is replaced by upwelling water) that can be as short as 50 meters, compared with larger streams lower in the watershed which may have turnover lengths as long as 77 km (Wondzell, 2011). The amount of hyporheic flow can also change due to climate or weather factors. Wondzell (2011) found that the ratio of hyporheic flow to total stream flow decreased in wet seasons or during storms as total stream discharge increases. In addition, the size of the hyporheic zone may be constrained by depth to the

bedrock, or even the presence of low-permeability sedimentary layers within the hyporheic zone or streambed (Gomez-Velez et al., 2014) because as a prerequisite for hyporheic exchange to occur, surface water must be able to flow through porous media within the streambed.

2.4 Inclusion of hyporheic exchange on water temperature and water quality modeling

Water temperature modeling in the past tended to focus on the streams interaction with the air or solar radiation as the overriding factors rather than interactions with, or processes occurring within the bed sediment. In some cases, a simplistic linear regression model between stream temperature and air temperature has been used predict water temperature (Crisp and Howson, 1982), with as high as 86-96% of stream temperature variance being explained by air temperature alone (when above 0°C). These types of models are useful for studying the effects of climate change and are often used in General Circulation Models because they are fairly accurate compared to other climate variables and have the added benefit of requiring only one input (Mohseni and Stefan, 1999), but they lack the specificity needed when examining and modeling individual stream systems. Air temperature can be considered an index for the net heat budget affecting the stream, the same as the Thornthwaite formula uses air temperature as a surrogate for the heat budget affecting potential evapotranspiration. Ironically, energy budget analyses of stream temperatures indicate that sensible exchange with the air is a minor part of the stream energy budget (Brown, 1969). Stream shading has also historically been an important variable when modeling stream temperatures (Rutherford

et al., 1997), and many modeling studies have been done on streams and watersheds subject to forestry practices and harvesting (Hewlett and Forston, 1982) to predict the effect that increased solar radiation reaching the stream surface will have on water temperatures.

When examining subsurface interactions, stream temperature models of the past have often included variables like groundwater discharge into the stream (Brown, 1969; LeBlanc et al., 1997), or the vertical temperature gradient of the streambed (Rutherford et al., 1997; Sinokrot and Stefan, 1993), but little has been included on hyporheic exchange processes. However, as these processes become better understood, they are beginning to be included in, or at least acknowledged as important for modeling studies. Using a steady-state, one-dimensional water quality model, and a new method for directing field sampling efforts to reduce model output variance called 'quantatively directed exploration' or 'QDE,' Supriyasilp et al. (2003) found that in a stream where hyporheic exchange is present, although local loading was the largest contributor to the total prediction variance, parameters related to the hyporheic zone were also shown to be contributors. In a 2011 study in British Columbia, Canada, Leach and Moore (2011) analyzed summertime stream temperature variability in two hydrogeomorphically distinct reaches, and a Lagrangian approach was used to model the system. The two reaches were found to be subject to similar surface heat inputs, but they exhibited differing stream temperature dynamics suggesting that either surface/subsurface interactions and/or bed heat conduction were important, although these interactions could not be measured directly. The authors found that in the upper sub-reach of the study area, the heat budget was modeled fairly accurately without the inclusion of subsurface inflow or bed

conduction, but in the lower sub-reach, stream temperatures could only be modeled with any accuracy when subsurface exchange was treated as a two-way flux. A 2006 modeling study by Kazezyilmaz-Alhan and Medina re-worked an earlier and commonly used transient storage model for simulating solute transport introduced by Bencala and Walters (1983), to include a new storage zone representing the hyporheic zone, which can be of varying thickness - the earlier modeling study had lumped the surface storage and hyporheic zone together in a single storage zone. Kazeyilmaz-Alhan and Medina (2006) suggest that the addition of this new zone, representing hyporheic transient storage, in dynamic stream water quality models would allow the simulation of damping effects that occur through interactions with the subsurface.

In one of the few modeling studies which explicitly takes into account heat transfer processes in the hyporheic zone, Loheide and Gorelick (2006) present a method to quantify both groundwater discharge and hyporheic exchange using detailed stream thermal signatures. Through a combination of aerial thermographic imagery and instream temperature measurements, thermal profiles were modeled using a one-dimensional energy budget/transport model, which included meteorological conditions, riparian shading, and other stream characteristics. The middle sub-reach in this study displayed buffered temperature and resulted in lower daily maximum temperature when compared with the upper and lower sub-reaches of Cottonwood Creek, indicating that increased baseflow and hyporheic exchange were more prevalent in this sub-reach (Loheide and Gorelick, 2006). In addition to lower maximum temperatures, the daily maximum temperature also occurred about two hours later in the day when compared with the other sub-reaches, suggesting not only a buffering, but also a lag in temperatures

in stream segments with hyporheic exchange (Loheide and Gorelick, 2006). Although the Loheide and Gorelick (2006) study was a large step forward in understanding how hyporheic exchange may affect stream temperatures, they state that their model-based estimates of hyporheic exchange were confounded because a number of different processes, including heat transferred by water flowing between the stream and the hyporheic zone, or by water flowing from the stream to "stagnant zones" within the channel, and heat conducted between the stream and the bed sediment, which may all have had equivalent buffering effects on temperatures, cannot be separated through this type of analysis .

In a more recent study that also explicitly takes into account hyporheic heat transfer processes, Marzadri et al. (2013) looked at heat transport resulting from complex flow patterns through a three-dimensional semi-analytical process-based model, specifically focusing on the pool-riffle bed form, rather than the more commonly used one-dimensional heat transport model (e.g. Loheide and Gorelick, 2006). This model was verified using summertime surface water and hyporheic water temperatures measured at Bear Valley Creek, Idaho. Results were best at shallow depths and when profiles along the center of the channel are examined, but showed that advection and longitudinal diffusion were the main mechanisms controlling the temperature distribution within the hyporheic zone. Like previous studies, the Marzadri et al. (2013) model revealed that upwelling water is characterized by a time lag and attenuation when compared to in-stream temperatures, whereas downwelling temperatures are the same as that of stream water. Attenuation is most evident in the deeper and slower hyporheic flows associated with large low-gradient streams, when compared with the shallow flow

fields associated with small streams – these effects are still apparent, but just smaller. (Marzadri et al., 2013).

Menichino and Hester (2014) used a computational fluid dynamics model to determine the effect of varying hydraulic conductivity across as range of sediment sizes on temperature dynamics and hydraulics within the hyporheic zone in another recent example of researchers overtly examining heat exchange though the hyporheic zone. This study demonstrated that both downwelling and upwelling temperatures showed cyclic diel patterns, and that these patterns were more similar to surface water as hydraulic conductivity increased. Using this model, Menichino and Hester (2014) also found that at low hydraulic conductivity, conduction was the dominant heat transfer mechanism, and advection became the overriding factor as hydraulic conductivity increased. Overall, there does seem to be movement in the literature towards an understanding that hyporheic exchange is important for stream temperature and water quality, but as of now there are only a few water quality and water temperature models that include hyporheic processes and fluxes as inputs.

The basic concepts behind hyporheic exchange have been well characterized within the literature, and conceptual models such as those presented by White (1993) and Boulton et al. (2010) are well accepted, however, because of the difficulties met when trying to measure these processes in the field, they are only rarely included in overall stream water temperature or water quality models. Even though hyporheic exchange is known to be ecologically significant, and important for water quality in some cases, this inability to adequately quantify hyporheic exchange also leads to problems when using

concepts involved in, or models using these exchange processes to make real-world decisions about stream management and restoration.

Figures

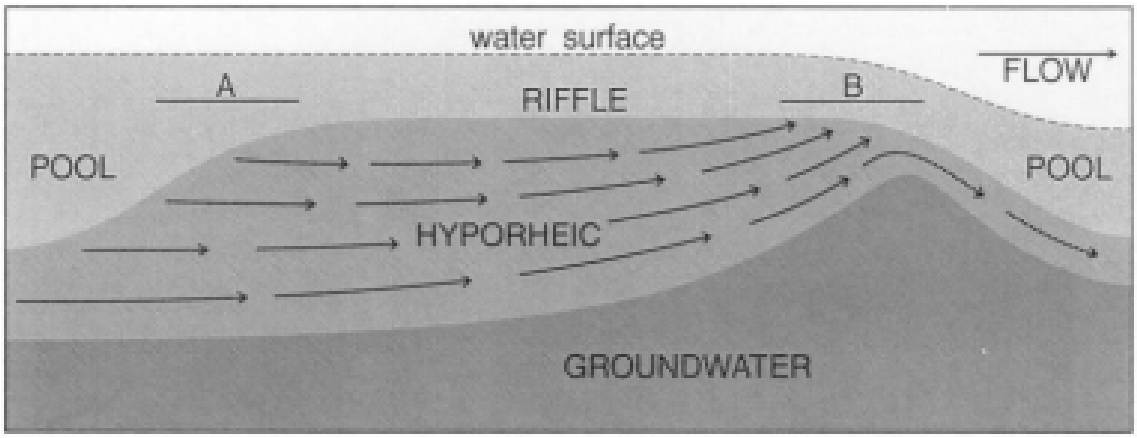

Figure 2.1: Conceptual longitudinal model of a pool-riffle-pool sequence (from White, 1993).

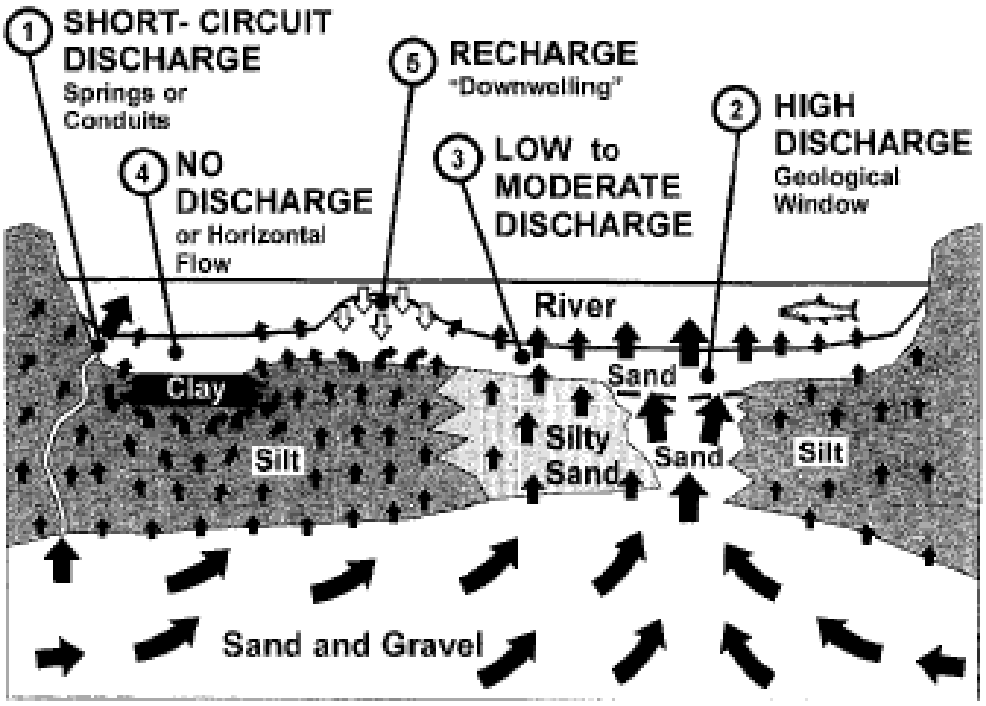

Figure 2.2: Conant's (2005) conceptual model showing different directions and magnitude of hyporheic flowpaths and sediment characteristics.

CHAPTER 3

THERMAL AND HYDRAULIC CHARACTERISTICS OF STREAM SUBSTRATES RELEVANT TO HYPORHEIC TEMPERATURE EXCHANGE

Movement of stream water from the channel, through the hyporheic zone, and back into the channel, is associated with heat exchange processes. This heat exchange alters the spatial distribution of temperatures within the channel, and has the capability to alter the diurnal temperature time series as well. The extent of this change depends on both the contact time with bed sediments and the thermal exchange characteristics of that sediment. This chapter will present information on typical reported characteristics of streambed and hyporheic sediments in order to inform a discussion about the mechanisms that may be responsible for temperature changes within the hyporheic zone.

Following the largely unexplored conceptualization of Burkholder et al. (2008), we are going to assume that the hyporheos acts as a heat exchanger for water moving from the stream, to the substrate, and back. As established in Chapter 1, the mean temperature of the hyporheos is generally the same as the mean temperature of the stream. Stream temperature time series feature seasonal and diurnal fluctuations driven largely by the time series of solar radiation, and although overall temperature ranges in the hyporheic zone are the same as stream water, Burkholder et al., (2008) and Arrigoni et al., (2008) demonstrated that the timing of maxima and minima within the temperature time series of the two system components is offset from each other. To understand and

have the potential to model hyporheic heat exchange between water and sediments, we must be able to answer the following relevant questions:

1. What are the ranges and likely values of sediment porosities and densities?

2. What are the ranges and likely values of sediment hydraulic conductivities through the hyporheos?

3. What are the ranges and likely values of path lengths and velocities for hyporheic flow?

4. What are the ranges and likely values of sediment specific heats and thermal conductivities?

5. What are the bulk heat transfer rates between sediments and water, and are these transfer rates dependent on sediment size class?

In this chapter, I will collect and synthesize reported literature values of hyporheic flux properties and the thermal conductivities and specific heats of several different types of bed sediments. I will also introduce, describe, and report upon lab experiments that examine time scales of conduction processes between water and sediment of differing temperatures. We hypothesize that complete heat transfer (to equilibrium temperatures between sediment and water) will occur on the scale of hours, and that heat transfer will be most rapid for particles with the largest surface area to volume ratio. These experiments, combined with known attributes of thermal exchange process associated with hyporheic flow, will act as a foundation on which to base some simple modeling experiments that will be introduced and developed in the next chapter in order to demonstrate how heat exchange may be occurring in the hyporheos.

3.1 Sediment porosities and densities

Streambed sediments display varying degrees of heterogeneity, and this can make estimation of sediment properties very difficult. In this and the following section, I will define the primary sediment characteristics that are important for understanding how water moves through and thermally interacts with hyporheic zone sediments. Then, a range of values for these different properties will be presented, obtained from a thorough review of the literature. Porosity of sediments refers to the fraction of void spaces within the total sediment volume, and can be affected by the ways in which sediments are packed, the shapes of the grains, and the size distribution of particles present in the sediment (Fetter, 2001); it is a determining factor in how much water the hyporheic zone can hold, and can affect how quickly water can be transported through this zone. For example, the porosity of a sediment will be lowered if it contains a mixture of different grain sizes, as smaller particles will fill in the void spaces created by the larger particles (Fetter, 2001); the smaller the pore size between sediment particles, the more slowly the water will move through it. Porosity within the hyporheic zone is quite variable (Table 3.1), with values generally falling between 0.2 and 0.6.

Bulk density is a property that is closely related to porosity, but also takes into account sediment particle densities. Bulk density refers to the dry mass of sediment per unit volume of the sediment and therefore considers both the solid and the void components of a sediment. Both porosity and bulk density of a sediment can be calculated if you know or can estimate the value of the other, using the following equation:

$$n = 1 - \frac{BD}{PD} \qquad \text{(Equation 3.1)}$$

where n is the porosity, BD is bulk density, and particle density (PD) refers to the actual density of the solid rock materials within a sediment or soil. Most sediment particles have quartz as a primary component, so if no information is available on the particle density of a given sediment, 2.65 g/cm^3 (the particle density of quartz) is assumed for purposes of using this equation.

Bulk densities will tend to fluctuate spatially within the hyporheic zone due to the inherent heterogeneity of the streambed, but the literature shows that there is a general trend of increasing bulk density with depth (Table 3.2). This trend is likely due to compaction caused by the weight of overlying sediments, a phenomenon that is also associated with decreased porosity. Bulk density and porosity inherently have an inverse relationship - as porosity decreases, bulk density increases; sediments with low porosity will have fewer void spaces, and therefore more mass within a given volume. This implies that hyporheic sediments with low porosity (few pore spaces) will be able to hold less water overall than hyporheic sediments with high porosity (many pore spaces). Table 3.3 shows porosities and calculated bulk densities for sediments comprised of various particle sizes (based on Table 12.1.2 from Shen and Julien, 1993), which range from 1.48 g/cm^3 for fine sand to 2.1995 g/cm^3 for coarse gravel and boulders. The bulk densities in this table were calculated from reported porosities using the above equation and a particle density of 2.65 g/cm^3. These bulk density values were shown to steadily increase with particle size. Bulk densities for hyporheic sediments are not often mentioned in the literature, but Table 3.4 lists some reported values for sand and gravel (although no size ranges given), which demonstrate values similar to those in Table 3.3,

and range from 1.36 – 2.25 g/cm^3, with gravel generally having a higher bulk density than sand.

3.2 Hyporheic hydraulic conductivities

The hydraulic conductivity of a porous media is defined by the specific flux rate of groundwater flow under a unit hydraulic gradient (a hydraulic gradient equal to one). This hydraulic property is a proportionality constant in Darcy's Law below:

$$Q = -KA\left(\frac{dh}{dl}\right) \qquad \text{(Equation 3.2)}$$

where Q is the discharge or flow, K is the proportionality constant (hydraulic conductivity), A is the cross-sectional area, dh/dl is known as the hydraulic gradient (dh is the change in head between points that are a distance of dl apart from each other). The negative sign in this equation indicates that water will always flow in the direction of decreasing hydraulic head. Discharge has the dimensions of volume/time. Darcy's Law can also be rewritten as,

$$q = \frac{Q}{A} \qquad \text{(Equation 3.3)}$$

where q = Q/A, and is known as the Darcian flux, which is the discharge per unit area. Darcy velocity has the dimensions of length/time, although it is not considered to be a true velocity because the cross-sectional area referred to in the equation is partially blocked by soil particles (Fetter, 2001). The actual velocity that water moves through the pore spaces within sediments is known as the pore velocity and can be calculated as the Darcy velocity divided by the porosity.

Conceptually, the hydraulic conductivity is a measure of how easily water moves through a permeable medium. The magnitude of the hydraulic conductivity is dependent upon total porosity, pore-size distribution and pore connectivity, or continuity (Rawls et al., 1993), but also on fluid properties such as density and viscosity, which are temperature dependent. Hydraulic conductivity is closely related to permeability, which is a function of the size of pore openings and the size of the sediment grains (Fetter, 2001). Smaller sized sediment grains have a larger surface area that the water can contact, which increases frictional resistance to flow and reduces intrinsic permeability. Well sorted grains will have a higher permeability than poorly sorted materials because, as mentioned earlier, finer materials can fill voids between larger particles, creating smaller voids with more surface area. Hydraulic conductivity can be measured or estimated in a variety of ways, including instream methods like slug tests (Morrice et al., 1997; Wondzell and Swanson, 1996), minipiezometers (Baxter et al., 2003), and tracers, like heat (e.g. Hatch et al., 2010), as well as numerical modeling (e.g. Yager, 1993), and there are even methods of hydraulic conductivity estimation based on grain-size analysis (Song, et al., 2009).

The hyporheic literature seems to split hydraulic conductivities into two separate, but closely related system segments – the hydraulic conductivity at the interface between the stream and the sediment, and the hydraulic conductivity within the hyporheic zone itself; the former controlling how water moves into the bed or hyporheic zone, and the latter controlling how it moves within this zone. Calver (2001) gives a thorough review of reported river channel-lining sediment permeabilities, and found that hydraulic conductivities of these materials ranged from below $1.0x10^{-9}$ to over $1.0x10^{-2}$ m/s, with

the majority of values falling between $1.0x10^{-7}$ and $1.0x10^{-3}$ m/s. Figure 3.1 is borrowed from Calver (2001) and shows the range of hydraulic conductivity values collected from various sources, including unpublished personal communications with other scientists. It is apparent from this data that hydraulic conductivities can be highly variable, ranging over orders of magnitude, even within the same study system. Table 3.5 lists hydraulic conductivity values for hyporheic zone sediments reported in the literature, rather than values only for bed-lining sediments. Not surprisingly, these values, which range from $6.9x10^{-7}$ m/s to $2.0x10^{-4}$ m/s, are generally in line with the range of common hydraulic conductivities collected by Calver (2001). Because hydraulic conductivity denotes how easily water can move through hyporheic sediments, it is one of the indicators of how long water will be in contact with these sediments.

Travel time is an important concept for understanding interactions within the hyporheic zone because travel time describes the contact time between the water and sediment. An equation for travel time can be formulated by relating the concepts of Darcy velocity and pore velocity. Darcy velocity (V_D) has the units of length per time, and can be calculated by the following equation:

$$q = -K\left(\frac{dh}{dl}\right) \qquad \text{(Equation 3.4)}$$

where the negative sign denotes the direction of flow from high head to low head. As mentioned earlier, Darcy velocity does not represent the true velocity because it doesn't take into account the portion of the cross-sectional area that is blocked by sediment. Pore velocity (V_P), however, does take this into account, and is calculated by dividing the Darcy velocity by the porosity:

$$V_P = \frac{q}{n} \qquad \text{(Equation 3.5)}$$

where n is the porosity. Both Darcy velocity and pore velocity have the dimensions of length per time, and the pore velocity equation can be rearranged to solve for the Darcy velocity,

$$V_D = V_P n = \left(\frac{L}{t}\right) n \qquad \text{(Equation 3.6)}$$

and the two solutions for Darcy velocity can be equated:

$$\left(\frac{L}{t}\right) n = K\left(\frac{dh}{dl}\right) \qquad \text{(Equation 3.7)}$$

This equation can be rearranged to solve for time (travel time):

$$t\ (travel\ time) = \frac{nL}{Ks} \qquad \text{(Equation 3.8)}$$

where s is channel slope, and will be used in place of the hydraulic gradient (dh/dl) for the purposes of the following calculations.

Travel time can be thought of in a number of ways. For example, "characteristic travel time" (T_C) would be the time it takes for water to travel one meter under a unit gradient, and can be calculated as,

$$T_C = \frac{n}{K} \qquad \text{(Equation 3.9)}$$

And a "unit travel time" (T_U) would be the time it takes to travel one meter:

$$T_U = \frac{n}{Ks} \qquad \text{(Equation 3.10)}$$

By using typical ranges of slope and characteristic travel time, one can examine how unit travel time may vary in characteristic hyporheic systems. As mentioned earlier, the majority of reported hydraulic conductivity values falls within the range of 1.0×10^{-7} and 1.0×10^{-3} m/s (Calver, 2001), and porosity values range from 0.2-0.6 (Table 3.1), so it is likely that characteristic travel times (n/K) will fall within the range of 600 – 2,000,000

seconds. Dade (1998) found that estimates of channel slope range from 10^{-5} to 10^{-2}. Figure 3.2 is a 3D graph of unit travel time as a function of these typical ranges of slope and characteristic travel time. This graph demonstrates that as slope decreases and characteristic travel time increases, unit travel time will increase. The shortest unit travel time calculated based on ranges of s and T_C was about 17 hours to travel one meter, and if these unit travel times are expanded to typical hyporheic flow path lengths, for example 1 – 100 m, then it becomes clear that travel times, and therefore contact times between hyporheic water and surrounding sediments, will likely be very long (e.g. it will take 340 hours for water to travel 20 meters, and 1700 hours for that same water to travel 100 m based on even the shortest calculated unit travel time).

3.3 Hyporheic path lengths and velocities

Hyporheic flow path lengths and velocities are important for understanding heat exchange in the hyporheos because they indicate how long waters flowing through the hyporheic zone are in contact with sediments, and therefore how long they have to interact with or be affected by the thermal properties of those sediments. Hyporheic flow path lengths can be highly variable and dependent on the same factors that control the amount of exchange that occurs - the hydraulic conductivity of the substrate, pressure gradients, and the depth to the bedrock. There is generally an increase of flow path length with increasing basin area due to the increased spacing, size, and importance of channel unit and morphologic features (Anderson et al., 2005), however, there seem to be few field studies that have directly measured flow path length, with most using subjective terms such as “short” and “long” to describe comparative path lengths.

Rather than directly measuring flow path lengths in some way, researchers often determine pool lengths and downwelling zone lengths, and infer hyporheic flow path lengths from that. In the Lookout Creek Basin within the H.J. Andrews Experimental Forest in the western cascade Mountains of Oregon, Anderson et al. (2005) predicted, through the use of a model, that pool lengths would increase from 2.31 m to 3.22 m, and downwelling zone lengths would increase from 2.40 m to 6.54 m over the surveyed stream reach, and that the downwelling zone length should increase by about 7% for every 1 km^2 increase in basin area. This implies an increase in hyporheic flow path lengths for larger streams with larger basin areas. Simulations of hyporheic exchange flows by Gooseff et al. (2006) in the same creek suggested that between second and fourth order streams, the upwelling zone lengths increased from 2.7 m to 7.6 m and downwelling zone lengths increased from 2.9 m to 6.0 m. Most path lengths referred to in the literature begin at the scale of meters and extend up to hundreds or even thousands of meters (Acuña and Tockner, 2009), but others describe path lengths that are almost infinitesimally small (Cardenas, 2008). The range of reported hyporheic path lengths from the literature are listed in Table 3.6.

Hydraulic velocity refers to the rate at which water moves through a sediment, or the distance it moves per unit of time, and is mostly reliant on the hydraulic conductivity (or ease of movement through that sediment). In fact, assessments of hydraulic conductivity alone have often been used to estimate velocities through the hyporheic zone. Heat itself is often used as a tracer to determine flow velocities, but this may result in an underestimation of real flow velocities because of retardation of heat within the surrounding media (Engelhardt et al., 2011). Some flow velocities reported in the

literature are listed in Table 3.7, with examples from Europe and the United States. These values are taken from a number of field studies that employed different measurement techniques such as seepage meters, fluorescein, NaCl, or temperature as a tracer. The flow velocities generally seem to fall within the range of 0.05 – 3 m/h. For comparison, the range of common hydraulic conductivities presented by Calver (2001) were $1.0x10^{-7}$ – $1.0x10^{-3}$ m/s, which translate to a range of 0.00036 – 3.6 m/hr. The flow velocities in Table 3.7 mostly fall well within the range of common hydraulic conductivities, suggesting that hydraulic conductivity measurements may be a suitable proxy for estimating hyporheic velocities in some cases.

3.4 Sediment specific heats and thermal conductivities

Thermal characteristics of sediment are important to know in order to understand the ways in which heat or energy can be transferred to water. Specific heat is a thermal characteristic that refers to the amount of heat per unit mass of a material that it would take to raise its temperature by one degree Celsius. The specific heat of hyporheic sediments are rarely mentioned in hyporheic exchange literature other than to say that values are considerably lower than that of water (Lee et al. 2013). Carslaw and Jaeger (1959) put the specific heat of granite (which is primarily made of quartz) at 0.21 cal/g·°C, compared to a value of 1.0 cal/g·°C for water, but warn that these values represent orders of magnitude rather than exact values. The specific heat capacity of a material is somewhat dependent on the initial temperature (Young, 1992), and this may lead to difficulties in estimation.

Thermal conductivity is another important thermal characteristic and refers to the way in which heat is transmitted through a solid - primarily through thermal vibrations of atoms. Atoms in hotter regions of a solid will, on average, have more kinetic energy than cooler regions, and the vibrations in hotter regions will transfer energy, and therefore heat, to neighboring cooler regions; the direction of heat flow is always from higher to lower temperature. The process of heat transfer can be understood using Figure 3.3 and the equation,

$$H = kA\frac{\Delta T}{L} \qquad \text{(Equation 3.11)}$$

where H is the rate of heat flow, or the heat current, k is the proportionality constant called thermal conductivity, A is the cross-sectional area, and ΔT/L is the temperature change or temperature difference per unit length (Young, 1992). Materials with a high k (thermal conductivity) are good conductors of heat, whereas materials with low k are poor conductors and insulators. The thermal conductivity of water is about 0.605 W/m·K (Ramires, 1995), and the thermal conductivity of quartz mineral is around 7.7 W/m·K (Horai, 1971), although different sources may give varying values for the thermal conductivity of quartz (for example, the website www.engineeringtoolbox.com lists the thermal conductivity of quartz as 3 W/m·K). The thermal conductivity of rock material containing quartz minerals can be highly variable owing to differing compositions, and therefore it may be difficult to accurately estimate the thermal conductivity of many types of sediment, and this will likely complicate any modeling of heat transfer within hyporheic zones that incorporates a conduction term.

3.5 Bucket experiments

In order to test how heat transfer occurs between water and sediments, ideally, there must be a way to measure the temperatures of both and then to monitor any changes that occur during their interaction. This type of interaction can be observed in a laboratory setting, but the ease of temperature measurement differs between rocks and water. Water temperature can be easily measured using small temperature loggers or temperature probes which can take automated measurements at specified time intervals, whereas measuring the temperature of a solid material is more complex. However, there are a number of ways that the temperature of a solid can be adjusted and estimated, and one is by immersing sediment in water that is unmoving and well-insulated, and allowing the sediment temperature and water temperature (which is easily measured) to reach equilibrium.

The initial experimental set-up to examine heat transfer between water and sediments used a series of thermally insulated buckets filled with sorted stream bed sediments collected from southern Appalachian streams. The purpose of this experiment was to determine how water at elevated or lowered temperatures would interact with sediment at or around room temperature, in order to investigate the rate at which heat transfer was occurring. Three sizes of sediment, determined based on the commonly used classification systems listed in Table 3.8, were chosen to give a full range of the sediments that may be present in streambed and hyporheic environments: sand, fine gravel, coarse gravel, and a mixture of the three (a proportional mix of sand, fine gravel, and coarse gravel). By observing how the different temperature sediment and water interact from the moment of contact, with measurements continuing until the

temperatures stabilized (through the use of a temperature time series), I was hoping to observe the types of rates and patterns of thermal processes that may be occurring within the hyporheic zone as surface water, which has been cooled or heated by the atmosphere and radiation, interacts with hyporheic sediments, and how this may ultimately affect downstream channel water temperatures as hyporheic water re-enters the channel.

For this experiment, it was necessary that each experimental unit was adequately insulated from the outside environment to ensure that all heat transfers being measured were occurring only between the water and the sediment. Each bucket (my experimental unit) was surrounded on all sides, including the bottom, with insulating foam, placed in a large cardboard box packed with crumpled newspaper, and the boxes were then placed in a group on several layers of flattened cardboard in order to ensure an adequately insulated environment. A small hole was drilled into the lid of each bucket to allow easy placement and removal of temperature probes into the buckets, and the lids were then also covered in a layer of foam (with a small slit to allow the probe wires out). During the experiment, the box tops were closed and the entire set-up was covered with a series of insulating blankets. Temperature was measured in two ways during this experiment – a temperature probe that could be hooked up to a laptop was used to give real-time data every half second to assist in determining when water temperatures had stabilized, and two internal temperature loggers buried within the sediments that took temperature measurements at a predetermined interval to be downloaded at the end of each trial run.

Each experimental unit contained 9 kg of either coarse sand (500 μm – 2 mm), fine gravel (4 – 8 mm), coarse gravel (16 – 32 mm), or a mixture of the three (3 kg coarse sand + 3 kg fine gravel + 3 kg coarse gravel). These sediments were covered with water

and allowed to come to an equilibrium temperature over the period of a few days. When the temperature of the interstitial water (measured by temperature probes) had reached a relatively steady temperature - and it was assumed that the sediment having been in contact with this water over a period of days would be the same temperature as that water - this water was then exchanged with an equal amount of water that was either 3 or 6°C cooler or warmer than the water it was replacing, and hence 3 or 6°C cooler than the sediment. The "new" water temperature was adjusted using ice or hot tap water, and monitored using a GoTemp! Temperature probe (Vernier), which allowed measurement of temperature changes in real time. When the desired water temperature was reached, the water in the experimental unit was quickly and carefully poured out and replaced with an equal amount of the new cooler or warmer water. The unit was then left untouched for a period of a few days, during which the temperatures of the water and the sediment would equilibrate. At this point, temperature data would be downloaded from each of two temperature loggers (Hobo® onset Pendant temp/light loggers) that were buried within the sediment in each bucket, and examined. Early on in this experiment, it was determined that the insulation was imperfect, and so a companion to each sediment trial was also set up to measure and quantify the temperature loss from the water alone to the surrounding room, and how affected the sediment trials may have been.

Three trials and their companion water buckets were run at a time, giving a total of 6 buckets for each experimental run, and the order of trials was randomized using a simple Matlab code. Overall within the experiment, there were three replicates of each sediment type/water temperature combination. At first, expecting this process of equilibration to take 24 hours or longer, I set the temperature recording time interval to 5

minutes, but after a first set of experimental runs, realized that I was missing the temperature peak from the added water, as my graphs, in many cases were a straight line with no apparent peaks or troughs. To try to capture the missing data from this experiment, the measurement time interval was shortened to two minutes to examine finer scale variations occurring from the initial water temperature change. Data from this experiment, including 3 replicates of each of the sediment-temperature change combination, proved to further demonstrate that the scale of change was even smaller than anticipated. Although, peaks and troughs were now visible in the temperature time series (see Figures 3.4 and 3.5 for examples), it was apparent that my data was still missing the initial, and apparently immediate temperature changes that were occurring. There should theoretically have been a point right when the water was added where temperature loggers within the experimental sediment bucket (and its corresponding water-only bucket) had the same reading – i.e., the set temperature of the heated or cooled water being added to each bucket (Figure 3.6), although this wasn't apparent in my data using a two-minute measurement time scale. These preliminary experiments demonstrated that equilibration between sediment and water of different temperatures seems to be occurring very quickly (in less than two minutes), and that changes on shorter time scales would have to act as a basis for understanding of heat exchange processes that may be occurring within the hyporheic zone.

3.6 Calorimeter experiments

The timescale of the bucket experiment was too coarse to capture the apparently rapid heat transfer processes occurring between sediment and water, so a new experiment

was developed, in which the same processes would be observed, but on a smaller scale. Small calorimeters replaced the large buckets of the previous experiment, and an oven and cooler were used to set the temperature of the sediments as different from room temperature water. Temperature change of the water as it interacts with the sediment would be measured on a much smaller time scale using GoTemp! Temperature Probes (Vernier), which have the ability to take readings every half-second. A set of three calorimeters was assembled, each containing 500 mL of room temperature water (Figure 3.7). Two of these experimental units were used to collect experimental data, while the third contained only water to ensure the adequate insulation of and unchanging temperature within the calorimeters.

As in the previous experiment, three sediment sizes were used (sand, fine gravel, coarse gravel, and a proportional mixture of the three), three replicate trials were completed with each sediment size/sediment temperature combination. Sediment samples were weighed (300 g) and placed in either an oven set to 38°C, or a cooler set to 4.4°C, where they remained in excess of a week to ensure their temperature equilibration to their environment – the sediments were then assumed to have reached those temperatures. The calorimeters were filled with room temperature water and instrumented with temperature probes hooked up to a laptop computer. The experiment was initiated when the temperature-adjusted sediment was added to the calorimeter. Temperature measurements of the water were taken every half second, beginning about 30 seconds prior to the sediment addition, and continued until there was no further discernable temperature change, which typically occurred within 18 minutes of the start of the experiment. Figures 3.8, 3.9, 3.10, and 3.11 show the temperature time series for sand, fine gravel,

coarse gravel, and the proportional mixture, respectively. Rather than looking at temperatures directly, I used the temperature change from the starting (or room) temperature as my independent variable as a way to normalize the data and allow more direct comparison between the different trials.

It is apparent from Figures 3.8-3.11 that the majority of the temperature change is occurring almost instantaneously, often within the first few seconds of sediment addition. Some curves, however, are smoother than others, and I believe that this may be due to the manner of sediment addition to the calorimeter rather than any inherent differences in the heat exchange processes between sediment sizes. Because sediment had to be carefully poured into a water-filled calorimeter, there was some initial turbulence of the water, especially associated with the larger grain sizes. In comparison, sand and fine gravel addition caused less turbulence because they were able to be added more gently, and the resulting graphs had smoother curves.

The purpose of this experiment was to look at the rates of heat transfer between sediment and water of differing temperatures, specifically from the point right as the temperature change occurs, or begins to occur, and indeed I did see an almost immediate temperature change in all cases. In addition, the water and sediment also seemed to reach equilibrium within this insulated system very quickly. This is an interesting finding because temperature fluxes in the hyporheic zone are sometimes thought to be dominated by advection and dispersion, with some, but perhaps minimal input from conduction. The rapid and immediate temperature changes seen in this experiment seem to suggest that conduction may be a significant energy flux during hyporheic exchange, especially when temperature differentials are large.

3.7 Calibration of specific heats of sediments

To more fully understand heat and energy fluxes that may be occurring within my laboratory experiment, and presumably within the hyporheic zone, I will now examine some of the thermal properties of streambed sediments more closely. To calculate the specific heat of the sediments used in my experiments and compare them to literature values, we must first start with the idea that during the heat transfer process, the amount of heat gained by the water is equal to the amount of heat lost by the rock (sediment),

$$\Delta H_W = -\Delta H_R \qquad \text{(Equation 3.12)}$$

To expand on this by looking at the components of heat transfer, we can make the equation,

$$-(T_e - T_{W_i})c\rho n = (T_e - T_{R_i})c_R\rho_R(1-n) \qquad \text{(Equation 3.13)}$$

where T_e is the equilibrium temperature, T_{Wi} is the initial water temperature, T_{Ri} is the initial rock temperature, c is the specific heat of water, c_R is the specific heat of the rock, ρ is the density of water, ρ_R is the particle density of the rock, n is the porosity (or the fraction that is water), and (1-n) is the fraction that is rock. To solve for c_R or the specific heat of the rock, the previous equation can be rearranged as follows,

$$c_R = \frac{-(T_e - T_{W_1})c\rho n}{(T_e - T_{R_1})\rho_R(1-n)} \qquad \text{(Equation 3.14)}$$

Based on the data collected in my calorimeter experiment, and the known values of specific heat and density of water, this equation can be solved to estimate the specific heat of the different types of sediment used in the calorimeter experiment.

To do this, I have created a table that lists the temperature values for the water, the sediment, and the final equilibrium temperature for each trial in my calorimeter study (Table 3.10). The sediments in the study were assumed to be primarily made of quartz,

giving a constant density value of 2.65 g/cm^3, as mentioned in an introductory section of this chapter. The porosity of the sediments were based on measurements made during the bucket experiments for each of the sediment types, and were compared to literature values, especially that of Shen and Julien, (1993; Table 3.3), and with hyporheic bulk densities listed for sand and gravel in Table 3.4, both of which show a mostly consistent pattern of sediments with larger grain sizes having higher bulk densities. The values of bulk density and porosity that I calculated based on my experimental data are shown in Table 3.9; these values were calculated during the bucket experiment by using the 9 kg mass weighed out for each sediment and dividing that by the volume of the bucket that was filled with sediment (the bucket was visualized as a frustum of a cone because the sides were not at right angles to the bottom as a cylinder would be). The estimated porosity differs only slightly from, but is consistently higher than the values listed in Table 3.3. As grain size increases, the porosity decreases, and the mix of different sediments has the lowest porosity, which is in agreement with Fetter (2001) who stated that in a mixture of different grain sizes, the smaller grains will fill the voids between the larger grains, thereby reducing porosity. The values used for the specific heat and density of water were 1 calorie/gram-°C and 1 g/cm^3, respectively. The calculated values for the specific heat of the sediments are listed in Table 3.10. When compared to the literature value for quartz (0.21cal/g·°C), we see that the calculated values seem to be an order of magnitude smaller.

3.8 Calibration of thermal conductivity

Estimating thermal conductivity based on my experimental data, and comparing it to literature values, proved to be more difficult and complex than for specific heat. Fourier's law is the basic rate equation for the conduction process, and states that the heat flux resulting from thermal conduction is proportional to the magnitude of the temperature gradient and has the opposite sign because conduction occurs in the direction of decreasing temperature (Fourier, 1955). This law can be expressed by the equation,

$$q = -K\frac{dT}{dx} \qquad \text{(Equation 3.15)}$$

where q is the heat flux vector, K is the thermal conductivity, and dT/dx is the temperature gradient in the direction of heat flow (which is negative). Assuming that the sediment grains are spherical in shape, and that there is a temperature gradient between the center and the outside of each spherical grain, then heat flow should be occurring in a radial direction outwards from the center of each sediment grain. Fourier's law in radial coordinates becomes,

$$q_r = -K\frac{dT}{dr} \qquad \text{(Equation 3.16)}$$

where q_r is the heat flow in the radial direction outwards, and dT/dr is the temperature gradient in a radial direction. Because equilibrium between the sediment and the water is almost instantaneous, we can make the simplifying assumption that the heat flow rates are equivalent to each other,

$$K_w\frac{\partial T_w}{\partial r} = K_R\frac{\partial T_R}{\partial r} \qquad \text{(Equation 3.17)}$$

where K_w is the thermal conductivity of the water surrounding the sediment grains, and K_R is the thermal conductivity of the rock (sediment grains). Here, we will also make the

simplifying assumption that the water is well-mixed. Using thermal conductivity values taken from the literature, and assuming the sediments are made primarily of quartz, we can find the general ratio of the temperature gradients between the water and the sediment,

$$\frac{K_R}{K_w} = \frac{\frac{\partial T_w}{\partial r}}{\frac{\partial T_R}{\partial r}} = \frac{7.7}{0.605} = 12.7 \qquad \text{(Equation 3.18)}$$

Thermal conductivity is more difficult to calibrate than specific heat, but will be useful in modeling heat transfer in hyporheic exchange, especially because it is apparent that conduction may be an important term when determining how water temperature might change as it moves through hyporheic sediments.

3.9 Conclusions

Through a thorough review of the literature, it is apparent that many sediment characteristics vary widely, with some, like hydraulic conductivity, varying over about 8 orders of magnitude, and pore spaces comprising anywhere from 20 – 60% of the bulk density of hyporheic sediments. This may cause difficulties when trying to make general statements about how hyporheic exchange processes occur. Another complicating factor when researching hyporheic sediment characteristics, is that many studies do not report values for variables that may have a large effect on contact times between water and sediments, such as hyporheic flow path length, and if they do, there is a lack of consistency in the methodology. In addition, many of the variables catalogued in this chapter are closely interrelated and interdependent. For example, porosity can have a large effect on the hydraulic conductivity, which may sometimes be used as an

approximation for hyporheic flow velocity, and the reporting of just one of these measures may imply information about the others. Thermal properties of hyporheic sediments are rarely mentioned in the literature, and when they are, values are listed as more of a standard or set value rather than being estimated within the frame of the study. It is possible to calculate the specific heat of sediments from laboratory experiments, as I have done in Table 3.10, although the calculated values seem to differ by about an order of magnitude from reported specific heat values from the literature, but calculating thermal conductivity appears to be a more complex concept.

My experimental investigations had a few false starts, but ultimately led to a better understanding of the time scales on which thermal interactions may occur as channel water comes in contact with hyporheic sediment. My initial hypothesis that heat transfer would occur on the scale of hours was refuted: conduction occurred almost instantaneously from the point where water and sediment were combined. My second hypothesis was that particles with a larger surface area to volume ratio (i.e. sand compared to gravel) would exhibit faster rates of heat transfer. Although this was somewhat apparent in the calorimeter experiment (this effect may have been slightly masked due to turbulence effects), heat transfer rates for all sediments were so fast that the effects of any differences in surface area to volume ratios were made effectively imperceptible. The rapid heat exchange occurring in these experiments may point to an apparent significance of conduction in the hyporheic exchange component of a stream system heat budget. This is perhaps the most interesting implication from these experiments, and one that has the potential to affect temperature modeling calculations in the future.

The investigations of thermal processes and hyporheic sediment characteristics presented here will hopefully lead to a better understanding of how and when heat transfer is occurring within a system where water and sediment of different temperatures meet, as occurs in the hyporheic zone in many streams. This chapter has presented measured ranges of sediment properties, which should act as an aid when developing models of natural systems. These concepts, especially conduction, will be examined more closely, in addition to other heat transfer processes like advection and dispersion, in the next chapter which looks at the ways in which hyporheic temperature may be damped compared to channel temperatures through the development and use of two simple models of heat movement through streambed sediments.

Tables

Table 3.1. Hyporheic porosities from the literature.

Porosity	**Notes**	**Reference**
0.387	Rio Calaveras, long reach, 1996	Fellows et al., 2001
0.38	Rio Calaveras, short reach, 1997	Fellows et al., 2001
0.393	Gallina Creek, lower reach, 1996	Fellows et al., 2001
0.375	Gallina Creek, upper reach, 1997	Fellows et al., 2001
0.25-0.35	range for sediment mixture of boulder, gravel, and sand	Fetter, 2001 (From Kasahara and Hill, 2006)
0.3-0.5	range for silt	Fetter, 2001 (From Kasahara and Hill, 2006)
0.324	Downwelling zone, Sycamore Creek	Jones et al., 1995
0.336	Upwelling zone, Sycamore Creek	Jones et al., 1995
0.177	Preflood, Kye Burn, New Zealand	Olsen et al., 2005
0.212	2 days after the flood event, Kye Burn, New Zealand	Olsen et al., 2005
0.202	1 month after the flood event, Kye Burn, New Zealand	Olsen et al., 2005
0.1932 +/- 0.0083	Site I, Sycamore Creek, AZ - estimated as water volume in saturated cores	Valett et al., 1990
0.2244 +/- 0.0067	Site II, Sycamore Creek, AZ - estimated as water volume in saturated cores	Valett et al., 1990
0.2328 +/- 0.0089	Site III, Sycamore Creek, AZ - estimated as water volume in saturated cores	Valett et al., 1990
0.51	Geometric mean, Aspen Creek	Wroblicky et al., 1998
0.64	Maximum, Aspen Creek	Wroblicky et al., 1998
0.47	Minimum, Aspen Creek	Wroblicky et al., 1998
0.51	Geometric mean, Rio Calaveras	Wroblicky et al., 1998
0.6	Maximum, Rio Calaveras	Wroblicky et al., 1998
0.39	Minimum, Rio Calaveras	Wroblicky et al., 1998

Table 3.2. Hyporheic bulk densities from the literature.

Bulk Density (g/cm^3)	**Notes**	**Reference**
1.96	at the surface of a second-order stream in the northwestern lowlands of Germany	Cleven and Meyer 1993
2.03	at the maximum depth in a second-order stream in the northwestern lowlands of Germany	Cleven and Meyer 1993
0.34	In 0-5 cm of core from Emmons Creek (based on dry mass)	Stelzer et al., 2011
0.9	In 20-25 cm of core from Emmons Creek (based on dry mass)	Stelzer et al., 2011

Table 3.3. Porosity and bulk density of sediments (based on Shen and Julien, 1993).

Classification	**Fine sand**	**Fine sand**	**Medium sand**	**Coarse sand**	**Coarse sand**	**Gravelly sand**	**Fine gravel**	**Medium gravel**	**Coarse gravel**	**Coarse gravel**	**Coarse gravel and boulders**
Size range (mm)	1/8 - 1/4	1/4- 1/2	1/2 - 1	1 - 2	2 - 4	4 - 8	8 - 16	16 - 32	32 - 64	64 - 128	128 - 256
Porosity	0.44	0.43	0.41	0.39	0.375	0.345	0.33	0.27	0.23	0.18	0.17
Bulk density (g/cm^3)	1.48	1.51	1.56	1.62	1.66	1.74	1.78	1.93	2.04	2.17	2.1995

Table 3.4. Bulk densities of sand and gravel taken from the literature.

Description	Sand BD	Gravel BD	Source
Sand, 2-6 ft. depth, from Old Bridge, NJ	1.47		Manger, 1963
Very fine sand	1.36		Manger, 1963
Terrace gravels from various locations in Montana (surface)		2.03	Manger, 1963
Gravel from Yellowstone River in Rosebud County, MT		2.19	Manger, 1963
Gravel from Fergus County, MT		1.89	Manger, 1963
Gravel (clinkered shale and sandstone) Tongue River, MT		1.36	Manger, 1963
Sevilleta 1 (0-5 cm depth) mean dry bulk density	1.49		Ritsema and Dekker, 1994
Sevilleta 2 (0-5 cm depth) mean dry bulk density	1.58		Ritsema and Dekker, 1994
Sevilleta 3 (0-5 cm depth) mean dry bulk density	1.56		Ritsema and Dekker, 1994
White Sands (0-5 cm depth) mean dry bulk density	1.31		Ritsema and Dekker, 1994
Juarez (0-5 cm depth) mean dry bulk density	1.72		Ritsema and Dekker, 1994
Kootwijk (0-5 cm depth) mean dry bulk density	1.63		Ritsema and Dekker, 1994
De Panne (0-5 cm depth) mean dry bulk density	1.56		Ritsema and Dekker, 1994
Terschelling (0-5 cm depth) mean dry bulk density)	1.65		Ritsema and Dekker, 1994
Ouddorp (0-5 cm depth) mean dry bulk density)	1.58		Ritsema and Dekker, 1994
Coarse sands (calculated from Representative Values of Porosity)	1.72-2.25		Smith and Wheatcraft, 1993

Table 3.5. Hyporheic hydraulic conductivities from the literature

Hydraulic Conductivity	**Notes**	**Reference**
$1.3x10^{-6}$ m/s	Aspen Creek - a sandstone-siltstone catchment with fine grained alluvium [a]	Morrice et al. (1997)
$12x10^{-6}$ m/s	Rio Calaveras - flows through volcanic tuff with alluvium of intermediate grain size [a]	Morrice et al. (1997)
$40x10^{-6}$ m/s	Gallina Creek - located in a granite/gneiss catchment of coarse, poorly sorted alluvium [a]	Morrice et al. (1997)
$200x10^{-6}$ m/s	McRae Creek, Oregon - mean for secondary channels [b]	Wondzell and Swanson (1996)
$90x10^{-6}$ m/s	McRae Creek, Oregon - mean for gravel bar [b]	Wondzell and Swanson (1996)
$47x10^{-6}$ m/s	McRae Creek, Oregon - mean for the floodplain [b]	Wondzell and Swanson (1996)
$0.69x10^{-6}$ m/s	Horizontal hydraulic conductivity of streambed sediments in Aspen Creek - geometric mean	Wroblicky et al. (1998)
$23x10^{-6}$ m/s	Horizontal hydraulic conductivity of streambed sediments in Rio Calaveras - geometric mean	Wroblicky et al. (1998)

[a] Hydraulic conductivity was conducted by slug or bail tests (Morrice et al. 1997)

[b] Saturated hydraulic conductivities calculated from falling-head slug tests

Table 3.6. Hyporheic flowpath lengths from the literature.

Length	Notes	Reference
5 m	Reach 1, Upwelling site 1 - Tagliamento River Basin, Italy[a]	Acuna and Tockner (2009)
15 m	Reach 1, Upwelling site 2 - Tagliamento River Basin, Italy[a]	Acuna and Tockner (2009)
30 m	Reach1, Upwelling site 3 - Tagliamento River Basin, Italy[a]	Acuna and Tockner (2009)
50 m	Reach 2, Upwelling site 1 - Tagliamento River Basin, Italy[a]	Acuna and Tockner (2009)
120 m	Reach 2, Upwelling site 2 - Tagliamento River Basin, Italy[a]	Acuna and Tockner (2009)
130 m	Reach 3, Upwelling site 1 - Tagliamento River Basin, Italy[a]	Acuna and Tockner (2009)
80 m	Reach 3, Upwelling site 2 - Tagliamento River Basin, Italy[a]	Acuna and Tockner (2009)
120 m	Reach 3, Upwelling site 3 - Tagliamento River Basin, Italy[a]	Acuna and Tockner (2009)
125 m	Reach 3, Upwelling site 4 - Tagliamento River Basin, Italy[a]	Acuna and Tockner (2009)
900 m	Reach 4, Upwelling site 1 - Tagliamento River Basin, Italy[a]	Acuna and Tockner (2009)
910 m	Reach 4, Upwelling site 2 - Tagliamento River Basin, Italy[a]	Acuna and Tockner (2009)
5.84-15.16 m	H.J. Andrews Experimental Forest, Oregon[b]	Anderson et al. (2005)
cm - >100m	Second-order mountain stream in the H.J. Andrews Experimental Forest, Oregon[c]	Haggerty et al. (2002)
~30-2000 m	estimates based on simulations of a high resolution model	Poole et al. (2008)
0.5-4.2 m	Drift Creek, Oregon[d]	Zarnetske et al. (2011)

[a]estimated length based on the distance between upwelling and downwelling locations
[b]measured as difference between STEPs (channel units with slope >13%)
[c]based on a pulse injection of a tracer
[d]estimated by electrical conductivity measurements

Table 3.7. Hyporheic flow velocities from the literature.

Velocity	Notes	Reference
3.3 m/h	Mean vertical velocity component of an infiltration site in Toss, Switzerland, using potentials + sediment	Brunke (1998) - taken from Saenger (2002)
1.56 m/h	Mean vertical velocity component of an exfiltration site in Toss, Switzerland, using potentials and sediment	Brunke (1998) - taken from Saenger (2002)
0.05-0.1 m/h	Mean vertical velocity component in a riffle of Nette, Germany, using temperature as tracer	Ingendahl (1999) - taken from Saenger (2002)
0.05-0.2 m/h	Mean vertical velocity component of a riffle in Brohl, Germany, using temperature as tracer	Ingendahl (1999) - taken from Saenger (2002)
0.17-3.13 m/h	Mean horizontal velocity component of a riffle in Nette, Germany, using NaCl tracer	Ingendahl (1999) - taken from Saenger (2002)
0.24-3.07 m/h	Mean horizontal velocity component of a riffle in Brohl, Germany, using NaCl tracer	Ingendahl (1999) - taken from Saenger (2002)
0.5 m/h	Mean vertical velocity component of an infiltration site in Lahn, Germany, using temperature as tracer	Lenk (2000) - taken from Saenger (2002)
0.25 m/h	Mean vertical velocity component of an infiltration site in Lahn, Germany, using temperature as tracer	Lenk (2000) - taken from Saenger (2002)
0.08 m/h	Mean vertical velocity component of an infiltration site in Lahn, Germany, using temperature as tracer	Lenk (2000) - taken from Saenger (2002)
0.74 (+/- 0.4) m/h	Mean horizontal velocity component of a riffle in Steina, Germany, using NaCl tracer	Pusch and Schwoerbel (1994) - taken from Saenger (2002)
0.1-0.2 m/h	Mean vertical velocity component of a riffle in Steina, Germany, using temperature as tracer	Pusch and Schwoerbel (1994) - taken from Saenger (2002)
0.2 m/h	Mean vertical velocity component of an infiltration site in Lahn, Germany, using potentials + sediment	Saenger (2000) - taken from Saenger (2002)
0.6 m/h	Mean vertical velocity component of an infiltration site in Lahn, Germany, using potentials + sediment	Saenger (2000) - taken from Saenger (2002)
<0.4 m/h	Mean vertical velocity component of an infiltration site in Lahn, Germany, using potentials + sediment	Saenger (2000) - taken from Saenger (2002)
0.2 m/h	Mean vertical velocity component of an infiltration site in Lahn, Germany, using potentials + sediment	Saenger (2000) - taken from Saenger (2002)

0.8 m/h	Mean vertical velocity component of an infiltration site in Lahn, Germany, using potentials + sediment	Saenger (2000) - taken from Saenger (2002)
0.6 m/h	Mean vertical velocity component of an infiltration site in Lahn, Germany, using potentials + sediment	Saenger (2000) - taken from Saenger (2002)
<0.4 m/h	Mean vertical velocity component of an infiltration site in Lahn, Germany, using potentials + sediment	Saenger (2000) - taken from Saenger (2002)
0.2-0.6 m/h	Mean horizontal velocity component of an infiltration site in Lahn, Germany, using fluorescein tracer	Saenger (2000) - taken from Saenger (2002)
0.5 m/h	Mean horizontal velocity component of an exfiltration site in Lahn, Germany, using a fluorescein tracer	Saenger (2000) - taken from Saenger (2002)
0.2-0.6 m/h	Mean horizontal velocity component of an infiltration site in Lahn, Germany, using fluorescein tracer	Saenger (2000) - taken from Saenger (2002)
2.23 m/h	Estimated subsurface flow measured by dye-injections in Sycamore Creek (Sonoran Desert stream)	Valett et al. (1990)
2.9 m/h	Mean horizontal velocity component of a riffle in Speed River, USA, using fluorescein tracer	Williams and Hynes (1974) - taken from Saenger (2002)
2.2 m/h	Mean horizontal velocity component of a riffle in Speed River, USA, using fluorescein tracer	Williams and Hynes (1974) - taken from Saenger (2002)
1.4 m/h	Mean horizontal velocity component of a riffle in Speed River, USA, using fluorescein tracer	Williams and Hynes (1974) - taken from Saenger (2002)
1.1 m/h	Mean horizontal velocity component of a riffle in Speed River, USA, using fluorescein tracer	Williams and Hynes (1974) - taken from Saenger (2002)
0.0467 m/h	Seepage meter upwelling velocity through the streambed at Aspen Creek (1.12 m/d)	Wroblicky et al. (1998)
0.0575 m/h	Seepage meter upwelling velocity through the streambed at Rio Calaveras (1.38 m/d)	Wroblicky et al. (1998)

Table 3.8. Different systems of classifying particle sizes (Soil Survey Division Staff, 1993).

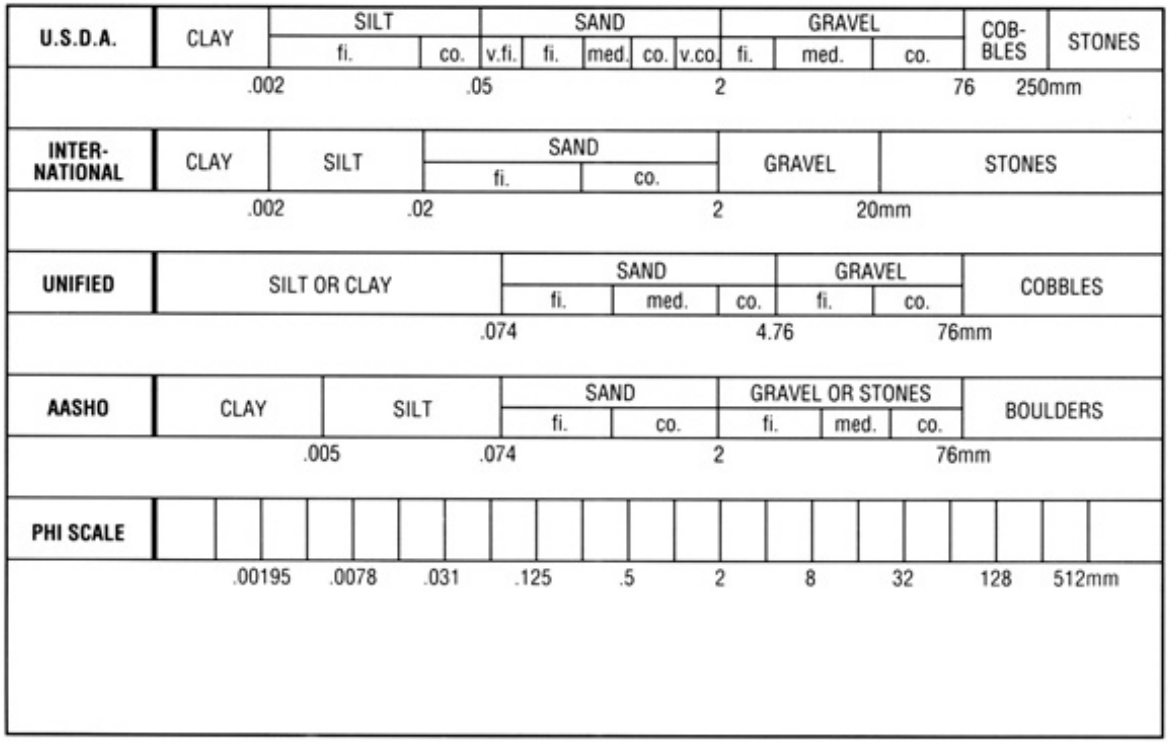

Table 3.9. Calculated bulk density and porosity of sediments used in bucket and calorimeter experiments.

Sediment Type	**Sand**	**Fine Gravel**	**Coarse Gravel**	**Mix**
Bulk Density (g/cm^3)	1.47	1.69	1.71	1.77
Porosity	0.45	0.36	0.35	0.33

Table 3.10. Calculated sediment specific heat (c_R) for each calorimeter trial. The sediment specific heat is calculated based on Equation 3.14, and has the units of cal/g·°C.

Trial	Water Temperature (°C)	Sediment Temperature (° C)	Equilibrium Temperature (°C)	Porosity	c_R
Heated Sand 1	19.9	38.0	21.6	0.45	0.032
Heated Sand 2	19.1	38.0	21.2	0.45	0.038
Heated Sand 3	19.6	38.0	21.3	0.45	0.033
Cooled Sand 1	19.7	4.4	18.5	0.45	0.026
Cooled Sand 2	19.2	4.4	18.0	0.45	0.027
Cooled Sand 3	19.5	4.4	18.3	0.45	0.026
Heated Fine Gravel 1	20.2	38.0	21.7	0.36	0.020
Heated Fine Gravel 2	19.6	38.0	21.1	0.36	0.019
Heated Fine Gravel 3	19.6	38.0	21.2	0.36	0.020
Cooled Fine Gravel 1	20.1	4.4	19.2	0.36	0.014
Cooled Fine Gravel 2	19.5	4.4	18.5	0.36	0.015
Cooled Fine Gravel 3	19.5	4.4	18.4	0.36	0.016
Heated Coarse Gravel 1	20.0	38.0	21.7	0.35	0.021
Heated Coarse Gravel 2	19.4	38.0	21.1	0.35	0.021
Heated Coarse Gravel 3	20.5	38.0	22.1	0.35	0.020
Cooled Coarse Gravel 1	19.9	4.4	19.3	0.35	0.008
Cooled Coarse Gravel 2	19.3	4.4	18.4	0.35	0.014
Cooled Coarse Gravel 3	20.4	4.4	19.3	0.35	0.014
Heated Mix 1	19.7	38.0	21.1	0.33	0.016
Heated Mix 2	19.6	38.0	21.2	0.33	0.017
Heated Mix 3	20.6	38.0	21.9	0.33	0.015
Cooled Mix 1	19.7	4.4	18.7	0.33	0.013
Cooled Mix 2	19.5	4.4	18.5	0.33	0.013
Cooled Mix 3	20.7	4.4	19.7	0.33	0.012

Figures

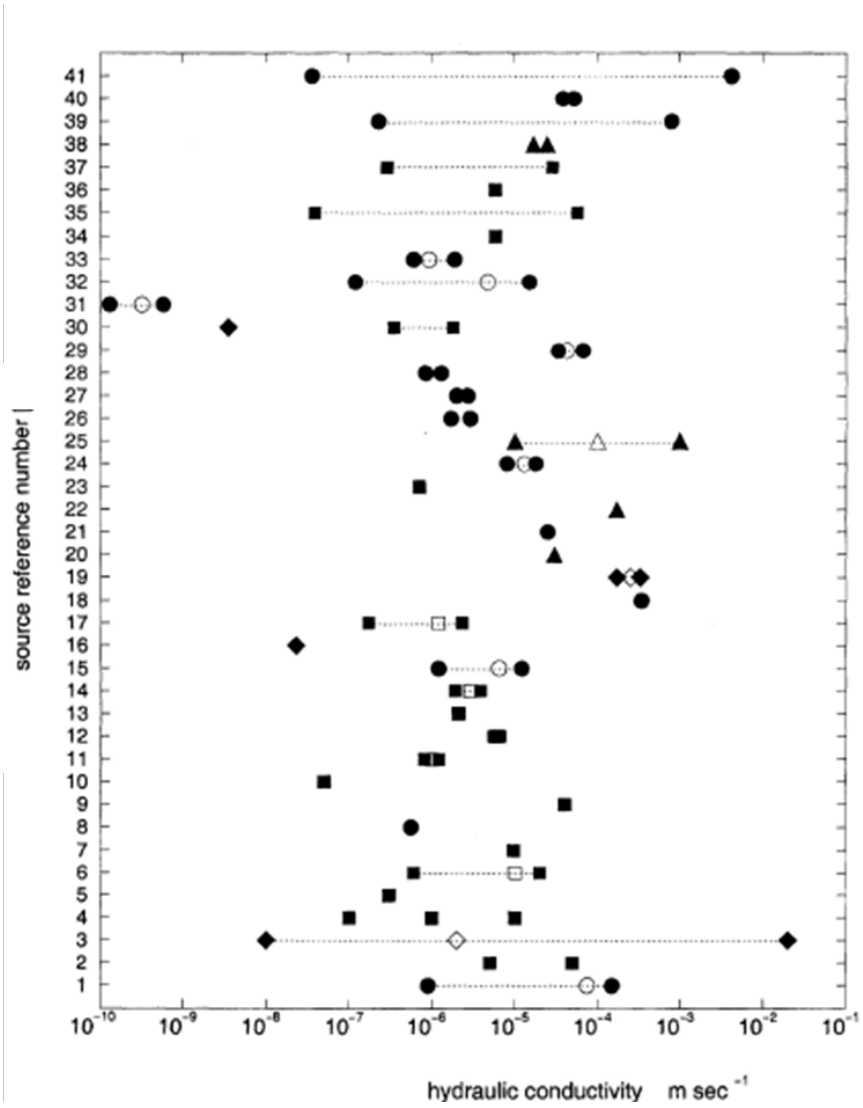

Figure 3.1: Values of hydraulic conductivity of river-lining materials (taken from Calver, 2001). Filled symbols denote single determinations or limits of ranges, and open symbols denote means. Ranges are indicated by dotted lines. Squares represent values derived from numerical modeling, circles from field studies, and diamonds from laboratory analyses. Triangles show values derived from hybrid methods.

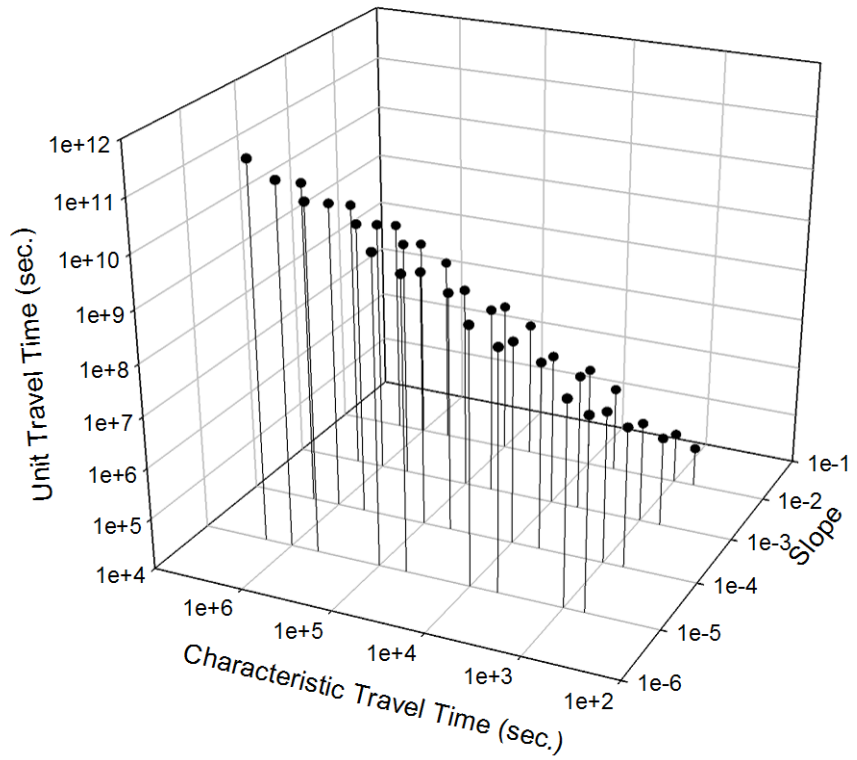

Figure 3.2: 3D plot of Unit travel time as a function of typical ranges of slope and characteristic travel time (all scales are logarithmic).

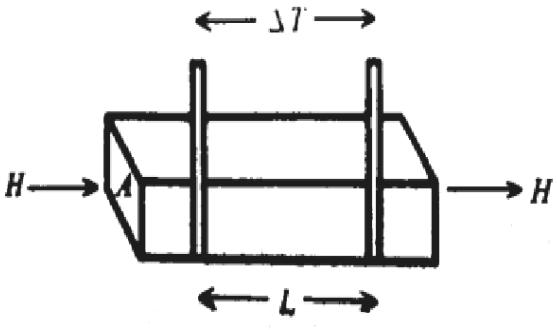

Figure 3.3: Principle of the steady-state longitudinal heat-flow method for measuring thermal conductivity (taken from Berman, 1976).

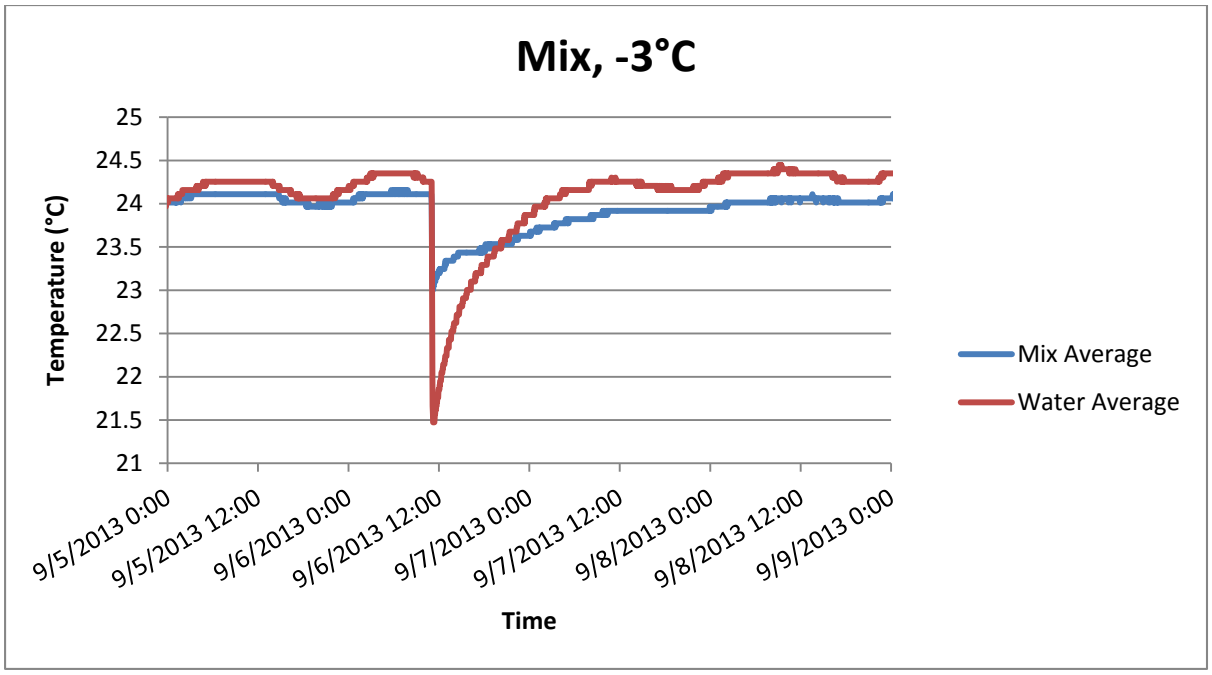

Figure 3.4: Bucket experiment: Mixed sediment trial temperature time series. The temperature time series for a trial of mixed sediment with added water that was 3°C cooler than the sediment it was added to. "Average" refers to the averaged temperature time series from two temperature loggers that were placed in each bucket. Here we see that the temperature time series for the sediment does not reach the same low point as the water-only bucket.

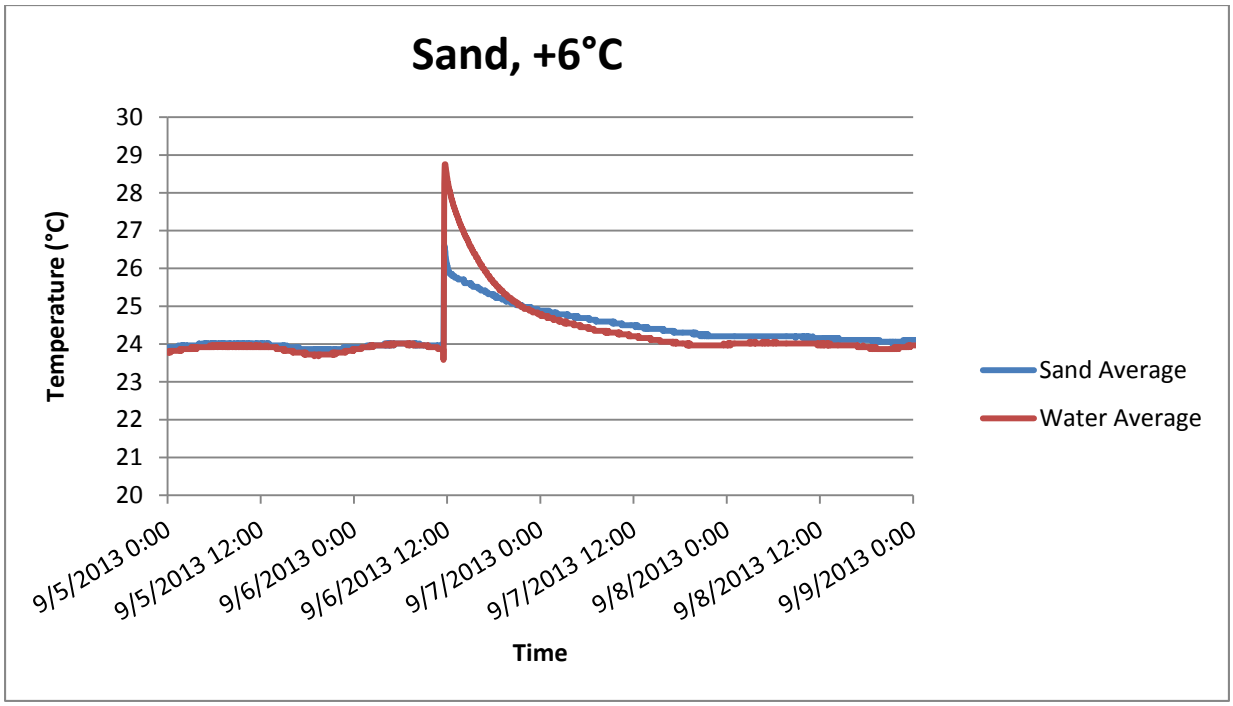

Figure 3.5: Bucket experiment: Sand trial temperature time series. The temperature time series for a trial of sand with added water that was 6°C warmer than the sediment it was added to. "Average" refers to the averaged temperature time series from two temperature loggers that were placed in each bucket. Here we see that the temperature time series for the sediment again does not reach the same peak as the water-only bucket.

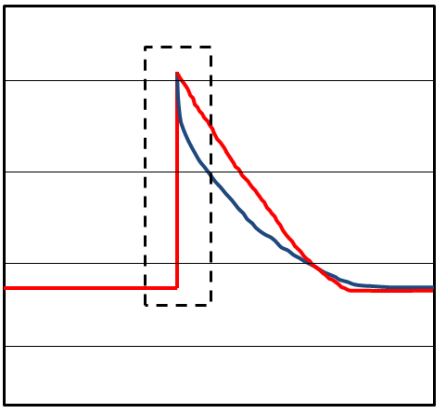

Figure 3.6: The hypothetical peak missing from temperature time series in the bucket experiment. The curve is based on Figures 3.5, the temperature peak of which is in the dashed box, and is what may be missing from the bucket experiment graphs due to the too coarse scale of temperature measurements.

Figure 3.7: The experimental set-up for the calorimeter study.

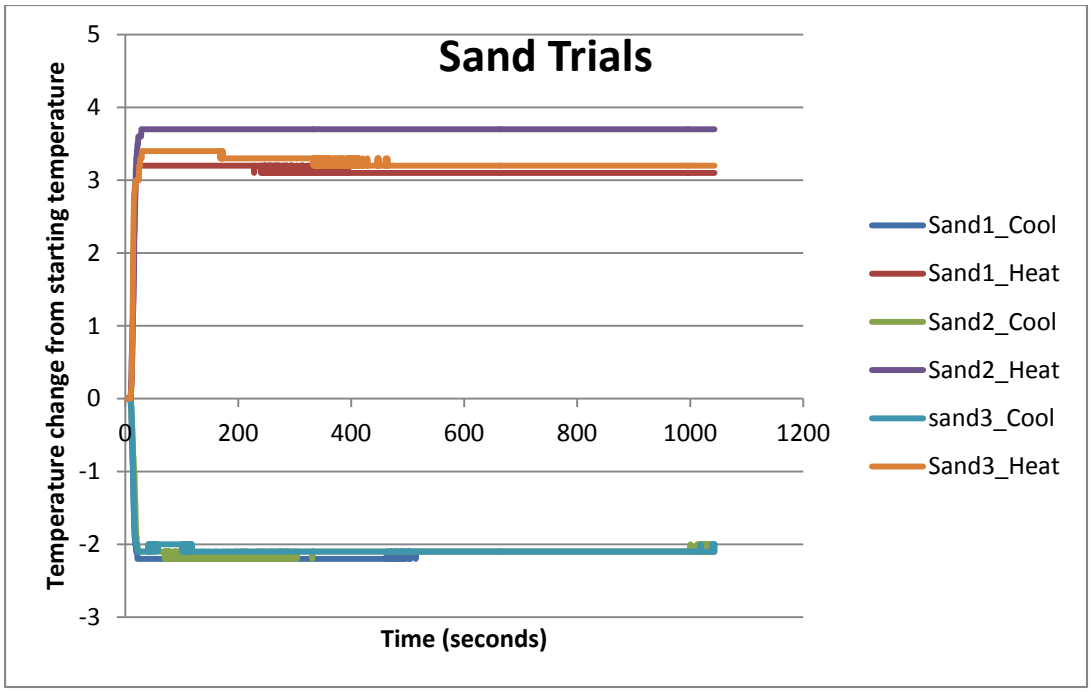

Figure 3.8: Temperature time series for the sand trials of the calorimeter experiment.

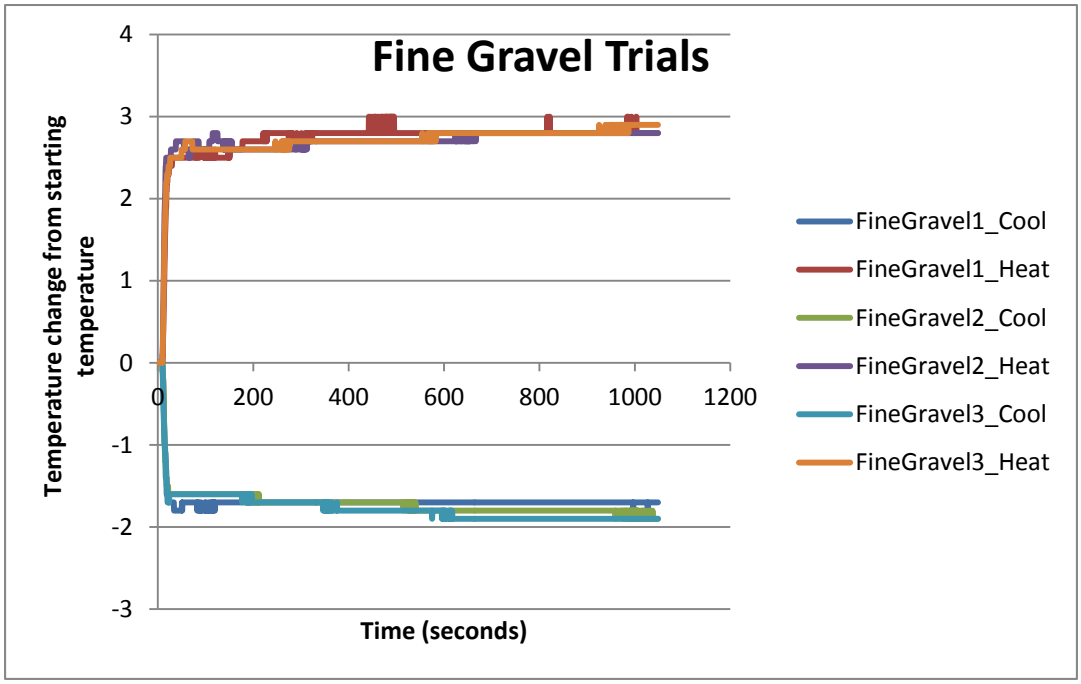

Figure 3.9: Temperature time series for the fine gravel trials of the calorimeter experiment.

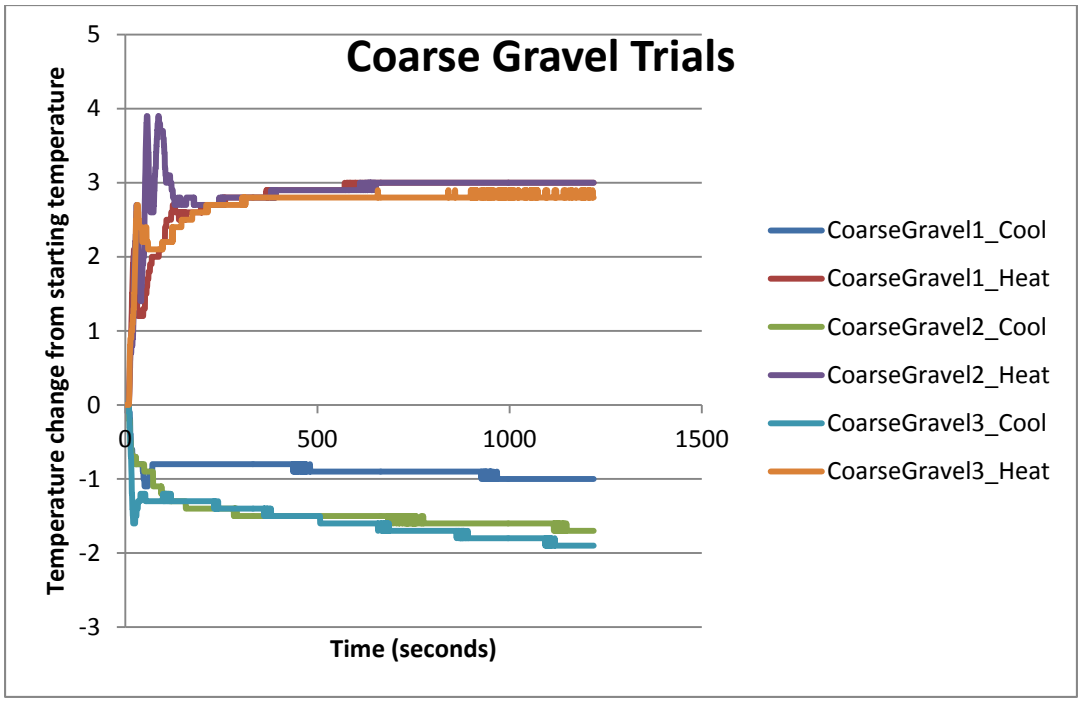

Figure 3.10: Temperature time series for the coarse gravel trials of the calorimeter experiment.

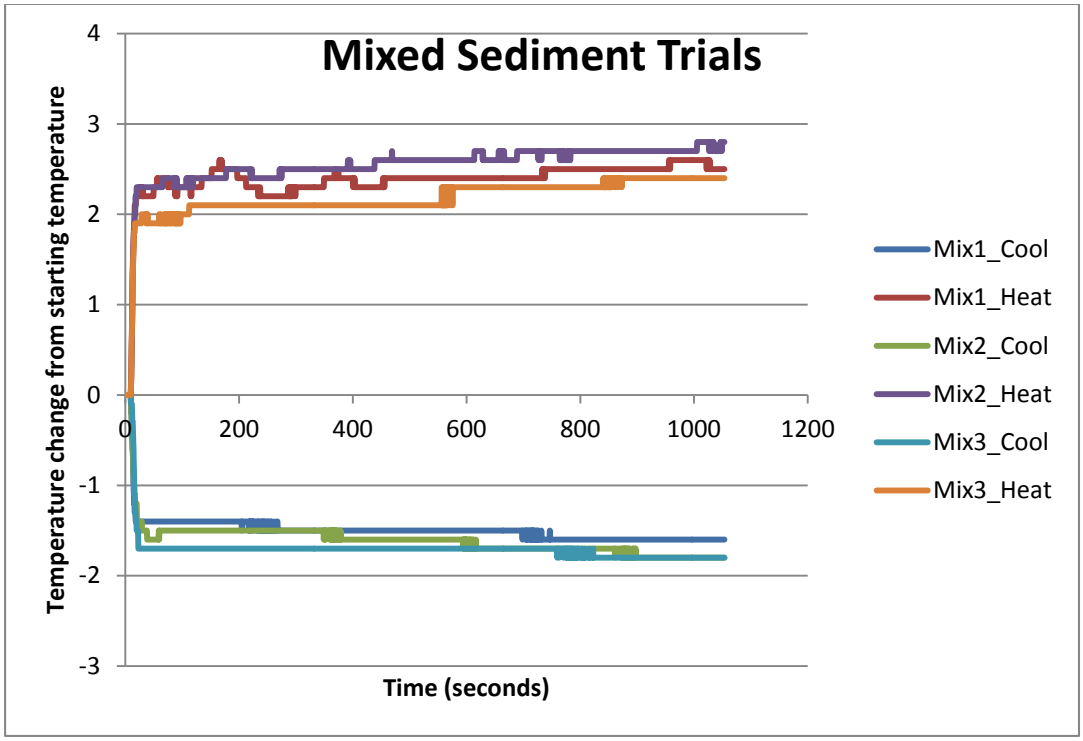

Figure 3.11: Temperature time series for the mixed sediment trials of the calorimeter experiment.

CHAPTER 4

DAMPING OF TEMPORAL TEMPERATURE VARIATION WITH HYPORHEIC TRAVEL

Modeling can be used as a tool for understanding how hyporheic processes work, and heat is commonly used as a tracer in this system because it is closely intertwined with the fluid fluxes passing through the hyporheos (Swanson and Cardenas, 2010). However, heat does not travel through porous media completely unchanged exactly like a conservative solute does (Vandenbohede et al., 2009). Few studies have examined how temperatures are modified within the hyporheic zone and what effect this may have when water is released back into the channel. One such study by Burkholder et al. (2008) determined that there is little effect on overall surface temperature patterns due to hyporheic exchange in a large gravel-bed river even though buffering and lagging of heat did create temperature variations within gravel bars when compared to the mainstem. The lack of substantial temperature effects on channel water was due to the proportion of water passing through the hyporheos being much smaller than the mainstem discharge. Despite this, the authors found that hyporheic discharge did create localized patches of water with different temperatures (Burkholder et al., 2008). It is possible that this type of discharge may have a larger effect on surface water temperatures within smaller streams where a larger proportion of channel water passes through hyporheic pathways.

This chapter will introduce two simple spreadsheet models that investigate how water temperature might change as it moves through hypothetical hyporheic flow paths. One model uses channel water temperature patterns as a basis of determining how patterns might shift due to the application of a "damping coefficient" based on contact times with hyporheic sediments. The second model more closely examines how the heat transfer mechanisms of advection, diffusion, and conduction will affect water temperatures in a single flow path. Interpretation of model results will hopefully give some insight into how rates of heat transport transfer to real-world effects for channel temperature patterns.

4.1 One-dimensional heat transfer equation

In order to examine how heat might flow through sediments during hyporheic exchange, it is often helpful to simplify the complex interactions and processes from their inherent three-dimensional properties into a one-dimensional equation which can then be expanded to include the other dimensions, if desired. In this case, we will examine how heat is transferred in the hyporheic zone with a one dimensional differential equation,

$$\frac{\partial T}{\partial t} = -v\frac{\partial T}{\partial x} + K_W\frac{\partial^2 T}{\partial x^2} - \overline{K}\frac{\Delta T}{r} \qquad \text{(Equation 4.1)}$$

where,

$$-v\frac{\partial T}{\partial x} = \text{The advection term}$$

$$K_W\frac{\partial^2 T}{\partial x^2} = \text{The diffusion term}$$

$$-\overline{K}\frac{\Delta T}{r} = \text{The simple conduction term}$$

and where ΔT is the temperature difference between the water and the rock, r is the particle radius, and $\overline{K}$ is the estimated thermal conductivity. Advection is a transport mechanism where matter or energy (like heat) is transferred by the physical movement of the water itself (Fetter, 2001). In the hyporheic zone, heat will be transferred in the direction of water flow through the interstitial spaces in the sediment and will be affected by all of the sediment characteristics discussed in earlier chapters that affect rates and amounts of hyporheic exchange. Diffusion can be defined as the net movement of a solute (or in this case, heat energy) down a concentration gradient, from areas of high concentration to areas of low concentration. The final term in this one-dimensional heat transfer equation is conduction. Conduction is a mechanism of heat transfer where heat flows between regions of different temperatures, always in the direction from higher to lower temperatures (Young, 1992). Some researchers have reported that conductive heat transport is responsible for an insignificant portion of the thermal variation within pool-riffle-pool sequences (Swanson and Cardenas, 2010), however, based on my laboratory experiments, which show that conduction is a near-instantaneous process, it may be worthy of further investigation.

4.2 Instantaneous conduction model for hyporheic damping

If hyporheic flow path lengths and velocities can be estimated, then we can also estimate water's travel time along a hyporheic flow path. Based on the evidence of damping processes within the hyporheic zone, as discussed by Arrigoni et al. (2008) and Burkholder et al. (2008), and using hyporheic sediment properties, it should be feasible to model potential temperature changes occurring in hyporheic flowpaths based on how

long water is present within an imagined flowpath. This model will use measured temperature time series of stream channel surface water and alter it based on a calculated "damping coefficient," with an assumed instantaneous rate of conduction, as justified by the very rapid heat transfer documented in the previous chapter.

For the purposes of this model, the flow path can be conceptualized as a sheet of water bounded above and below by sheets of rock, where the width of the flow path is equal to the average pore radius within a hyporheic flow path, and the velocity at which water is moving is equal to the pore velocity (Figure 4.1). Heat exchange within this proposed system, as it relates to conduction, can also be conceptualized (Figure 4.2), where in addition to advective heat transfer, or sheet flow in this model, there is also instantaneous conduction occurring between the water and the surrounding sediment (or rock layers). Water temperature patterns are cyclical, and one 24-hour period, which includes the maximum and minimum temperature for the day, is equivalent to one full cycle. These cyclical temperature patterns can be broken down into their component parts (Figure 4.3), and can be used to inform a damping model based on temperature time series data, with one full cycle representing one day (24 hours).

4.2.1 Model calculations

Using surface water temperatures alone as the model input, it we can estimate altered temperature time series of water within the hyporheic zone based on how long that water is in contact with sediments. The distance traveled in ½ cycle will be based on the timespan of the ½ cycle (12 hours or 0.5 day) and the flow path velocity (which can

be estimated). For example, with a hypothetical flow path velocity of 1 m/day, the ½ cycle travel distance will be:

$$L_{1/2} = Time \times V_p = 0.5\ day \times 1\ m/day = 0.5\ m \qquad \text{(Equation 4.2)}$$

Because of instantaneous conduction, the equilibrium temperature is such that the temperature of the rock is equal to the temperature of the water, and also that $\Delta H_r = -\Delta H_w$, or the changes in heat between the rock and water are equal (but opposite direction).

The heat input for the ½ cycle will be:

$$H_{in} = \rho L w c \Delta T \qquad \text{(Equation 4.3)}$$

where H_{in} is the heat input for a ½ cycle, ρ is the density, L is the travel distance, or length, w is the width of the pore space (or space between the sheets of rock where the water can flow), c is the specific heat, and ΔT is the change in temperature. Because the heat change between the water and the rock is equal, the earlier equation ($\Delta H_r = -\Delta H_w$) can be expanded to,

$$Lwc\rho(\Delta T - T_e) = Lw\left(\frac{1}{n} - 1\right) c_R \rho_R T_e \qquad \text{(Equation 4.4)}$$

Where $Lw\left(\frac{1}{n} - 1\right)$ is the length and width for the rock portion of the conceptual model (where n is the porosity), c_R and ρ_R are the specific heat and density of the rock, respectively, and T_e is the equilibrium temperature. When like terms are cancelled out, this equation becomes,

$$\Delta T - T_e = \frac{c_R}{c}\frac{\rho_R}{\rho}\left(\frac{1}{n} - 1\right) T_e \qquad \text{(Equation 4.5)}$$

$$\frac{\Delta T}{T_e} = 1 + \frac{c_R}{c}\frac{\rho_R}{\rho}\left(\frac{1-n}{n}\right) \qquad \text{(Equation 4.6)}$$

$$\frac{T_e}{\Delta T} = \frac{1}{1 + \frac{c_R}{c}\frac{\rho_R}{\rho}\left(\frac{1-n}{n}\right)} \qquad \text{(Equation 4.7)}$$

where $\frac{T_e}{\Delta T}$ is the proportion of the total temperature that is due to damping. When using known values for the specific heat and density of water (1 cal/g°C, and 1 g/cm^3, respectively), estimated values for the specific heat and density of rock given in the previous chapter (0.18 cal/g°C, and 2.65 g/cm^3, respectively), and an estimated porosity of 0.4 (based on the averaged porosity value calculated from the calorimeter experiment from the previous chapter), a damping coefficient per ½ cycle ($T_e/\Delta T$) can be calculated by inputting these values into the previous equation:

$$\frac{T_e}{\Delta T} = \frac{1}{1 + 0.72} = 0.58 \qquad \text{(Equation 4.8)}$$

So, when water is in contact with hyporheic sediments for ½ of a cycle (or 12 hours), the temperature maxima and minima would have been damped to 58% of those of the original temperature time series. This equation and coefficient can also be used to calculate the temperature of water that has been in contact with hyporheic sediment for longer than ½ of a cycle, and this idea can be used to create a set of possible temperature time series that may occur based on how long water has been in the hyporheic zone.

4.2.2 Spreadsheet model and results using a 24-hour stream channel temperature time series

A spreadsheet model was created using the equations from the previous section, with a 24-hour surface water temperature time series as the model input. Rather than using the absolute temperature data, each temperature point was recalculated based on its variation from the temperature average for that day. Using the same scale for all

temperature time series allowed for simpler comparison between data sets. To accomplish this, the original temperature time series data simply needs to be averaged, and then this average can be subtracted from each of the individual raw temperature measurements. This creates a variation of the temperature time series, which when graphed, shows the differences from the mean with the zero line on the y-axis being equal to the average, similar to the hypothetical cycle presented in Figure 4.3. This new normalized time series of channel water temperature can be multiplied by the damping coefficient that has been calculated per half cycle (12 hour period) to demonstrate how water temperatures will be affected when that water travels within the hyporheic zone for the length of that cycle. Each temperature measurement in the time series will be multiplied by the damping coefficient in order to represent what that temperature would have been if it had been in contact with hyporheic sediments for the specified time period. Damping coefficients can also be calculated for waters that are in contact with the hyporheic zone for longer than a half cycle. Table 4.1 lists damping coefficients calculated based on how many half cycles (12 hour periods) water is in contact with hyporheic sediments, and it is clear that the longer water is in the hyporheic zone, the more damped temperatures will be (e.g., if water is present within the hyporheic zone for 4 days, temperatures will only be 1% of what they originally were when in the stream channel, and will almost track the average exactly).

To test this model, temperature data was taken from two streams: Holloway Branch, located in the Wine Springs area of the Nantahala National Forest of western North Carolina; and Shope Fork, located about 21 km to the south-east near the Coweeta Hydrologic Laboratory (Figure 4.4). Holloway Branch (Figure 4.5) is a heavily shaded

2nd order cobble-bottom stream, and is located in a relatively undisturbed watershed dominated by eastern hemlock with a dense sub-canopy of rhododendron. There is little diurnal temperature variation in this stream, and the maximum and minimum temperatures for the collection period in question were different by less than 1°C. Shope Fork (Figure 4.6) is a fourth-order tributary of Coweeta Creek. Most of the stream is relatively undisturbed and lies in a mixed hardwood-conifer forest with an understory of rhododendron, mountain laurel, and dogwood (Petty and Grossman, 1996). The portion of the stream being monitored for temperature runs past the Coweeta offices, and lies in a man-made riparian gap where the stream surface is exposed to direct sunlight in this otherwise forested watershed. Shope Fork is wider and deeper than Holloway Branch, is cobble and boulder dominated, and is subject to greater temperature variation due to its location within a riparian gap than the densely shaded Holloway Branch – the daily temperature varied over 4°C. Stream location and characteristics for Holloway Branch and Shope Fork are listed in Table 4.1.

For this model, one daily cycle from each of the stream temperature time series was chosen. Any temperature time series can be used in this model, regardless of the collection period, but it may be most straightforward and informative to choose one full cycle (24-hour period) in order to examine how temperature extremes are affected by the damping behavior of the hyporheic zone. For Holloway Branch, the period from noon on June 6th to noon on June 7th 2014 was selected, with measurements taken every 30 minutes (Figure 4.7), and for Shope Fork, the period from 10 am July, 24th, 2012 to 10 am July, 25th, 2012 was selected, with measurements taken every 20 minutes (Figure 4.8). The measurement intervals differ between the datasets because they were borrowed

from previous projects, but should not affect the performance or validity of the model. These temperature time series were then normalized in the way described earlier (absolute temperature data was converted to read as the temperature deviation from the average) and subjected to the damping coefficients listed in Table 4.2. The model results for Holloway Branch and Shope Fork are shown in Figures 4.9 and 4.10, respectively, including a line showing the corresponding stream channel temperatures for comparison. It is clear that temperatures becomes more damped based on the number of half cycles that water is present within the hyporheic zone, and by 4 full cycles (or 4 days), there is hardly any temperature variation from the average within the time series at all, with temperatures only deviating from the average, at most, by about 0.003°C at Holloway Branch and 0.035°C at Shope Fork.

This model demonstrates how temperature damping may occur as stream water moves from the channel and into and through the hyporheic zone, and is dependent on how long that water is present within the zone and in contact with hyporheic sediments. The damping coefficient is calculated based on the properties of the sediment and water alone (including the thermal property of specific heat) without delving too deeply into exactly how these heat exchange processes and interactions are actually occurring. Despite this, the model has the potential to be very useful for understanding how water temperatures change as they move through hyporheic flow paths, and is practical in that the surface water temperature time series is the only significant model input. The next section will deal with a slightly more intricate, but conceptual model that takes a closer look at the specific heat exchange processes occurring within hyporheic zone flow paths.

4.3 Heat Flux EXCEL model

Another way to model heat exchange occurring within the hyporheic zone is to more closely examine the terms of the heat transfer equation introduced in Section 4.2. In this section, a simple conceptual model will be developed based on an understanding of how water and energy might move through a pathway in a hypothetical hyporheic system. This model is largely based on Rasmussen (1982), which examined how radionuclides are transported in groundwater through a fractured rock media. Flow through individual hyporheic flowpaths can be conceptualized simplistically in the same way as flow through a fracture in a rock, and if we can basically treat heat as a mass with respect to advection, it can be understood to be transported in similar ways to a solute. This model is not meant to be taken as a realistic hyporheic zone, but rather as an exercise in understanding the ways in which heat transfer theoretically may occur within a flowpath; therefore flowpath lengths are not taken into account. The values used in most cases will be hypothetical and/or based on literature values, but will serve to demonstrate how heat pulses are propagated through such systems.

Equations describing flux processes will be developed and described, and then these simple equations will be used as the basis for developing a conceptual model in Excel. Cells within this model will undergo advection, diffusion, and conduction as water moves downstream within the flowpath. First we will develop equations and a model that describes advection and diffusion – conceptualizing heat as a mass and using a mass balance equation to illustrate these processes. Dispersion, although actually representing a different process than diffusion (diffusion is a physical phenomenon, whereas dispersion is an empirical factor) may take a similar form and has a better

understood solution, so it will be used to loosely represent diffusion for simplicity in this model. Then, a conduction term will be added to the model as an internal process that occurs within each cell in the pathway, characterized as heat transfer between water and sediment based on porosity.

4.3.1 Advection and Diffusion

First, I will conceptualize the advection-dispersion process through the development of several equations. The following equations are based on Rasmussen (1982), but here, heat will be thought of as analogous to a solute, with energy as a mass. The fluid concentration, C, of a solute (or in this case energy) can be written as:

$$C = \frac{M}{V} \qquad \text{(Equation 4.9)}$$

where V is the volume of water in a cell, and M is the mass or energy in that cell. This equation can also be rearranged to read,

$$M = CV \qquad \text{(Equation 4.10)}$$

In this system, we can use the principle of conservation of mass to describe these processes. A mass balance can be written as,

$$M(i,j) = M(i,j-1) + [M_i - M_o] + [M_u - M_d] \qquad \text{(Equation 4.11)}$$

where $M(i, j)$ is the mass in cell i at time j, $M(i, j-1)$ is the mass in the same cell at the previous time step, M_i and M_o are the advective input and output of mass, respectively, from neighboring cells, and M_u and M_d are the dispersive fluxes from the neighboring upstream and downstream cells, respectively. This equation describes basic heat transport processes and will be used in this conceptual model.

Advection represents the mass flow of a solute at the average rate caused by the flux of water (Radcliffe and Šimůnek 2010). In this system, the advective input of mass can be calculated using the following equation:

$$M_i = \Delta V C(i-1, j-1) \qquad \text{(Equation 4.12)}$$

where *C(i-1, j-1)* is the concentration in the upstream node at the previous time step, and ΔV is the volume of water moving from the upstream node to the downstream node, found using the equation:

$$\Delta V = Q\Delta t \qquad \text{(Equation 4.13)}$$

where Q is the volumetric flow rate and Δt is the time step. The advective output of mass is similarly defined using the following equation:

$$M_o = \Delta V C(i, j-1) \qquad \text{(Equation 4.14)}$$

where *C(i, j-1)* is the concentration in the current node, but at the previous time step. It should be noted that the output for one cell then becomes the input for the next cell downstream. For advective-only flux (ignoring dispersion, which will be discussed later), the concentration calculation becomes:

$$C(i,j) = \frac{M(i,j)}{V} \qquad \text{(Equation 4.15)}$$

$$C(i,j) = \frac{M(i,j-1) + \Delta V C(i-1,j-1) - \Delta V C(i,j-1)}{V} \qquad \text{(Equation 4.16)}$$

$$= C(i,j-1) + \alpha[C(i-1,j-1) - c(i,j-1)] \qquad \text{(Equation 4.17)}$$

where $\alpha = \Delta V/V = Q\Delta t/V$ is a ratio of the advective volume being pushed downstream relative to the total volume in each element or node. In addition, it should be noted that $\tau = V/Q$ is the residence time of water in each cell, so that $\alpha = \Delta t/\tau$.

Transport mechanisms would be limited to advection if all solute molecules in flux were traveling at the same velocity as the average water velocity (Radcliffe and Šimůnek 2010); however, here and in typical hyporheic flow paths this is not the case. Diffusion, a second transport mechanism, refers to the movement of solute molecules in response to differences in concentration. As mentioned earlier, dispersion will be used in place of diffusion. Unlike the advective flux described earlier, which only moves mass one way (downstream), dispersive flux allows for movement in two directions: upstream and downstream. The dispersive flux can be calculated as:

$$M_i = M_u + M_d \qquad \text{(Equation 4.18)}$$

where M_u and M_d are the upstream and downstream exchanges, respectively. Fick's Law, which states that flux goes from regions of high concentration to regions of low concentration with a magnitude proportional to the concentration gradient, can then be used to define the upstream and downstream exchanges:

$$M_u = -DA\Delta t\frac{\Delta C}{\Delta x} = \frac{DA\Delta t}{\Delta x}[C(i-1,j-1) - C(i,j-1)] \qquad \text{(Equation 4.19)}$$

and

$$M_d = -DA\Delta t\frac{\Delta C}{\Delta x} = \frac{DA\Delta t}{\Delta x}[C(i,j-1) - C(i+1,j-1)] \qquad \text{(Equation 4.20)}$$

where D is the dispersion coefficient and A is the cross-sectional area across which the dispersion is occurring. Combining these two equations, the net exchange (M_n) can be calculated:

$$M_n = M_u - M_d = \frac{DA\Delta t}{\Delta x}[C(i-1,j-1) - C(i+1,j-1)] \qquad \text{(Equation 4.21)}$$

For dispersive-only flux, the calculation becomes:

$$C(i,j) = \frac{M(i,j)}{V} \qquad \text{(Equation 4.22)}$$

$$= C(i,j-1) + \beta[C(i-1,j-1) - C(i+1,j-1)] \qquad \text{(Equation 4.23)}$$

where

$$\beta = \frac{DA\Delta t}{V\Delta x} = \frac{D\Delta t}{L^2} \qquad \text{(Equation 4.24)}$$

with $L = \Delta x = V/A$.

By combining the advection and dispersion for flow through the system, there is a flux moving downstream through advection and a flux moving in an upstream and downstream direction through dispersion. To mathematically represent these processes, the above concentration calculations must be combined, resulting in the following equation:

$$C(i,j) = C(i,j-1) + \alpha[C(i-1,j-1) - C(i,j-1)] + \beta[C(i-1,j-1) - C(i+1,j-1) \qquad \text{(Equation 4.25)}$$

where, again α is that advection ratio term and β is that dispersion ratio term. By combining like terms, we get the following equation:

$$C(i,j) = [1-\alpha]C(i,j-1) + [\alpha+\beta]C(i-1,j-1) - \beta C(i+1,j-1) \qquad \text{(Equation 4.26)}$$

The Péclet number is a dimensionless number used in the study of transport of fluid flows and can be defined as the ratio of the rate of advection of a physical quantity by flow to the rate of diffusion of the same quantity driven by an appropriate gradient (Radcliffe and Šimůnek 2010). In our case, it can be defined as:

$$P_e = \frac{\alpha}{\beta} = \frac{\Delta t}{\tau}\frac{L^2}{D\Delta t} = \frac{L^2}{D\tau} \qquad \text{(Equation 4.27)}$$

so that $P_e >> 1$ is advection dominated (i.e., $\alpha >> \beta$), while $P_e << 1$ is dispersion dominated (i.e., $\alpha << \beta$).

4.3.2 Conduction

Conduction can be conceptualized as an aspect of advection when the advective flux takes into account the heat capacities of both the sediment material and the water within each cell. The energy balance equation is,

$$\frac{\Delta H}{\Delta t} = J_{in} - J_{out} \qquad \text{(Equation 4.28)}$$

where ΔH is the change in heat content (J) over the time interval, Δt (s), and J is the advective heat flux (J/s). The change in temperature, ΔT, of a volume of composite material (both solid rock and water), V (L), is:

$$\Delta T = \frac{\Delta H}{X_e V} \qquad \text{(Equation 4.29)}$$

where X_e is the effective heat capacity of a composite material, defined using,

$$X_e = \theta X_w + (1 - \theta) X_s \qquad \text{(Equation 4.30)}$$

where X_s is the heat capacity of the solid matrix, X_w is the heat capacity of the water, and θ represents porosity, or proportion of void spaces for the composite material.

The advective heat flux is,

$$J = X_w Q T \qquad \text{(Equation 4.31)}$$

where X_w is the volumetric heat capacity of water (J/L/°C), Q = ΔV/Δt is the flow rate (L/s), T is the water temperature (°C), and ΔV is the advective volume (L). Combining equations yields,

$$\Delta H = X_w(\Delta V_{in} T_{in} - \Delta V_{out} T_{out}) \qquad \text{(Equation 4.32)}$$

so that,

$$\Delta T = \frac{X_w(\Delta V_{in} T_{in} - \Delta V_{out} T_{out})}{X_e V} \qquad \text{(Equation 4.33)}$$

which, when $\Delta V = \Delta V_{in} - \Delta V_{out}$, yields,

$$\Delta T = \alpha(T_{in} - T_{out}) \qquad \text{(Equation 4.34)}$$

where,

$$\alpha = \frac{X_w}{X_e}\frac{\Delta V}{V} \qquad \text{(Equation 4.35)}$$

This creates the same advection equation as before, except with the addition of the ratio of heat capacities representing conduction processes. The next section will use these developed equations to generate a model of heat transfer in a hypothetical flow path.

4.3.3 Model Development

A hyporheic flow path can be conceptualized as a grid of cells simplistically representing flow both over space and through time. A system like this can be used to determine how the water within the flow path will react to an input of diurnally varying temperatures as it flows downstream. The concepts and equations introduced in the previous sections will be used to demonstrate how an input of hypothetical surface water with diurnally varying temperatures changes as it moves through a flow path, while being affected by heat transfer processes within the system including advection, dispersion/diffusion and conduction. Varying temperature or heat inputs into the system in a cyclical manner attempts to replicate the daily temperature cycles that a hyporheic flow path will likely encounter, as surface water moves into and through the hyporheic zone.

This system can be visualized as a series of cells in a straight line representing flow downstream through a flow path. The first (leftmost) cell is the most upstream point in the flow path, and adjacent cells to the right of this cell represent downstream locations within the same flow path, moving progressively downstream as you move to the right. The heat transfer processes previously described are occurring between and within these cells (Figure 4.11).

A model based on the conceptualization presented in Figure 4.11 was developed within Microsoft Excel as a two-dimensional grid, with distance downstream (x) running vertically as row headings, and time (t) running horizontally as column headings (Figure 4.12). The grid layout has 100 nodes, or cells, going downstream (x) and 200 time points (t). The row headings (x) do not have a length component associated with them, but rather represent the order, or placement of cells within the model (see Figure 4.11 for a graphic representation of this: the most upstream cell is designated by "1," the adjacent downstream cell is designated by a "2," and so on). This timescale was used because the cyclical pattern of the temperature input was not fully propagated through the system by the end of a single cycle (represented by 100 points), and model results were much more informative with the second temperature cycle added, as will be shown later. At time t = 0, the initial condition is set as a constant for all cells going downstream. Boundary conditions are first set to a constant upstream of the first cell and downstream of the last cell. When running the model the temperature/energy increases at a steady rate of 0.1°C per time step for 25 time steps, decreases at the same rate for 50 time steps, and then increases again for 25 time steps to end up at the temperature of the initial boundary condition, in an attempt to replicate a daily temperature cycle in shape, though not on the

same timescale. This pattern is then repeated for the next 100 time steps creating two full daily cycles in order for the change to propagate through the entire system (to see more fully how the cycle is altered at different spatial locations downstream). This cyclical temperature input allows for the viewing of concentration fluxes within the system over time and through space that replicate natural temperature patterns, however, the flow itself does not shift: this is a steady-state system.

For purposes of calculation, each time step is one minute, the volume of each cell is fixed at 100 L, and flow is arbitrarily set at 25 L/min. The volume of each cell is much larger than would be expected in real-world flowpaths, but is a useful arbitrary value because it allows easy conceptualization of advection within the system. If $\alpha = Q\Delta t/V$, or the ratio of inflow to the volume of the cell, then the advection ratio term, α, is 0.25. This merely means that ¼ or 25% of the volume of a cell is being moved downstream by advection at each time step. The dispersive-flux ratio, designated above as β, is arbitrarily assigned for simplicity. The equations introduced in the previous sections for advection and dispersion are used in the following way within the Excel model (as an Excel equation):

$$= B3 + \alpha * (C2 - B3) + \beta * (B2 - B4) \qquad \text{(Equation 4.36)}$$

where α is the advective ratio term and incorporates the cell volume of the same spatial location at the previous time point with the new addition of ¼ of the volume from the downstream adjacent cell, and β is the dispersive ratio term, that takes into account dispersive inputs from the directly adjacent upstream and downstream cells that occurred at the previous time step. Figure 4.13 indicates the cells within the Excel model that were used to calculate both advection and dispersion within the downstream cell.

Conduction is incorporated into this model by considering the influence of heat capacity, rather than any measure of thermal conductivity - which may be useful, but is more difficult to calculate. For the purposes of the model, the conduction term can be included as a factor within the advective ratio term, so the Excel equation will remain essentially the same as shown in Equation 4.36. The initial parameters used in this model are listed in Table 4.3, including parameters that are needed and/or calculated to incorporate conduction into the equation. The discharge, velocity, time interval are used to determine advection, there is an assigned dispersion factor that is considerably lower than the advection factor (the system is advection-dominated), and common porosity, and specific heats and densities of the water and the rock are needed to estimate conduction within the system. These latter values are the same as those used previously in the Damping Model - they are averages or values taken from the literature and should adequately represent appropriate values for hyporheic zone sediments. In this model, the advection term is much higher than the dispersion term, and therefore the Péclet number is greater than 1. Terms needed to understand instantaneous conduction within this model include the volumetric heat capacities of water and solid rock (C_w and C_s, respectively), which are calculated by multiplying the gravimetric heat capacity by the density of the corresponding material. Each cell within the model can be split into two volumes, the volume of water and the volume of solid material (quartz). Porosity (n) can be thought of as the volume of water whereas (n-1) is the volume of the rock. C_e is the effective heat capacity of a composite material that includes both the water and the solid rock that is present within each cell in the model, and is determined by the following equation:

$$C_e = nC_w + (1 - n)C_s \qquad \text{(Equation 4.37)}$$

where n is the porosity, C_w is the volumetric heat capacity of water, and C_s is the volumetric heat capacity of the solid rock. C_w/C_e is the ratio of heat capacities described in Equation 30, and the value now called the "ratio" (Table 4.3) is calculated in the same way as the advection equation mentioned earlier, but with the addition of the ratio of heat capacities representing conduction processes.

4.3.4 Implications for stream heat budgets

Results from the Heat Flux Model are shown in Figure 4.14. This figure displays the temperature pattern at different spatial locations over time within the hypothetical flow path. Because no flow path length is applied to the system itself and cells have no length specification, the patterns of the different curves can be seen to approximate what differences in temperature would be if hyporheic pathway were of these relative lengths compared to each other. The input temperature time series is also included within this graph for comparison.

The most striking feature of this figure is the visible damping of temperature patterns as you move downstream within the flow path. The further you go downstream (or this can be conceptualized as longer flow path lengths), the more the signal is damped, or the closer the maximum and minimum temperatures stay to the average. The temperature pattern at x = 1 almost directly tracks the temperature input, although it is very slightly damped and offset, and this demonstrates that for very short flow paths, hyporheic exchange will likely have very little impact on stream temperatures. It follows that at more extreme downstream locations than are exhibited in this graph, the

temperature signal should deviate little from the average, similar to the results seen for long travel times in the previously described Damping Model. Early within the model, it takes some time for the temperature signal to reach downstream locations, and once they do, they form damped cyclical patterns, with those further downstream taking longer to appear and being most damped. This model is also interesting because it seems to demonstrate lagging behavior in the temperature pattern in addition to damping, as was suggested by Arrigoni et al. (2008).

This model represents heat transfer through one flowpath within a hypothetical hyporheic zone, and attempts to simplistically compare these temperatures to channel water as an input of cyclical temperature changes. It is important to remember that this model only represents the hypothetical heat movement within one flowpath in a likely complex network of hyporheic flowpaths described by Poole at al. (2008), and therefore greatly simplifies the patterns that may be seen in actual hyporheic zone systems.

4.3.4 Relevant Analytical Solutions

Differential equations can be solved by an analytic approach, which searches for explicit formulas that describe behavior. There are a few analytic solutions that deal with dispersion in fractured or porous media that are relevant to this dissertation. The first is a 1961 Geological Survey Professional Paper by Ogata and Banks (1961). This solution looks at dispersion in a porous medium that is homogeneous and isotropic, and it assumes that solute transport, due to microscopic velocity variations in flow pathways, can be quantitatively expressed as the product of a dispersion coefficient and the concentration gradient. This solution was an improvement over previous solutions for dispersion of a

fluid moving through porous media because it allowed for an asymmetrical concentration gradient within the media.

The second relevant analytical solution was introduced by Grisak and Pickens (1981), and this paper examines a system where there is advection through fractured media, coupled with diffusion into the surrounding porous matrix. This solution was based on the heat exchanger conceptualization of Carslaw and Jaeger (1959), where a uniformly flowing fluid is in contact with a solid wall, and heat is transferred across the fluid-wall interface. Analytical solutions have advantages over numerical solutions, in that they are more easily solved, but are limited to constant values of system parameters, and therefore must assume homogeneous conditions (Grisak and Pickens, 1981).

4.4 Conclusions

The Excel and spreadsheet models introduced in this chapter demonstrate how temperature patterns can be propagated and changed as water passes through the hyporheic zone. Conduction within the hyporheic zone can be thought of as a mechanism that contributes to the damping of temperature cycles, where the maximum and minimum temperatures encountered during the cycle move closer to the mean, as described by Arrigoni et al. (2008). The longer water is in contact with these hyporheic sediments, the more damped the temperatures will be, until eventually temperatures will remain at or very close to the mean. This behavior is demonstrated through the use of the Instantaneous Conduction Model for Hyporheic Damping. The Heat Transfer Excel Model, deals with conduction and heat transport in a conceptual and more mechanistic way, and imagines the hyporheic zone as a two-dimensional grid of cells where each cell

is composed of water and solid rock (based on porosity). A heat signal is added to the system, and the model demonstrates how that signal is transformed as it moves through both time and space within a single flowpath of the system. This is a more theoretical model used to demonstrate that conduction is, in fact, having an effect on heat transfer processes, and therefore should not be excluded when modeling temperature in the hyporheic zone.

Tables

Table 4.1: Descriptive information for Holloway Branch and Shope Fork.

Stream Name	**Holloway Branch**	**Shope Fork**
Coordinates	35.209158, -83.605669	35.060173, -83.430131
Elevation	1123 m	684m
Stream Order	2^{nd}	4^{th}

Table 4.2: Damping coefficients based on number of half cycles that water is present in the hyporheic zone – used in Instantaneous Conduction Excel Model.

1/2 Cycles	**Damping**
1	0.58
2	0.34
3	0.2
4	0.11
5	0.07
6	0.04
7	0.02
8	0.01

Table 4.3: Initial parameters for Heat Flux Excel Model.

Parameter	Value	
Q (flow) =	25 L/min	
V (volume of cell) =	100 L	
Δt (time step) =	1 min	
α (advective ratio term)=	0.25	
β (dispersive ratio term)=	0.04 m^2/min	
n (porosity)=	0.4	
C_{pw} (specific heat of water)	1 cal/g/°C	gravimetric
C_{pr} (specific heat of quartz)	0.18 cal/g/°C	gravimetric
ρ_w (density of water)	1 g/cm^3	
ρ_r (density of quartz)	2.65 g/cm^3	
C_w (heat capacity of water)	1 cal/cm^3/°C	volumetric
C_s (heat capacity of quartz)	0.477 cal/cm^3/°C	volumetric
C_e (effective heat capacity of water and quartz)	0.6862 cal/cm^3/°C	volumetric
C_w/C_e (ratio of heat capacities)	1.457	
Ratio (calculated advection-conduction term)	0.364	

Figures

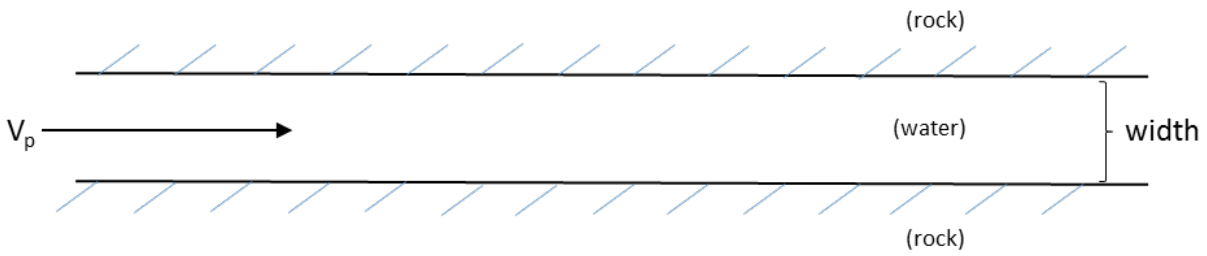

Figure 4.1: A schematic of water traveling through pores conceptualized as sheet flow.

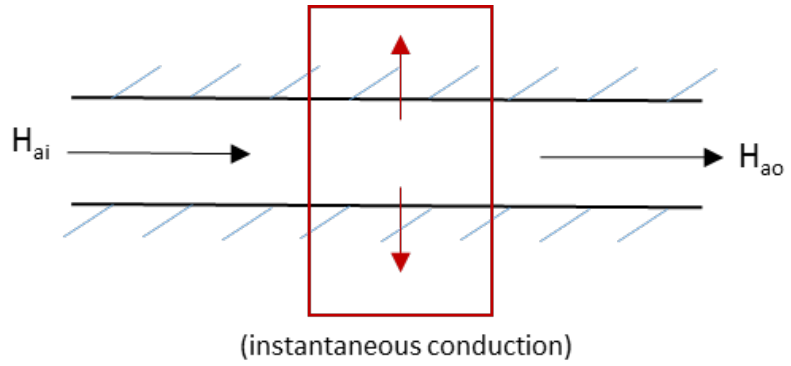

Figure 4.2: A schematic of how heat flow will occur within the sheet flow conceptualization of water movement through the hyporheic zone. This includes advective heat transfer in black and instantaneous conduction between the water and the rock in red.

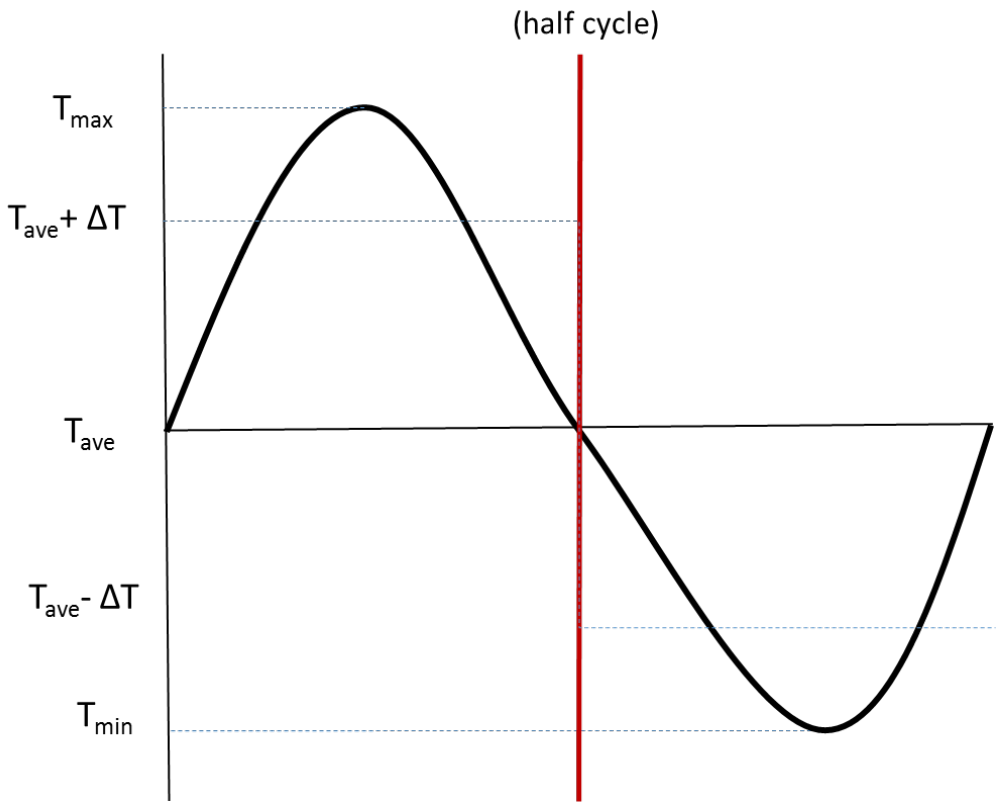

Figure 4.3: Schematic showing the components of a daily temperature time series

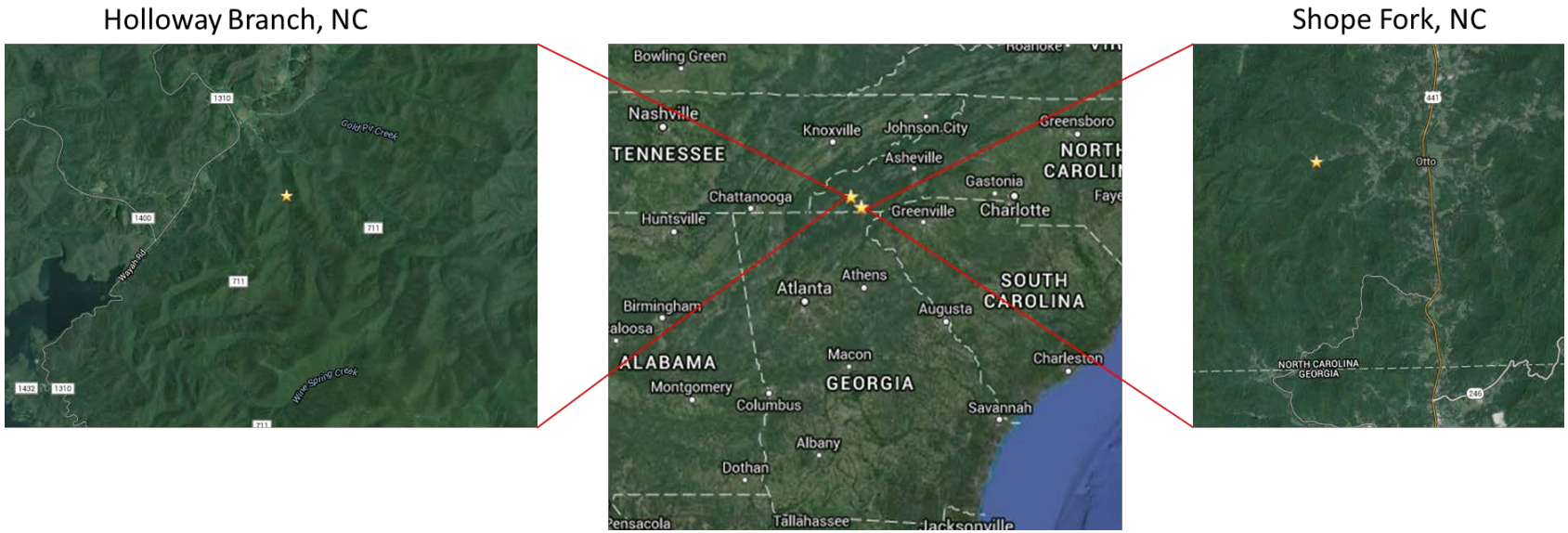

Figure 4.4: Locations of streams: Holloway Branch and Shope Fork, North Carolina

Figure 4.5: Holloway Branch, North Carolina

Figure 4.6: Shope Fork, North Carolina

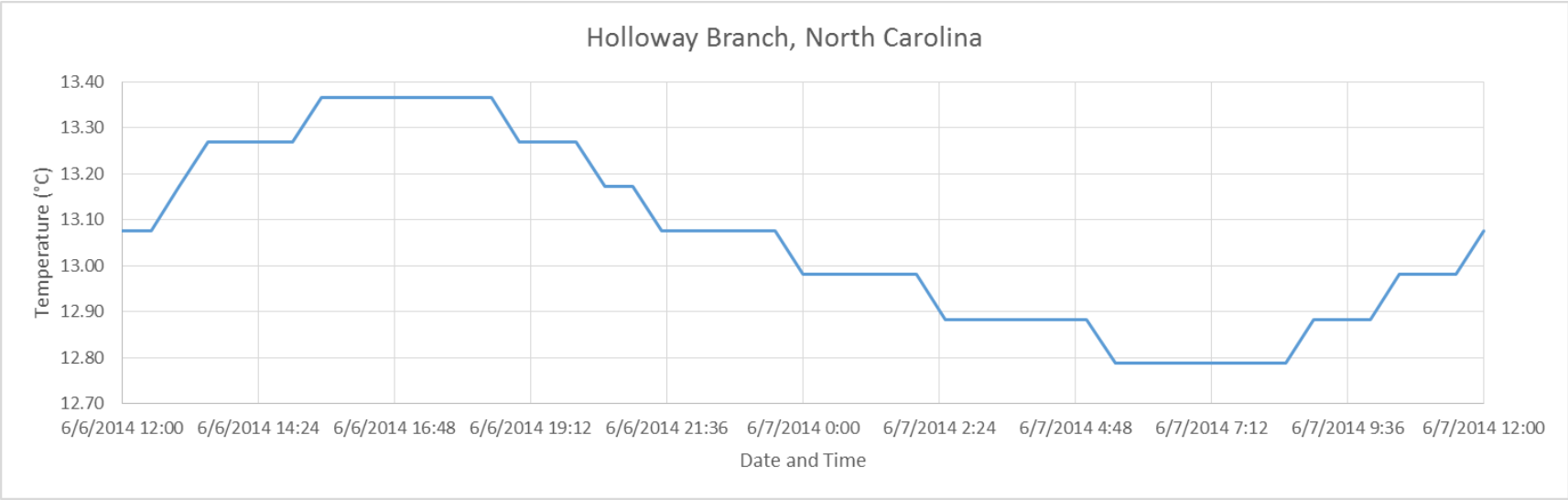

Figure 4.7: 24-hour temperature time series from Holloway Branch in the Nantahala National Forest, North Carolina.

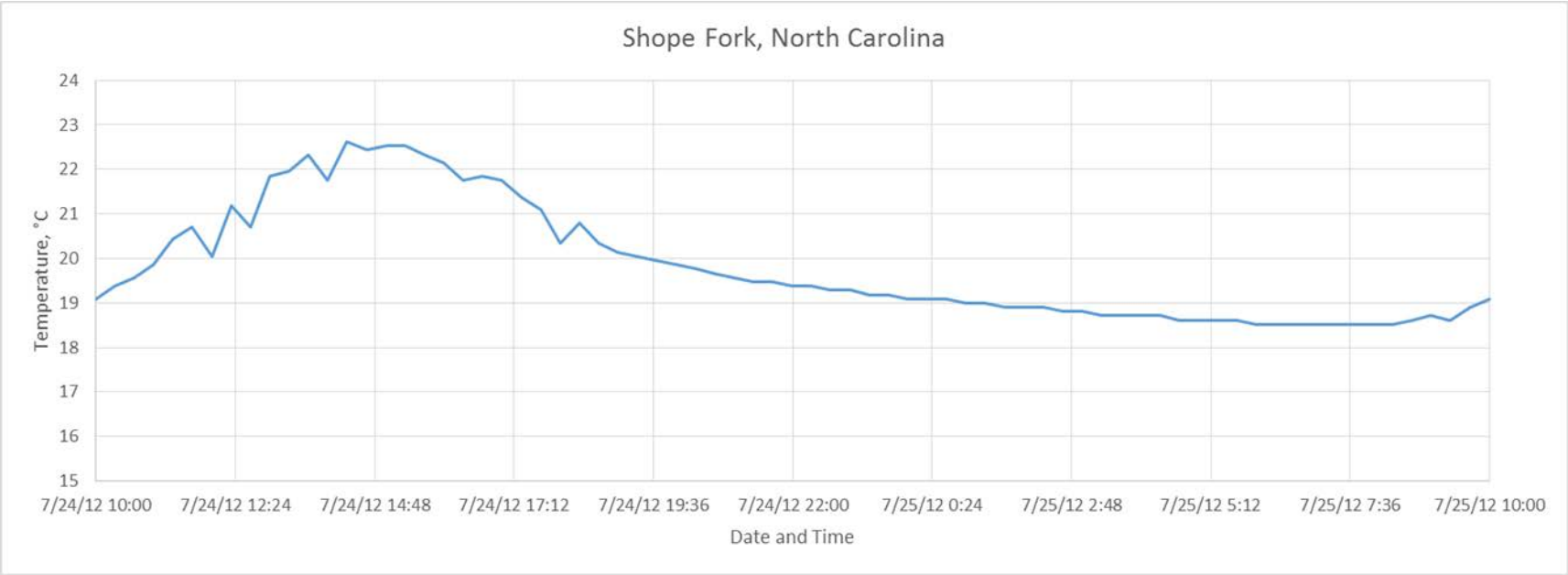

Figure 4.8: 24-hour temperature time series from Shope Fork, North Carolina.

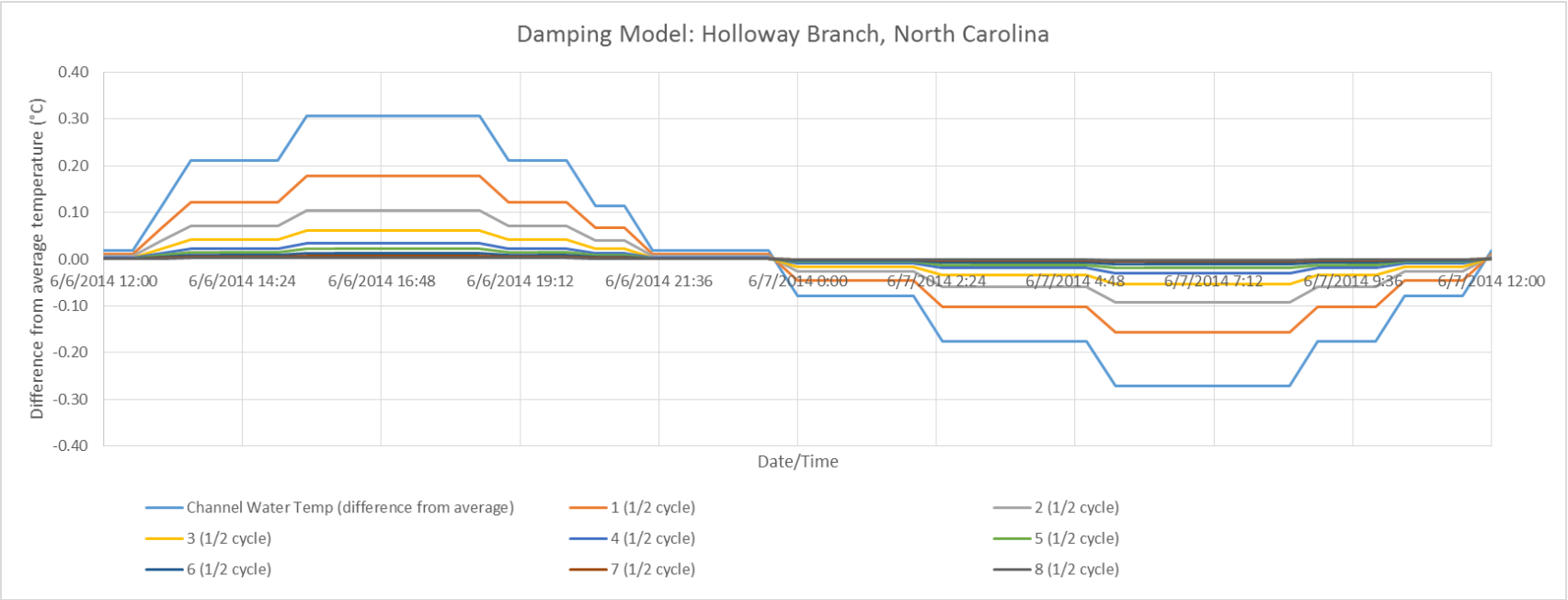

Figure 4.9: Model results for the Instantaneous Conduction Model at Holloway Branch, North Carolina, showing surface stream temperature as the difference from the average, and how damping occurs when water is in contact with hyporheic sediments for ½ a cycle and longer (up 4 full cycles, or 4 days).

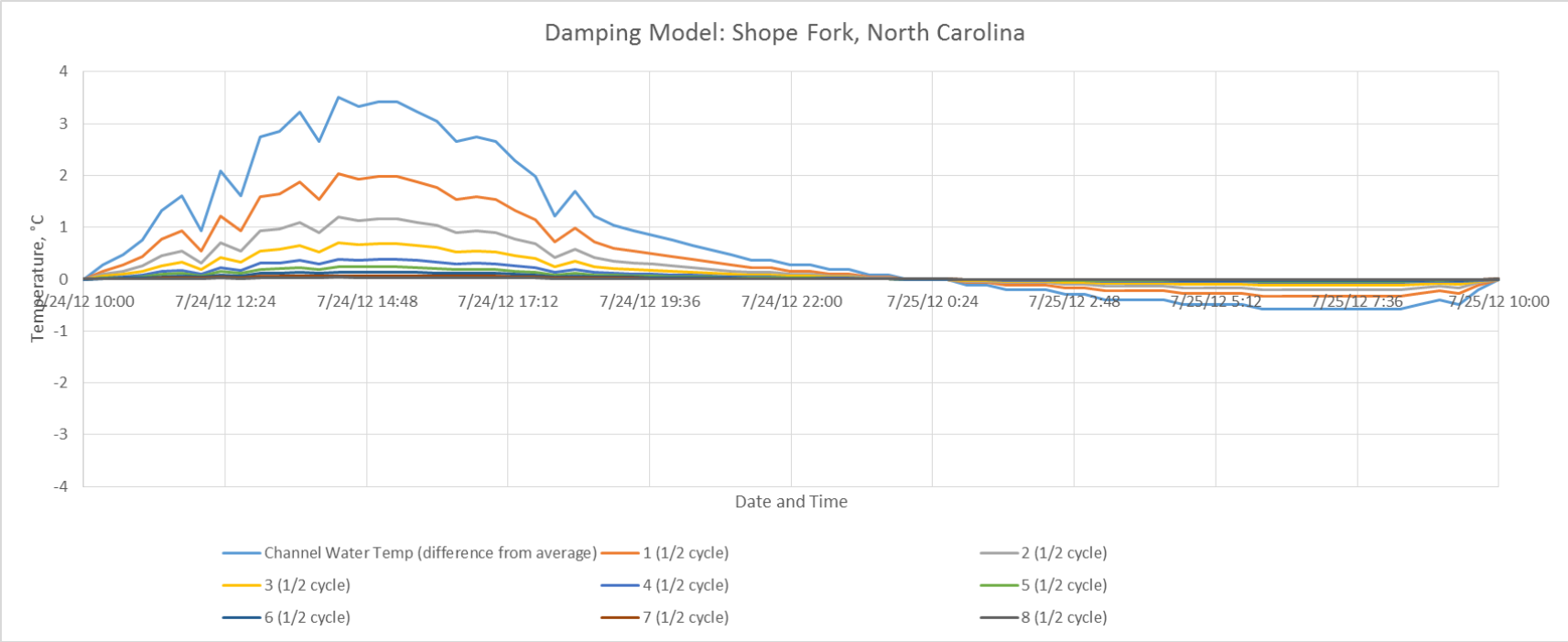

Figure 4.10: Model results for the Instantaneous Conduction Model at Shope Fork, North Carolina, showing surface stream temperature as the difference from the average, and how damping occurs when water is in contact with hyporheic sediments for ½ a cycle and longer (up to 4 full cycles, or 4 days).

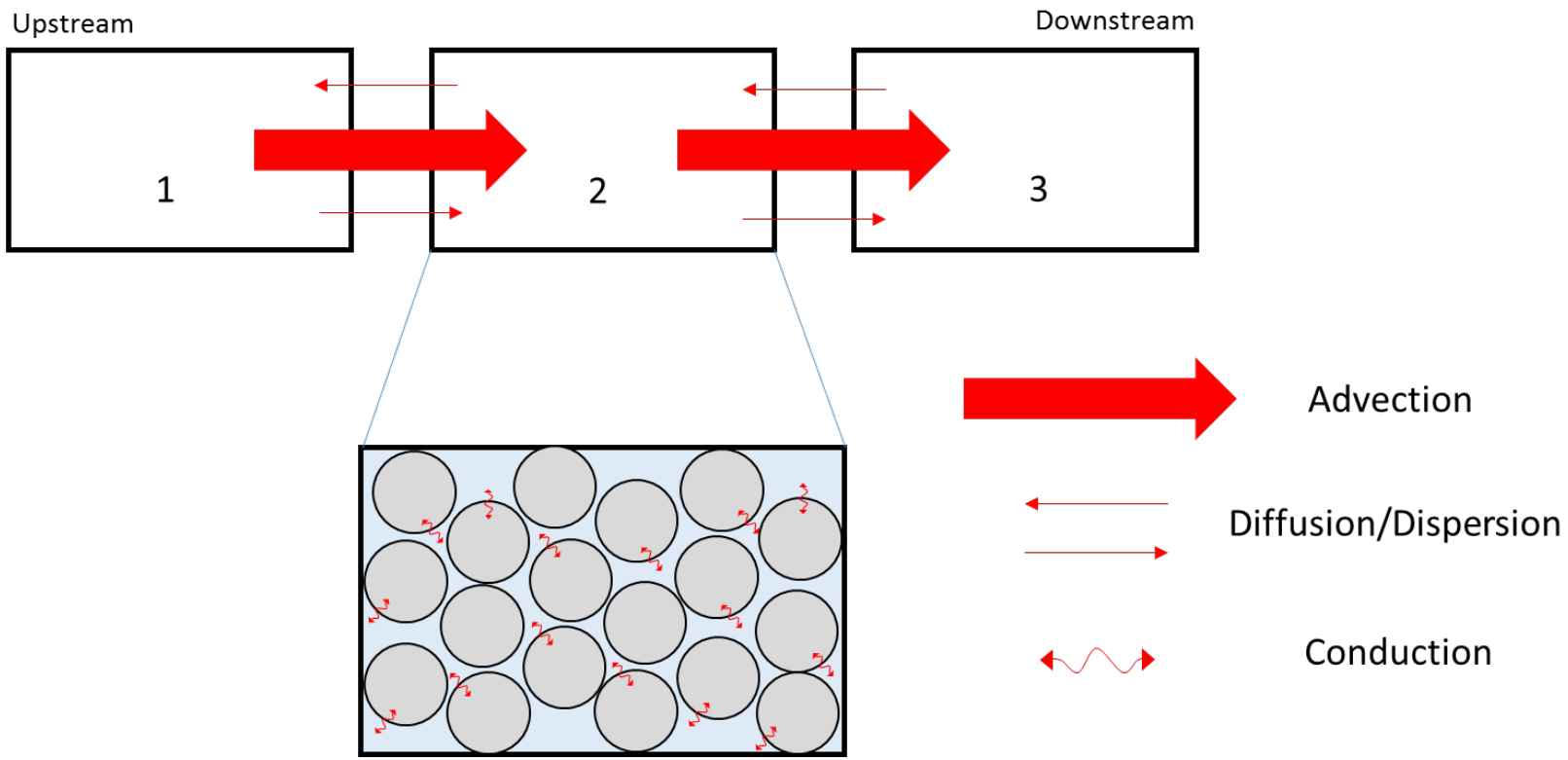

Figure 4.11: Conceptual visualization of Heat Flux model, with red arrows representing heat exchanges within the system. Numbers represent the spatial placement of the cell within the hypothetical flow path going downstream.

	A	B	C	D	E	F	G	H	I	J
1	x\t	0	1	2	3	4	5	6	7	8
2	0	12	17	17	17	17	17	17	17	17
3	1	12	13.25	14.38	15.20	15.79	16.20	16.49	16.68	16.81
4	2	12	12.31	12.88	13.54	14.20	14.81	15.34	15.77	16.11
5	3	12	12.08	12.29	12.63	13.08	13.58	14.10	14.60	15.07
6	4	12	12.02	12.09	12.24	12.47	12.78	13.16	13.58	14.02
7	5	12	12.00	12.03	12.08	12.19	12.35	12.58	12.87	13.20
8	6	12	12.00	12.01	12.03	12.07	12.15	12.27	12.44	12.65
9	7	12	12.00	12.00	12.01	12.03	12.06	12.12	12.20	12.33
10	8	12	12.00	12.00	12.00	12.01	12.02	12.05	12.09	12.16
11	9	12	12.00	12.00	12.00	12.00	12.01	12.02	12.04	12.07
12	10	12	12.00	12.00	12.00	12.00	12.00	12.01	12.02	12.03
13	11	12	12.00	12.00	12.00	12.00	12.00	12.00	12.01	12.01
14	12	12	12.00	12.00	12.00	12.00	12.00	12.00	12.00	12.01
15	13	12	12.00	12.00	12.00	12.00	12.00	12.00	12.00	12.00
16	14	12	12.00	12.00	12.00	12.00	12.00	12.00	12.00	12.00
17	15	12	12.00	12.00	12.00	12.00	12.00	12.00	12.00	12.00
18	16	12	12.00	12.00	12.00	12.00	12.00	12.00	12.00	12.00
19	17	12	12.00	12.00	12.00	12.00	12.00	12.00	12.00	12.00
20	18	12	12.00	12.00	12.00	12.00	12.00	12.00	12.00	12.00
21	19	12	12.00	12.00	12.00	12.00	12.00	12.00	12.00	12.00
22	20	12	12.00	12.00	12.00	12.00	12.00	12.00	12.00	12.00

Figure 4.12: A screenshot from Microsoft Excel showing how information within the Heat Flux model was organized. Row headings (in bold) represent the spatial component and column headings (in bold) represent the temporal component.

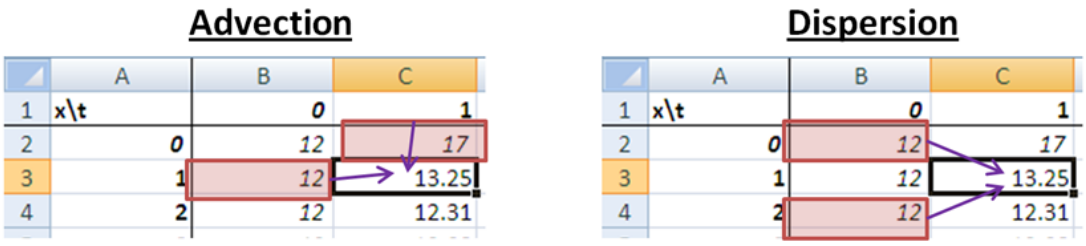

Figure 4.13: Screenshots from the Heat Flux model showing the components that were used to calculate advection and dispersion for downstream cells within the model.

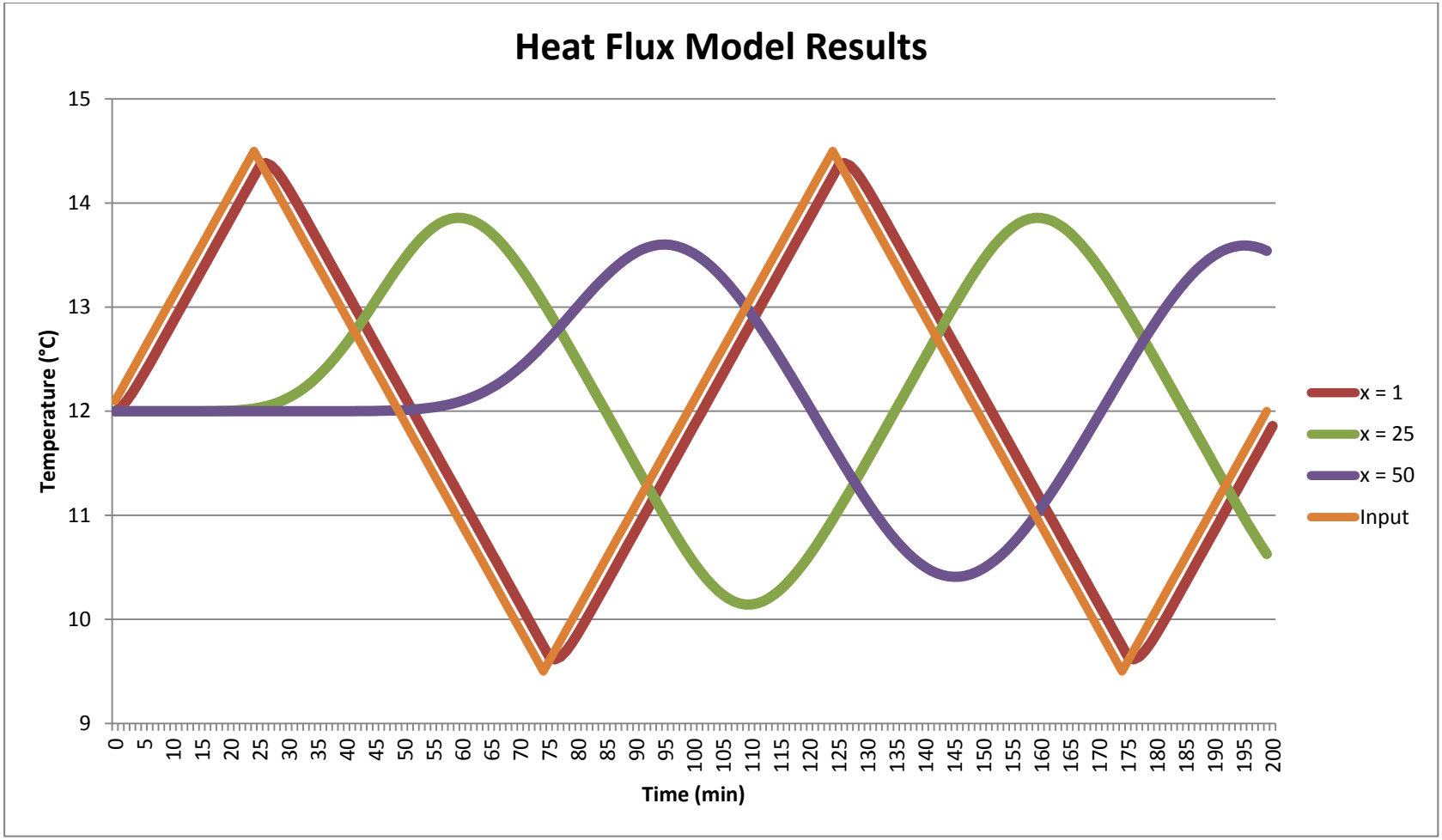

Figure 4.14: Results from the Heat Flux model, looking at heat concentrations through time for different locations within the grid of hyporheic cells, and including input temperatures. X is the location of the cell in the flow path: x = 1 is the first cell downstream of the starting boundary, x = 25 is the 25th cell downstream of the starting boundary, and x = 50 is the 50th cell downstream of that boundary.

CHAPTER 5

CONCLUSION

Hyporheic exchange is a relatively well-studied and well-understood concept, but one that is looked at differently depending on the field of study, and its effects on mainstem stream temperature are only now beginning to be more fully understood. As a result, hyporheic exchange is often excluded from stream temperature modeling studies because of either its complexity or its perceived lack of impact. There have been a number of studies in recent years (Loheide and Gorelick, 2006; Arrigoni et al., 2008; Marzadri et al., 2013) that have examined the heat exchange characteristics of the hyporheic zone and established that temperature time series are buffered and lagged when compared to surface water, but this dissertation really focuses on the contribution of conduction to these temperature behaviors.

A large range of literature values for hyporheic sediment characteristics were collected and presented to inform general knowledge about the hyporheos, as well as form the basis for the described modeling studies. Although sediment physical characteristics were commonly reported in hyporheic studies, values for thermal characteristics were harder to find, largely due to the fact that most hyporheic studies are not looking at temperature patterns, and if they are, they are specifically looking at temperature patterns within the hyporheos which can be directly measured quite easily. This made an understanding of heat exchange processes occurring somewhat more

difficult, but through the use of laboratory experiments, heat exchange rates could be better estimated.

This set of experiments has led to the conclusion that heat transfer between water and sediment of different temperature through conduction is extremely fast. Previous studies have estimated through dimensional analysis, that cobbles achieve thermal equilibrium with the surrounding water within one or two hours (Burkholder et al., 2008), but my calorimeter experiment seems to indicate that this process is almost instantaneous, and is therefore likely to exert a greater influence on temperature processes within the hyporheic zone than may have been previously thought. Although these experiments were done in a laboratory setting, excluding inherent heterogeneities found in the field, they do demonstrate the heat exchange rates of various natural sediments.

A more complex modeling study by Marzadri et al. (2013), published during the period that this study was being conducted, found very similar results. They examined the three-dimensional process-based model through a pool-riffle bedform that accounts for advection, diffusion, and conduction at downwelling and upwelling sites, and found that upwelling waters had a time lag and attenuation when compared with surface temperatures. Similar to my findings, they also discovered that in low-gradient streams with long residence times, most of the hyporheic zone had temperatures close to the mean daily surface temperature. However, rather than near-instantaneous conduction as their mechanism for this project, they inferred that advection and longitudinal diffusion were controlling the temperature distribution within the hyporheic zone.

Hopefully, this work will lead to a greater understanding of how heat transfer will occur as water passes through the hyporheic zone, and the modeling studies described

here may form a basis for being able to include a hyporheic exchange component to water temperature and water quality models. Because these models are so simple, especially the Damping Model which includes channel temperature time series as its only input, they may be useful in modeling the temperature complexity of stream systems that experience hyporheic exchange, and the finding that conduction rates are near-instantaneous may be useful in other stream temperature studies.

REFERENCES

Acuna, V., and K. Tockner. 2009. Surface – subsurface water exchange rates along alluvial river reaches control the thermal patterns in an Alpine river network. Freshwater Biology, 54: 306-320.

Anderson, J.K., S.M. Wondzell, M.N. Gooseff, and R. Haggerty. 2005. Patterns in stream longitudinal profiles and implications for hyporheic exchange flow at the H.J. Andrews Experimental Forest, Oregon, USA. Hydrological Processes, 19: 2931-2949.

Arrigoni, A.S., G.C. Poole, L.A.K. Mertes, S.J. O'Daniel, W.W. Wossner and S.A. Thomas. 2008. Buffered, lagged, or cooled? Disentangling hyporheic influences on temperature cycles in stream channels. Water Resources Research 44: W09418, doi: 10.1029/2007WR006480.

Bardini, L., F. Boano, M.B. Cardenas, R. Revelli, and L. Ridolfi. 2012. Nutrient cycling in bedform induced hyporheic zones. Geochimica et Cosmochimica Acta, 84:47-61.

Baxter, C.V., and F.R. Hauer. 2000. Geomorphology, hyporheic exchange, and selection of spawning habitat by bull trout (*Salvelinus confluentus*). Canadian Journal of Fisheries and Aquatic Sciences, 57(7): 1470-1481.

Baxter, C., F.R. Hauer, and W.W. Woessner. 2003. Measuring groundwater-stream water exchange: New techniques for installing minipiezometers and estimating

hydraulic conductivity. Transactions of the American Fisheries Society, 132(3): 493-502.

Bencala, K.E., and R.A. Walters. 1983. Simulation of solute transport in a mountain pool-and-riffle stream: A transient storage model. Water Resources Research, 19(3): 718-724.

Berman, R. 1976. Thermal conduction in solids. Claredon Press, Oxford, pp.193.

Booth, D.B., K.A. Kraseski, and C.R. Jackson. 2014. Local-scale and watershed-scale determinants of summertime urban stream temperatures. Hydrological Processes, 28: 2427-2438.

Boulton, A.J., T. Datry, T. Kasahara, M. Mutz, and J.A. Stanford. 2010. Ecology and management of the hyporheic zone: stream – groundwater interactions of running waters and their floodplains. Journal of the North American Benthological Society, 29(1): 26-40.

Boulton, A.J., S. Findlay, P. Marmonier, E.H. Stanley, and H.M. Valett. 1998. The functional significance of the hyporheic zone in streams and rivers. Annu. Rev. Ecol. Syst. 29: 59-81.

Brown, G. W. 1969. Predicting temperatures of small streams. Water Resources Research, 5(1): 68-75.

Brunke, M. and T. Gonser. 1997. The ecological significance of exchange processes between rivers and groundwater. Freshwater Biology, 37: 1-33.

Brunke, M. and T. Gonser. 1999. Hyporheic invertebrates – the clinal nature of interstitial communities structured by hydrological exchange and environmental gradients. Journal of the North American Benthological Society, 18(3): 344-362.

Burkholder, B.K., G.E. Grant, R. Haggerty, T. Khangaonkar, and P.J. Wampler. 2008. Influence of hyporheic flow and geomorphology on temperature of a large, gravel-bed river, Clackamas River, Oregon, USA. Hydrological Processes, 22: 941-953.

Caissie, D. 2006. The thermal regime of rivers. Freshwater Biology **51**: 1389-1406.

Calver, A. 2001. Riverbed permeabilities: Information from pooled data. Groundwater, 39(4): 546-553.

Cardenas, M.B. 2008. The effect of river bend morphology on flow and timescales of surface water – groundwater exchange across pointbars. Journal of Hydrology, 362: 134-141.

Cardenas, M.B. 2009. A model for lateral hyporheic flow based on valley slope and channel sinuosity. Water Resources Research 45: W01501, doi:10.1029/2008WR007442.

Carslaw, H.S., and J.C. Jaeger. 1959. Conduction of Heat in Solids. Clarendon Press, Oxford, pp. 510.

Cleven, E.-J., and E.I. Meyer. 2003. A sandy hyporheic zone limited vertically by a solid boundary. Arch. Hydrobiol., 157(2): 267-288.

Conant, B. 2005. Delineating and quantifying ground water discharge zones using streambed temperatures. Groundwater, 42(2): 243-257.

Cranswick, R.H., P.G. Cook, M. Shanafield, and S. Lamontagne. 2014. The vertical variability of hyporheic fluxes inferred from riverbed temperature data. Water Resources Research, 50: 3994-4010, doi: 10.1002/2013WR014410.

Crisp, D.T., and G. Howson. 1982. Effect of air temperature upon mean water temperature in streams in the north Pennines and English Lake District. Freshwater Biology, 12: 359-367.

Dade, W.B., and P.F. Friend. 1998. Grain-size, sediment-transport regime, and channel slope in alluvial rivers. Journal of Geology, 106: 661-675.

Dori, M.H.I. 2005. Climate change and changes in global precipitation patterns: What do we know? Environment International, 31(8): 1167-1181.

Ebersole, J. L., W. J. Liss and C. A. Frissell. 2003. Cold water patches in warm streams: physicochemical characteristics and the influence of shading. Journal of the American Water Resources Association, 39: 355-368.

Elliot, A.H., and N.H. Brooks. 1997. Transfer of nonsorbing solutes to a streambed with bed forms: Theory. Water Resources Research, 33(1): 123-136.

Engelhardt, I., M. Piepenbrink, N. Trauth, S. Stadler, C. Kludt, M. Schulz, C., Schüth, and T.A. Ternes. 2011. Comparison of tracer methods to quantify hydrodynamic exchange within the hyporheic zone. Journal of Hydrology, 400: 255-266.

Evans, E.C., G.R. McGregor, and G.E. Petts. 1998. River energy budgets with special reference to river bed processes. Hydrological Processes 12: 575-595.

Fellows, C.S., H.M. Valett, and C.N. Dahm. 2001. Whole-stream metabolism in two montane streams: Contribution of the hyporheic zone. Limnology and Oceanography, 46(3): 523-531.

Fernald, A.G., P.J. Wigington Jr., and D.H. Landers. 2001. Transient storage and hyporheic flow along the Willamette River, Oregon: Field measurements and model estimates. Water Resources Research, 37 (6): 1681-1694.

Fetter, C.W. 2001. Applied Hydrogeology. Prentice Hall, Upper Saddle River, New Jersey, pp. 598.

Findlay, S. 1995. Importance of surface-subsurface exchange in stream ecosystems: The hyporheic zone. Limnology and Oceanography, 40(1): 159-164.

Fourier, J. 1955. The analytical theory of heat. Dover Publications: New York, pp.466.

Fox, A., F. Boano, and S. Amon. 2014. Impact of losing and gaining streamflow conditions on hyporheic exchange fluxes induced by dune-shaped bed forms. Water Resources Research, 50(3): 1895-1907, doi: 10.1002/2013WR014668.

Fuller, C.C., and J.W. Harvey. 2000. Reactive uptake of trace metals in the hyporheic zone of a mining-contaminated stream, Pinal Creek, Arizona. Environ. Sci. Technol., 34: 1150-1155.

Gariglio, F.P., D. Tonina, and C.H. Luce. 2013. Spatiotemporal variability of hyporheic exchange through a pool-riffle-pool sequence. Water Resources Research, 49: 7185-7204, doi: 10.1002/wrcr.20419.

Geist, D.R., T.P. Hanrahan, E.V. Arntzen, G.A. McMichael, C.J. Murray, and Y. Chien. 2002. Physicochemical characteristics of the hyporheic zone affect red site selection by Chum salmon and Fall Chinook salmon in the Columbia River. North American Journal of Fisheries Management, 22(4): 1077-1085.

Gibert, J., M. Dole-Oliver, P. Marmonier, and P. Vervier. 1990. Surface water-groundwater ecotones. – In Naiman, R. J., and H. Decamps (eds). 1990. The ecology and management of aquatic-terrestrial ecotones. UNESCO, Paris, pp. 199-225.

Gomez-Velez, J.D., S. Krause, and J.L. Wilson. 2014. Effect of low-permeability layers on spatial patterns of hyporheic exchange and groundwater upwelling. Water Resources Research, 50: 5196-5215, doi:10.1002/2013WR015054.

Gooseff, M.N., J.K. Anderson, S.M. Wondzell, J. LaNier, and R. Haggerty. 2006. A modeling study of hyporheic exchange pattern and the sequence, size, and spacing of stream bedforms in mountain stream networks, Oregon, USA. Hydrological Processes, 20: 2443-2457.

Grisak, G.E., and J.F. Pickens. 1981. An analytical solution for solute transport through fractured media with matrix diffusion. Journal of Hydrology, 52: 47-57.

Haggerty, R., S.M. Wondzell, and M.A. Johnson. 2002. Power-law residence time distribution in the hyporheic zone of a 2nd-order mountain stream. Geophysical Research Letters, 29(13): doi: 10.1029/2002GL014743.

Hatch, C.E., A.T. Fisher, J.S. Revenaugh, J. Constantz, and C. Ruehl. 2006. Quantifying surface water-groundwater interactions using time series analysis of streambed thermal records: method development. Water Resources Research, 42: W10410, doi: 10.1029/2005WR004787.

Hendricks, S.P. 1993. Microbial ecology of the hyporheic zone: A perspective integrating hydrology and biology. Journal of the North American Benthological Society, 12(1): 70-78.

Herb, W. R., B. Janke, O. Mohseni, and H. G. Stefan. 2008. Thermal pollution of streams by runoff from paved surfaces. Hydrological Processes **22**: 987-999.

Hewlett, J.D., and J.C. Forston. 1982. Stream temperature under an inadequate buffer strip in the southeast Piedmont. Water Resources Bulletin, 18(6): 983-988.

Horai, K. 1971. Thermal conductivity of rock-forming minerals. Journal of Geophysical Research, 76(5): 1278-1308.

Isaak, D.J., S. Wollrab, D. Horan, and G. Chandler. 2012. Climate change effects on stream and river temperatures across the northwest U.S. from 1980-2009 and implications for salmonids fishes. Climatic Change, 113: 499-524.

Jones, J.B. Jr., S.G. Fisher, and N.B. Grimm. 1995. Nitrification in the hyporheic zone of a desert stream ecosystem. Journal of the North American Benthological Society, 14(2): 249-258.

Jones, J.B. Jr, and R.M. Holmes. 1996. Surface-subsurface interactions in stream ecosystems. Tree, 11(6):239-242.

Kaushal, S. S., G. E. Likens, N. A. Jaworski, M. L. Pace, A. M. Sides, D. Seekell, K. T. Belt, D. H. Secor and R. L. Wingate. 2010. Rising stream and river temperatures in the United States. Frontiers in Ecology and the Environment, 8(9): 461-466.

Kazezyilmaz-Alhan, C.M., and M.A. Medina Jr. 2006. Stream solute transport incorporation hyporheic zone processes. Journal of Hydrology, 329: 26-38.Leach, J. A. and R. D. Moore. 2011. Stream temperature dynamics in two hydrogeomorphically distinct reaches. Hydrological Processes, 25: 679-690.

Kinouchi, T. 2007. Impact of long-term water and energy consumption in Tokyo on wastewater effluent: implications for the thermal degradation of urban streams. Hydrological Processes, 21: 1207-1216.Leach, J.A., R.D. Moore, and S.G. Hinch. 2012. Estimation of forest harvesting-induced stream temperature changes and bioenergetics consequences for cutthroat trout in a coastal stream in British Columbia, Canada. Aquatic Sciences, 74: 427-441.

LeBlanc, R. T., R. D. Brown, and J. E. FitzGibbon. 1997. Modeling the effects of land use change on the water temperature in unregulated urban streams. Journal of Environmental Management 49: 445-469.

Lee, J.-Y., H.S. Lim, H.I. Yoon, and Y. Park. 2013. Stream water and groundwater interaction revealed by temperature monitoring in agricultural areas. Water, 5: 1667-1698; doi: 10.3390/w5041677.

Lenk, M. 2000. Hydraulische Austauschvorgänge zwischen fließender Welle und Interstitial – Felduntersuchungen in einer Pool-Riffle-Sequenz an der oberen Lahn. – Wasserbauliche Mitteilungen des Instituts für Wasserbau und Wasserwirtschaft, TU Darmstadt.

Li, G. 2006. Stream temperature and dissolved oxygen modeling in the lower Flint River basin, GA. PhD Dissertation, University of Georgia, Athens, GA, pp.240.

Li, G., C.R. Jackson, and K.A. Kraseski. 2012. Modeled riparian stream shading: Agreement with field measurements and sensitivity to riparian conditions. Journal of Hydrology, 428-429: 142-151.

Loheide II, S.P., and S.M. Gorelick. 2006. Quantifying stream – aquifer interactions through the analysis of remotely sensed thermographic profiles and in situ temperature histories. Environ. Sci. Technol., 40:3336-3341.

Long, S.L., and C.R. Jackson. 2014. Variation of stream temperature among mesoscale habitats within stream reaches: southern Appalachians. Hydrological Processes, 28(7): 3041-3052.

Luce, C., B. Stabb, M. Kramer, S. Wenger, D. Isaak, and C. McConell. 2013. Sensitivity of summer stream temperatures to climate variability in the Pacific Northwest. Water Resources Research, 50(4): 3428-3443.

Manger, G.E. 1963. Porosity and bulk density of sedimentary rocks. Geological Survey Bulletin 1144-E.

Marzadri, A., D. Tonina, and A. Bellin. 2013. Quantifying the importance of daily stream water temperature fluctuations on the hyporheic thermal regime: Implication for dissolved oxygen dynamics. Journal of Hydrology, 507: 241-248.

Menichino, G.T. and E.T. Hester. 2014. Hydraulic and thermal effects of in-stream structure-induced hyporheic exchange across a range of hydraulic conductivities. Water Resources Research, 50: 4643-4661, doi:10.1002/2013WR014758.

Morrice, J.A., H.M. Valett, C.N. Dahm, and M.E. Campana. 1997. Alluvial characteristics, groundwater – surface water exchange and hydrological retention in headwater streams. Hydrological Processes, 11: 253-267.

Ogata, A., and R.B. Banks. 1961. A solution of the differential equation of longitudinal dispersion in porous media. USGS Professional Paper 411-A.

Olsen, D.A., and C.R. Townsend. 2005. Flood effects on invertebrates, sediments and particulate organic matter in the hyporheic zone of a gravel-bed stream. Freshwater Biology, 50: 839-853.

Orghidan, T. 2010. A new habitat of subsurface waters: the hyporheic biotype. Fundam. Appl. Limnol., Arch. Hydrobiol., 176 (4): 291-302.

Petty, J.T., and G.D. Grossman. 1996. Patch selection by mottled sculpin (Pisces: Cottidae) in a southern Appalachian stream. Freshwater Biology, 35: 261-276.

Poole, G.C., S.J. O'Daniel, K.L. Jones, W.W. Woessner, E.S. Bernhardt, A.M. Helton, J.A. Stanford, B.R. Boer, and T.J. Beechie. 2008. Hydrologic spiraling: the role of multiple interactive flow paths in stream ecosystems. River Research and Applications 24: 1018-1031.

Pusch, M., and J. Schwoerbel. 1994. Community respiration in hyporheic sediments of a mountain stream (Steina, Black Forest). Arch. Hydrobiol., 130: 35-52.

Radcliffe, D.E. and J. Šimůnek. 2010. Soil Physics with HYDRUS: modeling and applications. Boca Raton, FL: CRC Press Taylor and Francis Group.

Ramires, M.L.V., C.A. Nieto de Castro, Y. Nagasaka, A. Nagashima, M.J. Assael, and W.A. Wakeham. 1995. Standard reference data for the thermal conductivity of water. Journal of Physical and Chemical Reference Data, 24: 1377-1381.

Rasmussen, T.C. 1982. Solute transport in saturated fractured media. Master's Thesis. University of Arizona.

Rawls, W.J., L.R. Ahuja, D.L. Brakensiek, A. Shirmohammadi. 1993. Infiltration and soil water movement. In Maidment, D.R. (ed). 1993. Handbook of Hydrology. McGraw Hill, New York, pp. 5.5.

Ritsema, C.J., and L.W. Dekker. 1994. Soil moisture and dry bulk density patterns in bare dune sands. Journal of Hydrology 154: 107-131.

Robertson, A.L. and P.J. Wood. 2010. Ecology of the hyporheic zone: origins, current knowledge and future directions. Fundam. Appl. Limnol., Arch. Hydrobiol., 176 (4):279-289.

Rutherford, J. C., S. Blackett, C. Blackett, L. Saito and R. J. Davies-Colley. 1997. Predicting the effects of shade on water temperature in small streams. New Zealand Journal of Marine and Freshwater Research, 31: 707-721.

Saenger, N. 2000. Identifikation von Austauschprozessen zwischen Fließgewässer und hyporheischer Zone. – Dissertation, Technische Univerität Darmstadt.

Saenger, N. 2002. Estimation of flow velocities within the hyporheic zone. Proceedings of the International Association of Theoretical and Applied Limnology, 28(4): 1790-1795.

Sear, D.A., I. Pattison, A.L. Collins, M.D. Newson, J.I. Jones, P.S. Naden, and P.A. Carling. 2014. Factors controlling the temporal variability in dissolved oxygen regime of salmon spawning gravels. Hydrologic Processes, 28: 86-103.

Shen, H.W., and P.Y. Julien. 1993. Erosion and sediment transport. In Maidment, D.R. (ed). 1993. Handbook of Hydrology. McGraw-Hill, New York, pp. 12.5-12.61.

Silliman, S.E., and D.F. Booth. 1993. Analysis of time-series measurements of sediment temperature for identification of gaining vs. losing portions of Juday Creek, Indiana. Journal of Hydrology, 146: 131-148.

Sinokrot, B.A., and H.G. Stefan. 1993. Stream temperature dynamics: measurements and modeling. Water Resources Research 27(7): 2299-2312.

Smith, J. W. N. 2005. Groundwater-surface water interactions in the hyporheic zone. Environment Agency Science Report SC030155/SR1, Bristol, UK.

Smith, L. and S.W. Wheatcraft. 1993. Groundwater Flow. In Maidment, D.R. (ed). 1993. Handbook of Hydrology. McGraw-Hill, New York, pp.6.9.

Soil Survey Division Staff. 1993. Soil survey manual. Soil Conservation Service. U.S. Department of Agriculture Handbook 18.

Song, J., X. Chen, C. Cheng, D. Wang, S. Lackey, and Z. Xu. 2009. Feasibility of grain-size analysis methods for determination of vertical hydraulic conductivity of streambeds. Journal of Hydrology, 375: 428-437.

Stanley, E.H., and A.J. Boulton. 1993. Hydrology and the distribution of hyporheos: Perspectives from a mesic river and a desert stream. Journal of the North American Benthological Society, 12(1): 79-83.

Stelzer, R.S., L.A. Bartsch, W.B. Richardson, and E.A. Strauss. 2011. The dark side of the hyporheic zone: depth profiles of nitrogen and its processing in stream sediments. Freshwater Biology, 56: 2021-2033.

Stonedahl, S.H., J.W. Harvey, A. Wörman, M. salehin, and A.I. Packman. 2010. A multiscale model for integrating hyporheic exchange from ripples to meanders. Water Resources Research, 46, W12539, doi: 1029/2009WR008865.

Supriyasilp, T., A.G. Graettinger, and S.R. Durrans. 2003. Quantitatively directed sampling for main channel and hyporheic zone water-quality modeling. Advances in Water Resources, 26: 1029-1037.

Swanson, T.E. and M.B. Cardenas. 2010. Diel heat transport within the hyporheic zone of a pool-riffle-pool sequence of a losing stream and evaluation of models for fluid flux estimation using heat. Limnology and Oceanography, 55(4): 1741-1754.

Taylor, C.A., and H.G. Stefan. 2009. Shallow groundwater temperature response to climate change and urbanization. Journal of Hydrology, 375: 601-612.

Valett, H.M., S.G. Fisher, and E.H. Stanley. 1990. Physical and chemical characteristics of the hyporheic zone of a Sonoran Desert stream. Journal of the North American Benthological Society, 9(3): 201-215.

Vandenbohede, A., A. Louwyck, and L. Lebbe. 2009. Conservative solute versus heat transport in porous media during push-pull tests. Transport in Porous Media, doi: 10.1007/s11242-008-9246-4

Vaux, W.G. 1968. Intragravel flow and interchange of water in a streambed. Fishery Bulletin 66(3): 479-489.

White, D.S. 1993. Perspectives on defining and delineating hyporheic zones. Journal of the North American Benthological Society 12(1): 61-69.

Williams, D.D. and H.B.N. Hynes. 1974. The occurrence of benthos deep in the substratum of a stream. Freshwater Biology, 4: 233-256.

Wondzell, S.M. 2006. Effect of morphology and discharge on hyporheic exchange flows in two small streams in the Cascade Mountains of Oregon, USA. Hydrological Processes 20: 267-287.

Wondzell, S.M. 2011. The role of the hyporheic zone across stream networks. Hydrological Processes 25: 3525-3532.

Wondzell, S.M. and F.J.Swanson. 1996. Seasonal and storm dynamics of the hyporheic zone of a 4th order mountain stream. I: Hydrologic processes. Journal of the North American Benthological Society, 15(1): 3-19.

Wroblicky, G.J., M.E. Campana, H.M. Valett, and C.N. Dahm. 1998. Seasonal variation in surface-subsurface water exchange and lateral hyporheic area of two stream-aquifer systems. Water resources Research, 34(3): 317-328.

Yager, R.M. 1993. Estimation of hydraulic conductivity of a riverbed and aquifer system on the Susquehanna River in Broome County, New York. U.S. Geological Survey Water-Supply Paper 2387.

Young, H.D. 1992. University Physics: Volume 1. Addison-Wesley: Reading, Massachusetts, pp.1132.

Zarnetske, J.P., R. Haggerty, S.M. Wondzell, and M.A. Baker. 2011. Dynamics of nitrate production and removal as a function of residence time in the hyporheic zone. Journal of Geophysical Research, 116: doi: 10.1029/2010JG001356.